

Effective Hamiltonian for cuprate superconductors derived from multi-scale *ab initio* scheme with level renormalization

Motoaki Hirayama¹, Takahiro Misawa², Takahiro Ohgoe³, Youhei Yamaji³, and Masatoshi Imada³

¹RIKEN Center for Emergent Matter Science, Wako, Saitama 351-0198, Japan

²Institute for Solid State Physics, University of Tokyo, Kashiwanoha, Kashiwa, Chiba, Japan and

³Department of Applied Physics, University of Tokyo,
7-3-1 Hongo, Bunkyo-ku, Tokyo 113-8656, Japan

Three-types (three-band, two-band and one-band) of effective Hamiltonians for the $\text{HgBa}_2\text{CuO}_4$ and three-band effective Hamiltonian for La_2CuO_4 are derived beyond the level of the constrained-GW approximation combined with the self-interaction correction (cGW-SIC) derived in Hirayama *et al.* Phys. Rev. B **98**, 134501 (2018) by improving the treatment of the interband Hartree energy. The charge gap and antiferromagnetic ordered moment show good agreement with the experimental results when the present effective Hamiltonian is solved, indicating the importance of the present refinement. The obtained Hamiltonians will serve to clarify the electronic structures of these copper oxide superconductors and to elucidate the superconducting mechanism.

I. INTRODUCTION

Mechanism of high temperature superconductivity in copper oxide superconductors discovered more than thirty years ago¹ is still under active debates. One of the reasons of the controversies is severe competitions of completely different orders, particularly, *d*-wave superconductivity, antiferromagnetism and charge inhomogeneous states such as charge/spin stripe-ordered states suggested by experiments²⁻¹³ as well as by highly accurate numerical studies on theoretical models such as the Hubbard model¹⁴⁻²¹, while they are still controversial. Therefore, more quantitative *ab initio* studies are needed based on the realistic parametrization of the cuprate superconductors to reach conclusive, and quantitative understanding of the mechanism.

Recently, several first principles effective Hamiltonians for low-energy degrees of freedom of electrons near the Fermi level in the cases of Hg based and La based cuprate superconductors have been derived after eliminating the high-energy electronic degrees of freedom far from the Fermi level²², based on the multi-scale *ab initio* scheme for correlated electrons (MACE)²³⁻²⁵, which is expected to be the basis of quantitative realistic studies of the cuprate superconductors without adjustable parameters. The derivation of the effective Hamiltonians is based on the constrained GW (cGW) calculation, where the exchange correlation energy and the Hartree energy in the density functional theory (DFT) in the level of the local density approximation (LDA) is carefully removed to exclude the double counting of the Coulomb interaction in the low-energy effective Hamiltonians. Other attempts to determine parameters of effective Hamiltonians were also reported²⁶⁻²⁸.

In this paper, we propose a more accurate and realistic description of the low-energy effective Hamiltonians by taking account effects called energy *level renormalization* (LR) of the orbitals consisting of the low-energy effective Hamiltonians. In the present framework, effects of the Hartree energy between the low-energy orbitals con-

tained in the effective Hamiltonians and the high-energy orbitals outside of them already eliminated in the effective Hamiltonians are calculated more accurately. This Hartree energy contribution has been of course taken into account in the GW level. However, when we solve the low-energy effective Hamiltonians more accurately beyond the GW, the charge density is improved and the Hartree energy is modified. This correction is not taken into account in Ref.22 and generate the LR.

We further take into account the feedback from the LR to the GW global band structure. By using the renormalized global band structure, we derive an improved effective Hamiltonian using the cGW calculation. By this correction, we show that the level distance in the low-energy orbitals is renormalized to smaller values and the resultant enhanced mutual screening between these orbitals drives the effective interaction weaker in the low-energy Hamiltonians. We show that the improved Hamiltonian well reproduces the charge gap and antiferromagnetic ordered moment of the experimental results in the mother materials.

In Sec. II we show the method of the improved downfolding. The three effective Hamiltonians for $\text{HgBa}_2\text{CuO}_4$ are derived in Sec. III.A. The result obtained by the variational Monte Carlo method (VMC)^{31,32} to incorporate the feedback is also shown in Sec. III.A. Three-band effective Hamiltonians for La_2CuO_4 are derived in Sec. III.B. We summarize the paper in Sec. IV.

II. METHOD

A. Downfolding method

1. cGW-SIC

The aim of MACE is to derive an *ab initio* effective Hamiltonian for the low-energy degrees of freedom from the whole band structure of all electronic degrees of free-

dom, particularly for strongly correlated electron systems. The effective Hamiltonian in the low-energy space is given in the form of extended Hubbard-type Hamiltonian without any adjustable parameters as,

$$\begin{aligned} \mathcal{H}_{\text{eff}}^{\text{cGW-SIC}} = & \sum_{ij} \sum_{\ell_1 \ell_2 \sigma} t_{\ell_1 \ell_2 \sigma}^{\text{cGW-SIC}}(\mathbf{R}_i - \mathbf{R}_j) d_{i\ell_1 \sigma}^\dagger d_{j\ell_2 \sigma} \\ & + \frac{1}{2} \sum_{i_1 i_2 i_3 i_4} \sum_{\ell_1 \ell_2 \ell_3 \ell_4 \sigma \eta \rho \tau} \left\{ W_{\ell_1 \ell_2 \ell_3 \ell_4 \sigma \eta \rho \tau}^r(\mathbf{R}_{i_1}, \mathbf{R}_{i_2}, \mathbf{R}_{i_3}, \mathbf{R}_{i_4}) \right. \\ & \left. d_{i_1 \ell_1 \sigma}^\dagger d_{i_2 \ell_2 \eta} d_{i_3 \ell_3 \rho}^\dagger d_{i_4 \ell_4 \tau} \right\}, \quad (1) \end{aligned}$$

where $d_{i\ell\sigma}^\dagger$ ($d_{i\ell\sigma}$) is the creation (annihilation) operator of an electron for the ℓ th Maximally localized Wannier function (MLWF) with spin σ centered at unit cell \mathbf{R}_i . The terminology ‘‘extended Hubbard Hamiltonian’’ is used in this paper as the lattice fermion Hamiltonian containing longer-ranged transfers as well as longer-ranged and/or off-diagonal Coulomb interactions to represent first principles parameters accurately beyond the simple Hubbard model containing only the onsite interaction and the nearest-neighbor transfer. Here, the single particle term is represented by

$$t_{\ell_1 \ell_2 \sigma}^{\text{cGW-SIC}}(\mathbf{R}) = \langle \phi_{\ell_1 \mathbf{0}} | H_K^{\text{cGW-SIC}} | \phi_{\ell_2 \mathbf{R}} \rangle, \quad (2)$$

and the interaction term is given by

$$\begin{aligned} & W_{\ell_1 \ell_2 \ell_3 \ell_4 \sigma \eta \rho \tau}^r(\mathbf{R}_{i_1}, \mathbf{R}_{i_2}, \mathbf{R}_{i_3}, \mathbf{R}_{i_4}) \\ = & \langle \phi_{\ell_1 \mathbf{R}_{i_1}} \phi_{\ell_2 \mathbf{R}_{i_2}} | H_{W^r}^{\text{cGW-SIC}} | \phi_{\ell_3 \mathbf{R}_{i_3}} \phi_{\ell_4 \mathbf{R}_{i_4}} \rangle, \quad (3) \end{aligned}$$

where $\phi_{\ell \mathbf{R}_i}$ is the ℓ th MLWF centered at \mathbf{R}_i . In the previous approach^{22,24,25}, the one-body term $H_K^{\text{cGW-SIC}}$ and the 2-body term $H_{W^r}^{\text{cGW-SIC}}$ were calculated by the cGW with the self-interaction correction (SIC) and the constrained random phase approximation (cRPA), respectively, using the Green’s function of the band structure of all degrees of freedom. It should be noted that all the parameters in Eq.(1), namely $t^{\text{cGW-SIC}}$ and W^r , are given from the first principles calculation without any adjustable parameters. In this research, we follow the basic strategy of MACE and use the whole band structure obtained by the GW approximation (GWA) beyond the DFT to derive the *ab initio* Hamiltonian. As is widely known, the band gap, or more generally, energy difference between low-energy bands, is underestimated in the DFT scheme using the LDA, while it is improved by the GW method²⁹. Both the one-body and two-body parts in the *ab initio* Hamiltonian, therefore, are also expected to be more accurate by using the GW method.

In the cGW^{24,25}, the band dispersion is determined from the self-energy and the polarization by excluding the contribution within the low-energy degrees of freedom to remove the double counting. These contributions from the low-energy degrees of freedom are taken into account afterwards when the low-energy effective Hamiltonian is solved in the same way as the LDA+cRPA scheme based on the LDA Kohn-Shame Hamiltonian. However, in contrast to the LDA+cRPA, the cGW method can explicitly

exclude the double counting of the exchange correlation energy in the effective Hamiltonian because the contributions from high- and low-energy degrees of freedom to the exchange correlation energy can be disentangled in the GW scheme³⁰ while their contributions cannot be separated in the DFT. Furthermore, in the GW-based scheme, the electron correlation from the degrees of freedom outside of the effective Hamiltonian is better taken into account than the LDA²². The self-interaction included in the LDA is also removed by the self-interaction correction (SIC) that subtracts the Hartree energy estimated from the LDA charge density of the Wannier orbitals in the low-energy effective Hamiltonian. The double counting of Hartree energy is subtracted when the effective Hamiltonian is solved. Furthermore, the frequency dependent part of the interaction ignored in the low-energy Hamiltonian is taken into account as the renormalization factor in the one-body part.

2. Error in cGW-SIC

Even with this cGW-SIC formalism, an important correction to the Hartree energy contribution is missing. When the low-energy effective Hamiltonian is solved, the high-energy degrees of freedom are already traced out, and the ground state is determined only from the energy of the low-energy degrees of freedom. In the solution, the spatial distribution of the electron density (the primary part is the electron occupation in the Wannier orbitals in the low-energy degrees of freedom) changes in general from that in the GW (or DFT). This change in the electron density makes a difference in the Hartree interaction between the low- and high-energy degrees of freedom, which is not taken into account in the low-energy solver. However, this difference of the interband Hartree energy can be substantial, because the number of high-energy bands are large and, thus, a small change in charge density may induce a large change in the interband Hartree energy.

3. Rigidity of orbital occupation

The number of degrees of freedom and the scale of total energy are greatly different between the all-electron calculation and the low-energy effective Hamiltonian. The electron density in the all-electron calculation is determined by the bare Coulomb interaction of about 20 eV at the on-site and several eV at most at off-sites. On the other hand, the electron density in the low-energy effective Hamiltonian is determined only by the screened interaction between the low-energy degrees of freedom, which is one order of magnitude smaller than the bare Coulomb interaction. In the low-energy effective Hamiltonian, the high-energy degrees of freedom is traced out, and it is impossible to account for the change in the total energy of the high-energy degrees of freedom due to

the change of the electron density of the low-energy degree of freedom. Since the change in the charge distribution causes significant increase in the Hartree energy, the charge distribution is hardly affected by further improving accuracy of the *ab initio* methods (see Appendix A). The interband energy in the Hartree level determined from the global electronic structure is actually properly calculated in the GW energy and the resultant stable charge distribution is reliable. In fact, the Hartree level of energy and resultant charge density is estimated both by the LDA and GW with very similar values. For example, the occupation numbers for the Cu $x^2 - y^2$ and the O $2p$ orbitals in the LDA/GW are 1.450 and 1.775/1.437 and 1.781 in the Hg system, 1.396 and 1.802/1.350 and 1.825 in the La system, respectively, and the LDA and GW show no appreciable difference. The charge density may not be affected even when more accurate *ab initio* treatments are used. This means that the orbital occupation is rigid and should be fixed at the values of the GW (or similar LDA) results in the solution of the low-energy solver. This rigidity of the orbital occupation is expected to be more accurate if the Wannier orbitals belong to different atoms, because the Hartree energy is expected to be very different for orbitals belonging to different atoms and even a small redistribution of the charge in the low-energy orbitals results in large cost of interband Hartree energy.

4. Chemical potential shift

Then a better solution of the low-energy solver is obtained by shifting the chemical potential of each orbital in the effective low-energy Hamiltonian to adjust and reproduce the occupation in each orbital to the value given by the GW. We call the method to use the effective Hamiltonian simply obtained by such a shift of the chemical potential to the cGW-SIC Hamiltonian, cGW-SIC+ $\Delta\mu$.

We note here about a subtlety of the cGW-SIC+ $\Delta\mu$. First, the ground state of the effective Hamiltonian obtained by the low-energy solver may show spontaneous symmetry breaking while the GW solution is paramagnetic: The ground state of the effective Hamiltonian at half filling obtained by the VMC has antiferromagnetic order, while the paramagnetic ground state is obtained by the present GW calculation. This difference in the ground state character may introduce the possible correction arising from the exchange splitting effect, which is taken into account in the VMC result while it is not in the GW energy. Another subtlety is the off-diagonal part of the density fitting. Although it is a secondary effect, the Hartree energy contains not only the diagonal part of density ($d_i^\dagger d_i$ and $d_j^\dagger d_j$) but also the off-diagonal part ($d_i^\dagger d_j$ and $d_j^\dagger d_i$) in the atomic orbital basis of d_i and d_j . This off-diagonal part may also be adjusted between the GW and the VMC results. These secondary effects will be discussed in a future publication.

5. Renormalized level feedback

The renormalized level determined in the cGW-SIC+ $\Delta\mu$ can further be used to improve the full GW electronic structure. We call this improvement level renormalization feedback (LRFB). In the LRFB, the chemical shifts are added to the self-energy to update the full GW Green's function, where we call the updated one GW+LRFB Green's function. For better self-consistency, we use the GW+LRFB Green's function to perform the cGW-SIC calculations again. In this paper, we employ the level-renormalized revised effective Hamiltonians by taking into account the feedback effect in this way. We name this scheme cGW-SIC+LRFB. The outline of cGW-SIC+LRFB method is illustrated in Fig. 1. The present procedure can be self-consistent by repeating the LRFB in the cGW-SIC+ $\Delta\mu$ until the the cGW-SIC+LRFB effective Hamiltonian covers (as shown in Fig. 1), while it is beyond the scope of the present paper. We describe details of cGW-SIC+LRFB below.

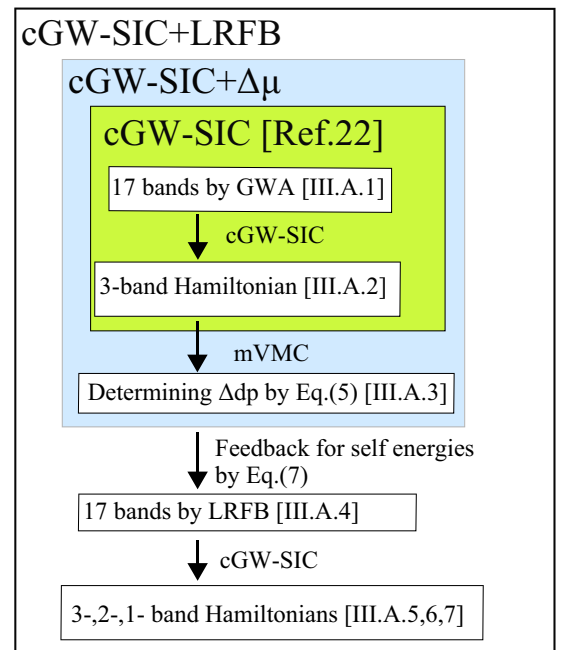


FIG. 1. (Color online) Overview of cGW-SIC+LRFB method. As an example, we show the calculation flow of cGW-SIC+LRFB method for the cuprate superconductors.

The cGW-SIC+ $\Delta\mu$ and cGW-SIC+LRFB are expected to reach a non-negligible improvement of the low-energy effective Hamiltonian. To demonstrate the improvement, here, we take an example of the three-band Hamiltonian for the cuprates derived in Ref.22, where the Wannier orbitals of d and p belong to different atoms, namely Cu and O, respectively. If the LRFB is applied, the level difference between the oxygen p_σ and the copper $d_{x^2-y^2}$ orbital decreases in comparison to the GW results, as we show later. This also means that the effective

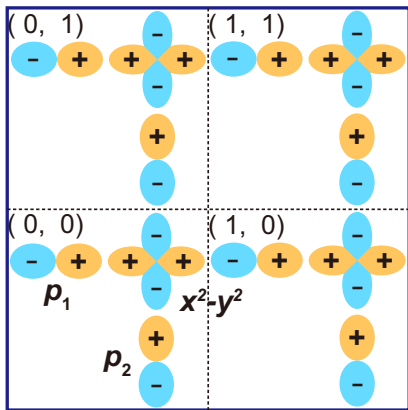


FIG. 2. (Color online) Position of the Cu $x^2 - y^2$ and O $2p$ orbitals and definition of the 2×2 sublattice in the VMC for the three-band Hamiltonian. Phases of the orbitals are denoted by \pm .

one-band Hamiltonian for the anti-bonding band resulting from the hybridized $d_{x^2-y^2}$ and p_σ orbitals has to be further improved because of the level shift and increased screening from the p_σ orbital. More precisely, after the hybridization of the Cu d and O p orbitals, the GW results are given by the bonding, non-bonding, and anti-bonding bands. Since the LR leads to stronger hybridization and screening effects arising from the bonding and non-bonding bands, they may make the effective interaction of the one-band Hamiltonian weaker. For example, as we will show later, nearest-neighbor hopping $t(1,0,0)$, the on-site screened Coulomb interaction U , and $U/t(1,0,0)$ for the one-band Hamiltonian of $\text{HgBa}_2\text{CuO}_4$ are -0.461 , 4.37 , and 9.5 in the cGW, and -0.509 , 3.85 and 7.6 in the GW+LRFB.

B. Multi-scale correction for occupation number of low-energy effective Hamiltonian

The improved transfer integral with the correction of the chemical potential \tilde{t} is

$$\tilde{t}_{\ell_1\ell_2\sigma}^{\text{cGW-SIC}}(\mathbf{R}) = t_{\ell_1\ell_2\sigma}^{\text{cGW-SIC}}(\mathbf{R}) + \Delta\mu_{\ell_1\sigma}(\mathbf{0})\delta_{\ell_1\ell_2}, \quad (4)$$

where $\Delta\mu$ is the chemical potential shift to reproduce the occupation number of each Wannier orbital by the GW calculation, even after solving the effective Hamiltonian by an accurate low-energy solver.

Instead of DFT, in the GWA, the Green's function and various physical quantities such as the self-energy are calculated in a self-consistent manner based on the Hedin's equation. In actual calculations, Hartree interaction is often not updated during the self-consistent calculation, but it is empirically known that the band structure is improved compared to that in the DFT. Therefore, in this study, we employ the electron density of each Wannier orbital in the GWA in Eq. (4) as the density to

be reproduced in the solution of the low-energy effective Hamiltonian.

C. Calculation by low-energy solver to correct orbital occupation number

We have several possibilities for the choice of the low-energy solver when we solve the effective Hamiltonians derived by the cGW-SIC+LRFB. Here, we employ the VMC method using the variational wave functions with various correlation factors and projection operators operated to pair product wave functions³² as the low-energy solver. The VMC is a method to optimize the variational parameters in the wave function to reach a good variational many-body ground-state.

We replace $t^{\text{cGW-SIC}}$ in the effective Hamiltonian (1) by $\tilde{t}^{\text{cGW-SIC}}$ defined in Eq.(4) and solve the modified effective Hamiltonian by sweeping the chemical potential $\Delta\mu$ of each orbital²⁵. Then we adjust the chemical potential of each orbital so that the VMC solution of the effective Hamiltonian, $|\psi\rangle$, reproduces each orbital occupation obtained by the GWA, i.e.,

$$n_\nu^{\text{VMC}} = n_\nu^{\text{GW}}, \quad (5)$$

where $n_\nu^{\text{VMC}} = N_s^{-1} \sum_{i=1}^{N_s} \sum_{\sigma=\uparrow,\downarrow} \langle \psi | d_{i\nu\sigma}^\dagger d_{i\nu\sigma} | \psi \rangle$.

By employing the adjusted chemical potential suggested in the VMC result to satisfy Eq.(5), and shifting the chemical potential in the cGW-SIC Hamiltonian, the cGW-SIC+ $\Delta\mu$ Hamiltonian is obtained.

D. Downfolding with cGW-SIC+LRFB

In the cGW-SIC+LRFB method, a static 1-body term $H_K^{\text{cGW-SIC}}$ is obtained from the dynamical 1-body term by renormalizing the frequency dependence using renormalization factors Z_H^{cGW} . By multiplying the chemical potential shift $\Delta\mu$ by $(Z_H^{\text{cGW}})^{-1}$, the correction from the frequency dependence of the dynamical 1-body term is taken into account. The revised GW self-energy $\Sigma^{\text{LRFB}}(\omega)$ is then given by

$$\Sigma^{\text{LRFB}}(\omega) = \Sigma^{\text{GW}}(\omega) + [Z_H^{\text{cGW}}(0)]^{-1}\Delta\mu. \quad (6)$$

The second term in Eq. (6) is a contribution of correlation effect beyond the GWA. The Hamiltonian in the GW+LRFB is

$$H = Z^{\text{LRFB}}(0)[H^{\text{LDA}} - V^{\text{xc}} + \Sigma^{\text{LRFB}}(0)], \quad (7)$$

where H^{LDA} is the Kohn-Sham Hamiltonian, V^{xc} is the exchange correlation energy in the LDA results, and Z^{LRFB} is the renormalization factor of Σ^{LRFB} at $\omega = 0$

$$Z^{\text{LRFB}}(0) = \left\{ I - \frac{\partial \text{Re} \Sigma^{\text{LRFB}}}{\partial \omega} \Big|_{\omega=0} \right\}^{-1}. \quad (8)$$

$Z^{\text{LRFB}}(0)$ is nearly the same as $Z^{\text{GW}}(0)$ because the ω dependence of Σ^{LRFB} originates from Σ^{GW} . In the Hamiltonian in the GW+LRFB, the LR in the full GW level is mostly given by $Z^{\text{GW}}(0)[Z_{\text{H}}^{\text{cGW}}(0)]^{-1}\Delta\mu$. One might think that the LR in the full GW level is smaller than $\Delta\mu$ because $Q \equiv Z^{\text{GW}}(0)/Z_{\text{H}}^{\text{cGW}}(0) < 1$. However this is reasonable because after the cGW calculation, the LR is $\Delta\mu$ and the contribution from the low energy degrees of freedom gives further renormalization given by Q .

We use the corrected self-energy (6) for the Green's function. Then we perform the cGW-SIC again, which generates cGW-SIC+LRFB Hamiltonian.

E. Application to the cuprates

In this paper, we apply the method to derive three types of effective Hamiltonian for the the cuprate superconductors $\text{HgBa}_2\text{CuO}_4$ and La_2CuO_4 : (1) Three-band effective Hamiltonian consisting of the Cu $d_{x^2-y^2}$ and two O $2p_\sigma$ Wannier orbitals, (2) two-band Hamiltonian consisting of the Cu $d_{x^2-y^2}$ and Cu $d_{3z^2-r^2}$ Wannier orbitals and (3) one-band Hamiltonian for the anti-bonding band of hybridized Cu $d_{x^2-y^2}$ and O p_σ Wannier orbitals.

In the present application to the cuprates, we apply the orbital level shift to the three-band cGW-SIC Hamiltonian in the form of Eq. (1) so that the relative level of O $2p_\sigma$ orbital is adjusted relative to the level of Cu $d_{x^2-y^2}$ orbital. To analyze the three-band Hamiltonian with the level shift, we use the mVMC method. In the mVMC calculation, we only consider the density-density type interactions ($W_{\ell_1\ell_2\ell_3\ell_4\sigma\sigma\rho\rho}^r(\mathbf{R}_{i_1}, \mathbf{R}_{i_1}, \mathbf{R}_{i_2}, \mathbf{R}_{i_2})$) and ignore the exchange term because their effects are small.

The present scheme is summarized in the following (see Fig. 1). Following the treatment employed in Ref.22, the effective Hamiltonian for the 17 bands near the Fermi level is first derived. For this purpose, the global band structure is obtained by the DFT with LDA. Then the Green's functions for the bands other than the 17 bands are fixed in this LDA form all through the calculations. The band structure of the 17 bands are first derived from the self-energy of the 17 bands calculated from the one-shot full GW calculation. Next, by using the GW Green's function for the 17 bands, the cGW-SIC calculation is performed to derive the effective Hamiltonian for the 17 bands with the one-body term obtained from the cGW and the interaction term using the cRPA. Then from this Hamiltonian, the three types of effective Hamiltonians are derived as we detail below. Up to here the procedure is the same as that employed in Ref.22.

By adding additional chemical potentials $\Delta\mu_d$ and $\Delta\mu_p$ for the Cu d and O p orbitals, respectively as parameters, $\Delta\mu_{dp} \equiv \Delta\mu_p - \Delta\mu_d$ dependence of the orbital fillings is calculated by the mVMC for the three-band Hamiltonian. In general the orbital fillings in the mVMC solution are not the same as the full GW result if $\Delta\mu_{dp} = 0$. Then the relative chemical potential $\Delta\mu_{dp}$ is shifted to the value so that the orbital fillings in the mVMC solution be-

come the same as the full GW result. By employing this level shift to the cGW-SIC Hamiltonian, cGW-SIC+ $\Delta\mu$ Hamiltonian is obtained. By taking into account the effect of nonzero $\Delta\mu_{dp}$, we recalculate the cGW-SIC to rederive the effective cGW-SIC-LRFB Hamiltonian with the LRFB correction.

F. Computational Conditions

1. Conditions for DFT, and GW

For the crystallographic parameters, we employ the experimental results reported by Ref. 40 for $\text{HgBa}_2\text{CuO}_4$ and those reported by Ref. 41 for La_2CuO_4 . We take the lattice constants of the tetragonal unit cell as $a = 3.8782/3.7817\text{\AA}$ and $c = 9.5073/13.2487\text{\AA}$ for the Hg/La compound. In the Hg compound, the height of Ba atom measured from CuO_2 plane is $0.2021c$ and the apex oxygen height is $0.2940c$. In the La compound, the La and apex oxygen heights measured from the CuO_2 plane are $0.3607c$ and $0.1824c$, respectively. Other atomic coordinates are determined from the crystal symmetry. Here, the crystallographic parameters of $\text{HgBa}_2\text{CuO}_{4+\delta}$ is employed because the mother compound is not available. The mother compound La_2CuO_4 has an orthorhombic symmetry and has slightly different lattice parameters from those listed above. We employ the tetragonal symmetry for the effective Hamiltonian with the crystallographic parameters of $\text{La}_{1.85}\text{Ba}_{0.15}\text{CuO}_4$ at 10K. We neglect this difference.

Computational conditions are as follows. The band structure calculation is based on the full-potential linear muffin-tin orbital (LMTO) implementation⁴². The exchange correlation functional is obtained by the local density approximation of the Ceperley-Alder type⁴³ and spin-polarization is neglected. The self-consistent LDA calculation is done for the $12 \times 12 \times 12$ k -mesh. The muffintin (MT) radii are as follows: $R_{\text{Hg}(\text{HgBa}_2\text{CuO}_4)}^{\text{MT}} = 2.6$ bohr, $R_{\text{Ba}(\text{HgBa}_2\text{CuO}_4)}^{\text{MT}} = 3.6$ bohr, $R_{\text{Cu}(\text{HgBa}_2\text{CuO}_4)}^{\text{MT}} = 2.15$ bohr, $R_{\text{O1}(\text{HgBa}_2\text{CuO}_4)}^{\text{MT}} = 1.50$ bohr (in CuO_2 plane), $R_{\text{O2}(\text{HgBa}_2\text{CuO}_4)}^{\text{MT}} = 1.10$ bohr (others), $R_{\text{La}(\text{La}_2\text{CuO}_4)}^{\text{MT}} = 2.88$ bohr, $R_{\text{Cu}(\text{La}_2\text{CuO}_4)}^{\text{MT}} = 2.09$ bohr, $R_{\text{O1}(\text{La}_2\text{CuO}_4)}^{\text{MT}} = 1.40$ bohr (in CuO_2 plane), $R_{\text{O2}(\text{La}_2\text{CuO}_4)}^{\text{MT}} = 1.60$ bohr (others). The angular momentum of the atomic orbitals is taken into account up to $l = 4$ for all the atoms.

The cRPA and GW calculations use a mixed basis consisting of products of two atomic orbitals and interstitial plane waves⁴⁴. In the cRPA and GW calculation, the $6 \times 6 \times 3$ k -mesh is employed. By comparing the calculations with the smaller k -mesh, we checked that these conditions give well converged results. We include bands in $[-26.4: 122.7]$ eV (193 bands) for calculation of the screened interaction and the self-energy. For entangled bands, we disentangle the target bands from the global Kohn-Sham bands⁴⁵.

We expect that the difference arising from the choice of basis functions (for instance, plane wave basis or localized basis) in the DFT calculation is small as was shown in a previous work⁴⁶. The $3d$ orbital of Cu is relatively localized among that of the transition metals. Therefore, the bare Coulomb interaction v and the screened Coulomb interaction calculated from v are sensitive to the accuracy of the wave function near the core. When calculating with a plane wave basis, we would improve the accuracy of interaction by using hard pseudo potentials.

2. Method and Conditions for VMC

We use the open-source software mVMC^{32–35} that implements the VMC with the variational wave function defined as

$$|\psi\rangle = \mathcal{P}_G \mathcal{P}_J \mathcal{L}^S |\phi_{\text{pair}}\rangle, \quad (9)$$

where \mathcal{P}_G and \mathcal{P}_J are the Gutzwiller factor³⁶ and the Jastrow factor³⁷, respectively. The variational wave function $|\psi\rangle$ is capable of describing various phases such as magnetic, superconducting, and spin liquid phases in a unified fashion. We employ the total spin projection \mathcal{L}^S to restore the symmetry of the Hamiltonian³⁸. In most part of the calculations, we use spin singlet total spin projections ($S = 0$), which is expected to be the ground-state quantum number. The pair-product part $|\phi_{\text{pair}}\rangle$ is the generalized pairing wave function defined as

$$|\phi_{\text{pair}}\rangle = \left[\sum_{i,j=1}^{N_s} \sum_{\nu,\mu=1}^{N_{\text{orb}}} f_{ij\nu\mu} a_{i\nu\uparrow}^\dagger a_{j\mu\downarrow}^\dagger \right]^{N_e/2} |0\rangle, \quad (10)$$

where f_{ij} denotes the variational parameters, N_{orb} is the number of the orbitals, and N_s is the number of the lattice sites. In this calculations, we take 2×2 sublattice shown in Fig. 2 to consider off-site correlations. The translational symmetry is assumed beyond this supercell. We have $2 \times 2 \times N_{\text{orb}}^2 \times N_s$ independent variational parameters for pair-product part. All the variational parameters are simultaneously optimized by using the stochastic reconfiguration method^{32,39}.

III. RESULT

A. HgBa₂CuO₄

1. Band structure in the GWA

We show the band structure of HgBa₂CuO₄ obtained by the GWA in Fig. 3. The 17 Wannier functions are constructed from the 20 bands near the Fermi level²². Full GW self-energy is introduced to the 17 bands near the Fermi level originating from the Cu $3d$ and O $2p$ orbitals, which are relatively well isolated from higher-energy bands. The Cu $3d$ orbitals are split into t_{2g} and

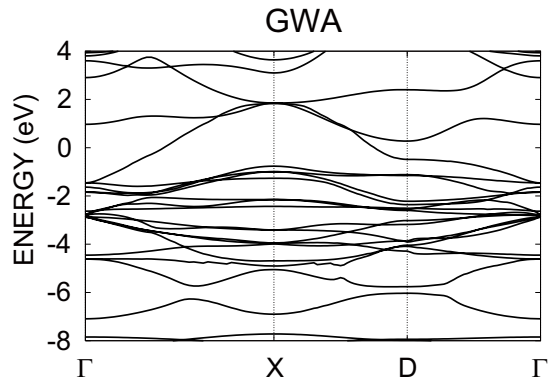


FIG. 3. (Color online) Electronic band structures of HgBa₂CuO₄ obtained by the GWA. Self-energy is calculated only for the 17 bands originating from the Cu $3d$ and O $2p$ orbitals near the Fermi level indicated by red (gray in black and white plot) bands. The zero energy corresponds to the Fermi level.

e_g orbitals by the octahedral crystal field, and the e_g orbitals are further split into higher $x^2 - y^2$ and lower $3z^2 - r^2$ by the crystal field mainly from the distorted octahedron of the oxygen ions surrounding the copper ions. The Cu e_g and O $2p$ orbitals are strongly hybridized with each other and make a covalent bond. Especially, the Cu $x^2 - y^2$ orbital has a strong σ -bonding with the O $2p_\sigma$ orbitals directed to the Cu atom, which makes large band width ~ 3.5 eV. The s -band originating from the Hg atom is also hybridized with 17 bands near the Fermi level. The one-body Hamiltonian parameters at the level of full GWA is listed in Table I.

2. Three-band Hamiltonian in the cGW-SIC

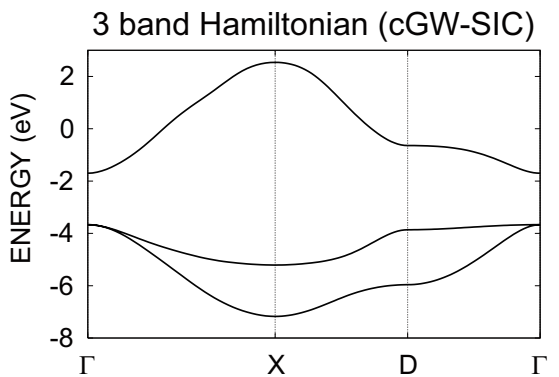


FIG. 4. (Color online) Electronic band structure of three-band Hamiltonian in the cGW-SIC originating from the Cu $d_{x^2-y^2}$ and O $2p$ Wannier orbitals for HgBa₂CuO₄. The zero energy corresponds to the Fermi level.

The three-band Hamiltonian consists of the Cu $d_{x^2-y^2}$ and O $2p_\sigma$ orbitals. The energy window for the Wannier

functions is set as the same as that in the GWA for the 17 bands. Band structure of the one-body part of three-band Hamiltonian in the cGW-SIC is shown in Fig. 4. In the calculation of the cGW-SIC and the cRPA, we use the Green's function obtained by the GWA. The difference in the chemical potential between the Cu $x^2 - y^2$ and O $2p$ orbitals is 2.42 eV. The nearest-neighbor hopping between the Cu $x^2 - y^2$ and O $2p$ orbitals is calculated to be 1.26 eV, which makes a strong covalent bond. The on-site interaction for the Cu $x^2 - y^2$ orbital is strong (8.84 eV), while that in the O $2p$ orbital is relatively weak (5.31 eV). Details are discussed in Ref. 22 and the Hamiltonian parameters are reproduced in Table I.

3. Chemical potential correction for three-band Hamiltonian by VMC

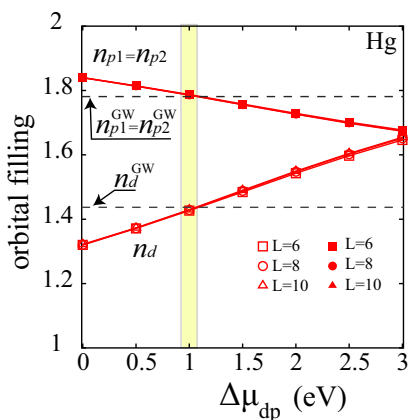


FIG. 5. (Color online) $\Delta\mu_{dp}$ dependence of the orbital fillings n_ν for the mother material of Hg compound calculated by VMC for the Hamiltonian (1) with the system size $L \times L$. Dashed lines show the orbital fillings obtained by the GW calculation. The proper chemical potential shift is estimated as $\Delta\mu_{dp} = 1.0$ eV for the Hg compound.

By using the mVMC, we here analyze the three-band (dp) Hamiltonian of $\text{HgBa}_2\text{CuO}_4$ obtained above by the cGW-SIC in the form of Eq.(1)²². The matrix elements of the Hamiltonian are listed in Table I, but the relative level difference between the Cu $d_{x^2-y^2}$ and O $2p_\sigma$ Wannier orbitals, $\Delta\mu_{dp} = \Delta\mu_p - \Delta\mu_d$, is added to tune the orbital fillings.

Figure 5 shows the orbital fillings of the Cu $d_{x^2-y^2}$ and O $2p_\sigma$ orbitals as a function of $\Delta\mu_{dp}$ added to the cGW-SIC Hamiltonian. Here, we note that $\Delta\mu_{dp} = 0$ corresponds to the cGW-SIC Hamiltonian used in the previous studies^{22,47} after eliminating the double counting in the Hartree terms. Increasing $\Delta\mu_{dp}$, in other words, decreasing the level difference, enhances the hybridization between the Cu $d_{x^2-y^2}$ and O $2p_\sigma$ orbitals. The O $2p_\sigma$ orbital component becomes larger in the anti-bonding band crossing the Fermi level, and the filling of the O $2p_\sigma$ Wannier orbital decreases. By taking $\Delta\mu_{dp} = 1.0$ eV, the fill-

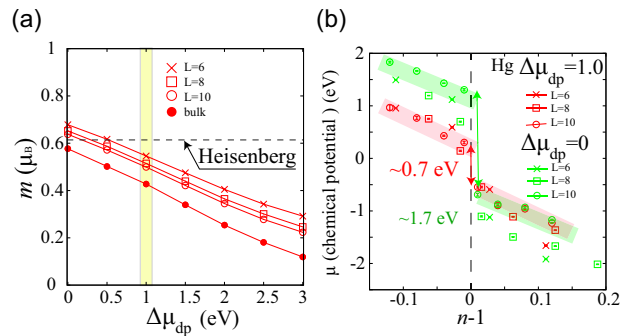


FIG. 6. (Color online) mVMC results for the Hg three-band Hamiltonian (1) with the system size $L \times L$; (a) $\Delta\mu_{dp}$ dependence of the magnetic ordered moment. By performing extrapolation with the least square fitting for magnetic ordered moments in finite system sizes, we obtain the bulk (thermodynamic) limit of the magnetic ordered moment. At the appropriate correction ($\Delta\mu_{dp} \sim 1\text{eV}$), we obtain $m \sim 0.4$ (μ_B). For comparison, we show the magnetic ordered moment in the Heisenberg model on the square lattice⁴⁸ by the dashed line. (b) Doping dependence of the chemical potential μ . At the appropriate corrections, The charge gap is estimated as $\Delta_c \sim 0.7$ eV.

ings of the O $2p_\sigma$ and Cu $d_{x^2-y^2}$ Wannier orbitals meet the values in the GWA.

By using the correction, we calculated the magnetic ordered moment m for $\text{HgBa}_2\text{CuO}_4$ (Fig. 6(a)), which is defined as

$$m = 2 \left[\frac{1}{N_s} \sum_{i,j} \langle \mathbf{S}_i \cdot \mathbf{S}_j \rangle e^{i\mathbf{Q} \cdot (\mathbf{r}_i - \mathbf{r}_j)} \right]^{\frac{1}{2}},$$

where $\mathbf{Q} = (\pi, \pi)$ is the ordering vector. The cGW-SIC Hamiltonian without $\Delta\mu$ ($\Delta\mu_{dp} = 0$) shows the magnetic ordered moment, whose amplitude is very close to that of the square lattice Heisenberg model as shown in Fig. 6(a). Since the existing copper oxide Mott insulators typically show the ordered moment smaller than that of the Heisenberg model⁴⁹, the ordered moment is apparently overestimated. On the other hand, when the correction ($\Delta\mu_{dp} > 0$) is taken into account, the correlation of the system weakens and the magnetic ordered moment is reduced to a more appropriate value smaller than that in the Heisenberg limit.

The *ab initio* matrix elements of the effective Hamiltonian of the cGW-SIC+ $\Delta\mu$ are listed in Table I. The difference from cGW-SIC in the same Table is only the level of the p orbital.

By introducing the chemical potential correction, the Mott gap of the effective Hamiltonian at half filling is also estimated using the mVMC. The Mott gap ΔE_{MG} is estimated from the total energy difference as $\Delta E_{\text{MG}} = (E(N+2) + E(N-2) - 2E(N))/2 = \mu(N+1) - \mu(N-1)$, where $E(N)$ and $\mu(N)$ are the ground state energy and the chemical potential of the N -electron system, respectively. Since the Mott gap is formed by strong short-ranged Coulomb repulsion, the system size dependence

is small and the value is a good estimate of the thermodynamic limit. Here, by introducing the chemical potential correction leading to a positive $\Delta\mu_{dp}$, the hybridization between the dp orbitals becomes stronger and, thus, makes the correlation of the system weaker than that without the correction. The Mott gap ΔE_{MG} , indeed, depends on $\Delta\mu_{dp}$: While the Mott gap ΔE_{MG} without the correction is calculated to be 1.7 eV, ΔE_{MG} with the correction $\Delta\mu_{dp} = 1$ eV is reduced to 0.7 eV, which proves the weaker correlation in the $cGW\text{-SIC}+\Delta\mu$ Hamiltonian, as shown in Fig. 6(b). Unfortunately, there exists no mother material in the Hg system. However, in the next section for the La compound, we will show that our *ab initio* estimate of the Mott gap indeed agrees with the experimental value, in contrast to the estimate without the $\Delta\mu$ correction.

4. $GW+LRFB$ band

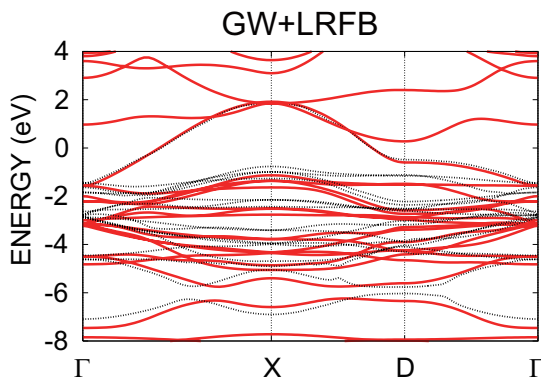


FIG. 7. (Color online) Electronic band structure of $\text{HgBa}_2\text{CuO}_4$ obtained by the $GW+LRFB$ (red solid line). Self-energy in the GWA is calculated only for the 17 bands originating from the Cu $3d$ and O $2p$ orbitals near the Fermi level. The feedback effect is counted only to the O $2p$ orbital directed to the Cu atom. The zero energy corresponds to the Fermi level. For comparison, the band structure in the GWA is also given (black dotted line).

Next, we calculate the band structure in the GW combined with LRFB by adding the on-site correction of the O $2p$ orbitals estimated by the VMC ($\Delta\mu_{dp} = 1.0$ eV) to the self-energy in the GWA Green's function. The chemical potential multiplied by the inverse of the renormalization factor in the $cGW\text{-SIC}$ is added to the GW self-energy of the 17 bands near the Fermi level. We obtain Fig. 7 by expanding self-energy to the frequency around the energy eigenvalue of the DFT and diagonalizing the Hamiltonian as the same as that in the usual GWA. Since there is no frequency dependence in the on-site correction, the frequency dependence of the self-energy remains the same as the GWA, and the renormalization factor is nearly the same as that in the GWA. The largest change in the $GW+LRFB$ band from the GWA is the hybridiza-

tion between the Cu $x^2 - y^2$ and O $2p$ orbitals. Also, due to the change in the energy level of the O $2p$ orbitals, the 17 bands around the Fermi level is slightly modified through the hybridization.

5. Three-band Hamiltonian in $cGW\text{-SIC}+LRFB$

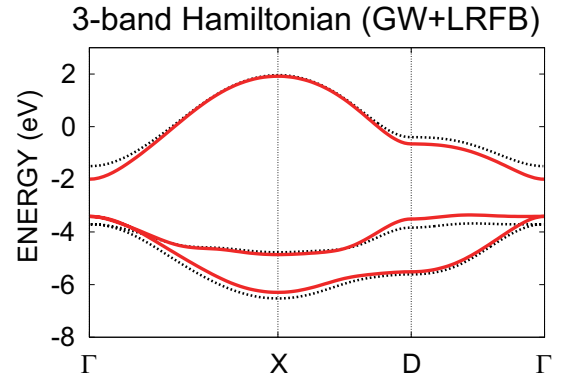


FIG. 8. (Color online) Electronic band structure of three-band Hamiltonian in the $GW+LRFB$ originating from the Cu $d_{x^2-y^2}$ and O $2p$ Wannier orbitals for $\text{HgBa}_2\text{CuO}_4$. The zero energy corresponds to the Fermi level. For comparison, the band structure of the Wannier function in the original GWA is also given (black dotted line).

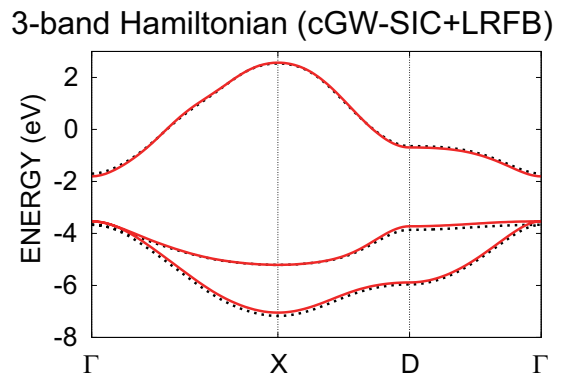


FIG. 9. (Color online) Electronic band structure of three-band Hamiltonian consisting of the Cu $d_{x^2-y^2}$ and O $2p$ Wannier orbitals for $\text{HgBa}_2\text{CuO}_4$ by using the $cGW\text{-SIC}+LRFB$. The zero energy corresponds to the Fermi level. For comparison, the band structure in the $cGW\text{-SIC}$ is also plotted (black dotted line).

We derive the 3-band Hamiltonian at the $cGW\text{-SIC}$ level based on the Green's function obtained by the $GW+LRFB$. Before deriving $cGW\text{-SIC}+LRFB$, we first show in Fig. 8 the band structure of the 3-band Hamiltonian obtained by the Wannier function in the level of $GW+LRFB$. We set the energy window for the Wannier functions as the same as that in the GWA and $GW+LRFB$. Then, the Wannier function of $GW+LRFB$

is close to the atomic orbital similarly to the Wannier function of the GWA. The bands indicated by the dotted line in the figure is those obtained by the Wannier function in the GWA constructed under similar conditions. The one-body Hamiltonian parameters of GW+LRFB are listed in Table II. The chemical potential difference between the Cu $x^2 - y^2$ and O $2p$ Wannier orbitals in the GW+LRFB is 1.48 (eV), while that in the GWA is 2.31 (eV) (see Table I for GWA). The decrease in the chemical potential difference (0.83 eV) is slightly smaller than $\Delta\mu_{dp}$ (1.0 eV) due to the renormalization factor derived from the static low-energy effective Hamiltonian. Since the Cu $x^2 - y^2$ and the O $2p$ orbitals are not hybridized at the Γ point due to the symmetry, the chemical potential change is clearly visible at Γ point (Fig. 8). On the other hand, at the X point, the width of the bonding and anti-bonding bands increases because the energy difference between the Cu $x^2 - y^2$ and O $2p$ orbitals decreases. The correction is a static chemical potential, the dp hopping hardly changes between the GWA (1.18 eV) and the GW+LRFB (1.19 eV), and therefore the increase in the bandwidth of the anti-bonding band is due to purely increase of covalency between the Cu $x^2 - y^2$ and O $2p$ orbitals in the GW+LRFB.

The band structure obtained by the cGW-SIC+LRFB is shown in Fig. 9. The three-band Hamiltonian in the cGW-SIC+LRFB is close to that without the feedback (namely cGW-SIC in Table I). The Hamiltonian parameters are listed in Table II. The chemical potential difference between the Cu $x^2 - y^2$ and the O $2p$ orbitals is 2.17 eV in the cGW-SIC+LRFB, which is close to 2.42 eV in the cGW-SIC obtained from the GW band structure. Also, the magnitude of the nearest-neighbor hopping between the Cu $x^2 - y^2$ and the O $2p$ orbitals is 1.261 eV, which is nearly the same value as 1.257 eV in the cGW-SIC. The effect of the correction is very small in the three-band Hamiltonian. This is because the enhanced mutual screening between the Cu $x^2 - y^2$ and the O $2p$ orbitals ascribed to the reduced level difference of these two bands is not taken into account at this stage of the derived three-band Hamiltonian. The screened on-site Coulomb interaction between the Cu $x^2 - y^2$ orbitals is 8.99 eV in the cGW-SIC+LRFB, while it is 8.84 eV and nearly the same in the cGW-SIC. Because of this similarity, the effective three-band Hamiltonian is well represented by cGW-SIC+ $\Delta\mu$ when one solves by low-energy solvers.

Figure 10 shows the doping concentration (δ) dependence of the orbital fillings for the Cu $3d_{x^2-y^2}$ and two O $2p_\sigma$ Wannier orbitals (in (a)) as well as for the Wannier orbitals representing diagonalized bands in Fig. 9 (in (b)) obtained by VMC using the cGW-SIC+ $\Delta\mu$ Hamiltonian given in Table I. Figure 9(a) shows a kink at zero doping indicating different character of carriers between electron and hole doping. More remarkably, only the $3d_{x^2-y^2}$ carriers look doped in the electron doped side and only the $2p$ carriers look doped in the hole doped side around the zero doping, because the filling of the other orbital stays

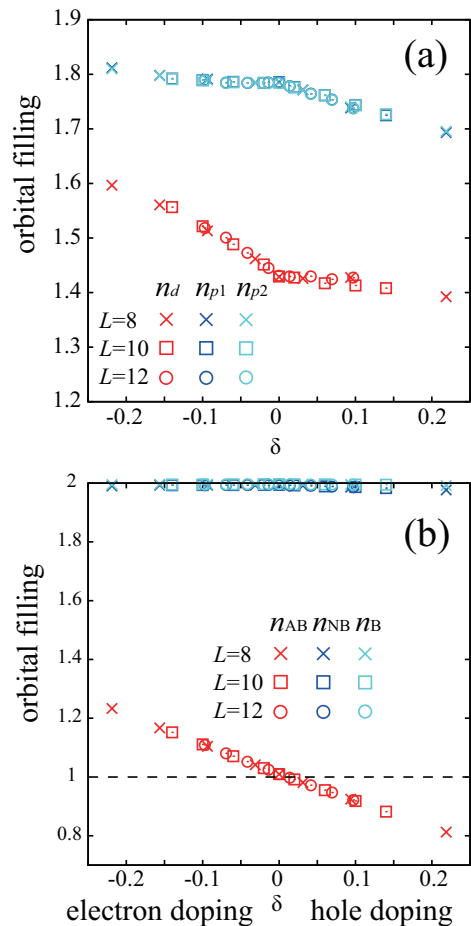


FIG. 10. (Color online) Doping dependence of the occupation number of the Cu $x^2 - y^2$ (n_d) and O $2p$ (n_{p1} , n_{p2}) orbitals for the Hg compound calculated by the VMC for the cGW-SIC+ $\Delta\mu$ Hamiltonian. (a) Orbital occupation in the basis of $d_{x^2-y^2}$ and $2p_\sigma$ atomic-like Wannier orbitals (b) Orbital occupation in the basis of bonding, nonbonding and antibonding Wannier orbitals, which represents three diagonalized bands in Fig. 9, respectively.

nearly constant, as was already suggested by the picture of charge transfer insulator⁵⁰. This means that carriers doped in the so-called Hubbard band and lower Hubbard band consist of different orbitals. However, it is interesting to see the same doping in the Wannier basis functions that represent the bonding, nonbonding and antibonding bands in Fig. 9, it turns out that the carriers are doped only in the highest antibonding band, as is expected. This shows that such different characters of carriers in (a) arise only within the carriers belonging to the original anti-bonding band⁵¹. Therefore the present apparent charge transfer insulator is well represented by the single-band framework of the antibonding band, which consists of strongly hybridized d and p atomic-like Wannier orbitals.

6. Two-band Hamiltonian in cGW-SIC+LRFB

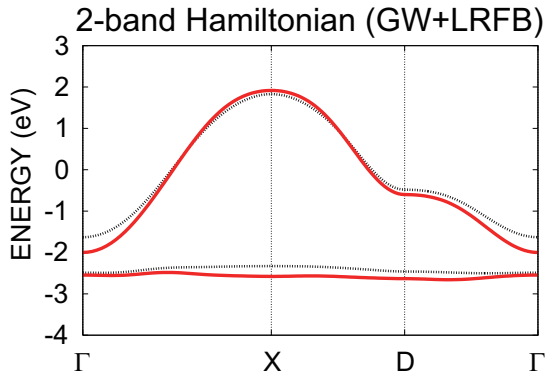


FIG. 11. (Color online) Electronic band structure of two-band Hamiltonian in the GW+LRFB originating from the Cu e_g Wannier orbitals for $\text{HgBa}_2\text{CuO}_4$. The zero energy corresponds to the Fermi level. For comparison, the band structure of the Wannier function in the GWA is also given (black dotted line).

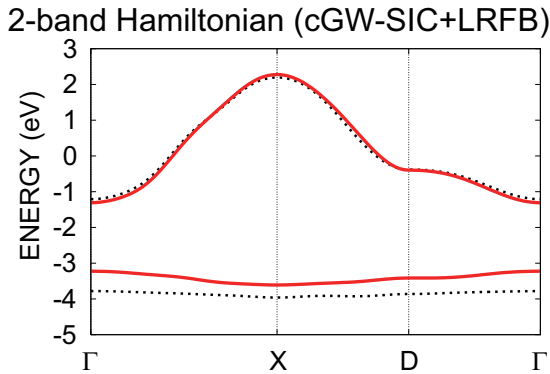


FIG. 12. (Color online) Electronic band structure of two-band Hamiltonian in the cGW+LRFB originating from the Cu e_g Wannier orbitals for $\text{HgBa}_2\text{CuO}_4$. The zero energy corresponds to the Fermi level. For comparison, the band structure in the cGW-SIC obtained from the GWA is also given (black dotted line).

Next, we discuss the two-band Hamiltonian in the cGW-SIC calculated from the GW+LRFB band structure (namely cGW-SIC+LRFB band). The 17 bands around the Fermi level is included to the energy window for the Wannier functions, where the bonding and non-bonding bands of the O $2p$ orbitals are not included. The one-body parameters obtained from the full GWA and the cGW-SIC Hamiltonian parameters obtained using the full GW Green's functions are listed in Table III. Interaction parameters in the level of cGW-SIC based on the full GW Green's function are calculated by the cRPA and listed in Table III as well. Then the level renormalization of O p_σ orbital is taken into account for the full GW calculation as GW+LRFB in the same

way as the three-band calculation. Figure 11 shows the GW+LRFB band structure. The one-body parameters by the GW+LRFB are listed in Table IV. Then the cGW-SIC for the purpose of constructing the two-band (Cu $d_{x^2-y^2}$ and O p_σ) Hamiltonian is performed²². The one-body parameters for the cGW-SIC+LRFB are listed in Table IV. The interaction parameters for the cGW-SIC+LRFB Hamiltonian are calculated using cRPA applied to the GW+LRFB Green's functions and are listed in Table IV as well.

The energy difference between the anti-bonding orbital and Cu z^2 orbital is 2.45 eV in the GW+LRFB, which is nearly the same as that in the GWA (2.43 eV). On the other hand, the nearest-neighbor hopping is 0.512 eV in the GW+LRFB, which is factor 1.13 larger than the value of 0.453 eV in the GWA. This is because the on-site correction increases the contribution of the O $2p$ orbitals to the anti-bonding orbital and then the hopping through the O $2p$ orbital increases.

Band structure in the cGW-SIC+LRFB is shown in Fig. 12. The Cu anti-bonding orbitals in the cGW-SIC with the feedback (cGW-SIC+LRFB) is substantially different from that without the feedback (cGW-SIC). The effective Hamiltonian parameters are listed in Table IV. The hybridization amplitude ((nearest-neighbor) transfer integral) of Cu $x^2 - y^2$ orbitals with the O $2p$ increases from the cGW-SIC (-0.426 eV) to cGW-SIC+LRFB (-0.455 eV), because the Wannier function of the anti-bonding orbital expands. Due to the expansion, the effective interaction decreases. For instance, the onsite interaction U for the anti-bonding ($d_{x^2-y^2}$) orbital decreases from 4.508 eV (cGW-SIC) to 4.029 eV (cGW-SIC+LRFB). Then the ratio U/t substantially decreases from 10.6 to 8.85.

7. One-band Hamiltonian in cGW+LRFB

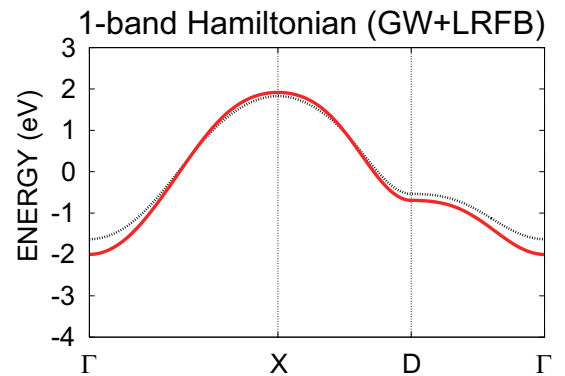


FIG. 13. (Color online) Electronic band structure of one-band Hamiltonian in the GW+LRFB originating from the Cu $d_{x^2-y^2}$ Wannier orbitals for $\text{HgBa}_2\text{CuO}_4$. The zero energy corresponds to the Fermi level. For comparison, the band structure of the Wannier function in the GWA is also given (black dotted line).

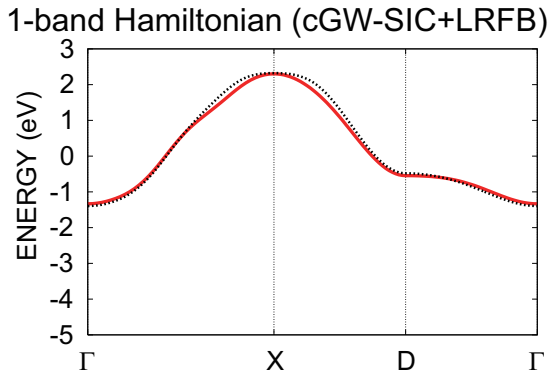


FIG. 14. (Color online) Electronic band structure of one-band Hamiltonian in the cGW obtained from the GW+LRFB band structure originating from the Cu $d_{x^2-y^2}$ Wannier orbitals for $\text{HgBa}_2\text{CuO}_4$. The zero energy corresponds to the Fermi level. For comparison, the band structure in the cGW obtained from the GWA is also given (black dotted line).

The band structure of effective one-band Hamiltonian in the level of GW+LRFB is shown in Fig. 13 and the Hamiltonian parameters are listed in Table V. The band structure and the one-band Hamiltonian parameters at the level of cGW+LRFB is derived similarly after considering the level correction and feedback, which are shown in Fig.14 and Table VI, respectively. In the case of the one-band Hamiltonian, we do not need to consider the SIC. The cGW+LRFB Hamiltonian is distinct from the cGW Hamiltonian, where the transfer amplitudes are increased from -0.461 (0.119) eV to -0.509 (0.127) eV for the transfers between the nearest-neighbor sites t (between the next-nearest-neighbor sites t'), while the matrix elements of the Coulomb repulsion are decreased from 4.37 (1.09) to 3.85 (0.83) eV for onsite interaction U (nearest-neighbor interaction V). The combined effect drives the system into weaker correlation, where $U/|t|$ is modified from 9.48 to 7.56.

Finally, the parameters for the three types of the effective Hamiltonians for the Hg compounds are summarized in Table VII.

B. La_2CuO_4

1. Band structure in the GWA

The band structure of La_2CuO_4 based on the GWA is calculated in the same way as the Hg compound and plotted in Fig. 15.

2. Three-band Hamiltonian in the cGW-SIC

The three-band effective Hamiltonian based on the cGW-SIC given in Ref.22 is reproduced in Fig.16.

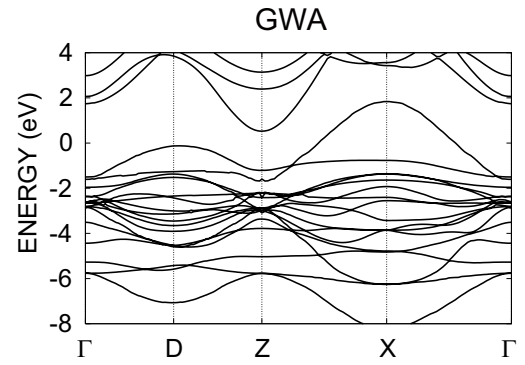


FIG. 15. (Color online) Electronic band structure of La_2CuO_4 obtained by the GWA. Self-energy is calculated for the 17 bands originating from the Cu $3d$ and O $2p$ orbitals near the Fermi level and the 28 conduction bands originating from the La $4f$ orbitals. The zero energy corresponds to the Fermi level. The 17 bands are drawn in red color (gray in black and white print).

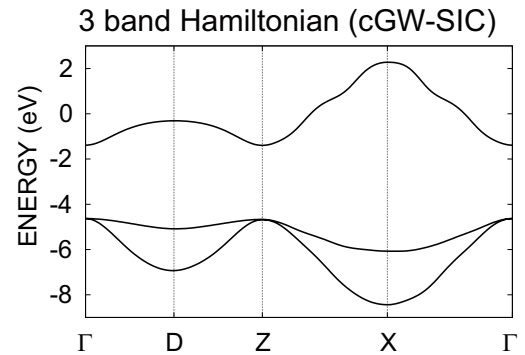


FIG. 16. (Color online) Electronic band structure of three-band Hamiltonian in the cGW-SIC originating from the Cu $d_{x^2-y^2}$ and O $2p$ Wannier orbitals for La_2CuO_4 ²². The zero energy corresponds to the Fermi level.

3. On-site potential correction for three-band Hamiltonian obtained by the VMC: cGW-SIC+ $\Delta\mu$

Figure 17 shows $\Delta\mu_{dp}$ dependence of the orbital fillings for La_2CuO_4 . We find that the proper LR (corrections in the chemical potential) are given by $\Delta\mu_{dp} \sim 2.5$ eV for La_2CuO_4 . Therefore we add $\Delta\mu_{dp} \sim 2.5$ eV to the chemical potential of O p orbital. The revised Hamiltonian parameter on the level of cGW-SIC+ $\Delta\mu$ is listed in Table VIII

This modified Hamiltonian was solved by mVMC. The obtained magnetic ordered moments and the chemical potentials are shown in Figs. 18(a) and (b), respectively. Our calculations show that the magnetic ordered moment for La_2CuO_4 is about $0.6 \mu_B$ in agreement with the neutron scattering result, $0.60 \pm 0.05 \mu_B$ ⁵². The charge gap is about 2 eV, which is consistent with the available experimental result, for instance the optical conductivity⁵³.

Since the Hamiltonian parameters are remarkably sim-

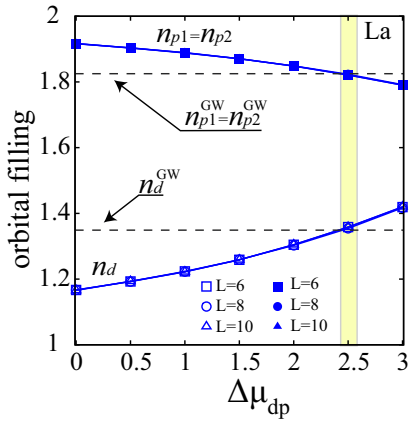


FIG. 17. (Color online) $\Delta\mu_{dp}$ dependence of the orbital fillings n_ν for the La compound calculated by the VMC at the system size $L \times L$. Dashed lines show the orbital fillings obtained by the GW calculation. The appropriate LR (chemical potential correction) is estimated as 2.5 eV.

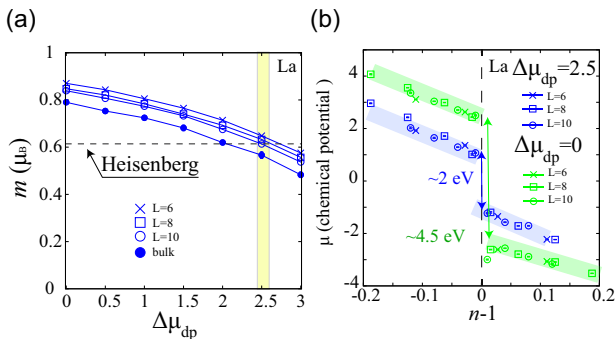


FIG. 18. (Color online) VMC results of the La compound at the system size $L \times L$; (a) $\Delta\mu_{dp}$ dependence of the magnetic ordered moment. At the proper LR, we obtain $m \sim 0.6$ (μ_B). (b) Doping dependence of the chemical potential μ . At the proper LR, The charge gap is estimated to be $\Delta_c \sim 2\text{eV}$.

ilar for the Hg compounds between the cGW-SIC and cGW-SIC+LRFB, we also assume that the parameters for the La compounds estimated by the cGW-SIC+LRFB change little from the cGW-SIC parameters and we do not list here. Therefore when one solves by using the low-energy solver, the effective three-band Hamiltonian is given just by raising up the chemical potential of O p orbitals with the amount of 2.5 eV as listed in Table VIII as cGW-SIC+ $\Delta\mu$. The interaction parameters to be used by the low-energy solver are given in the same table, which are obtained by cRPA with the GW-LRFB Green's function.

Figure 19 shows that the carrier character is different between the hole and electron doping in the atomic-like Wannier orbitals in (a) while carriers are solely doped in the antibonding band in (b) similarly to the Hg compound. This suggests that the two compounds belong to the same class of three-band level scheme, which is essentially described by the single-band framework.

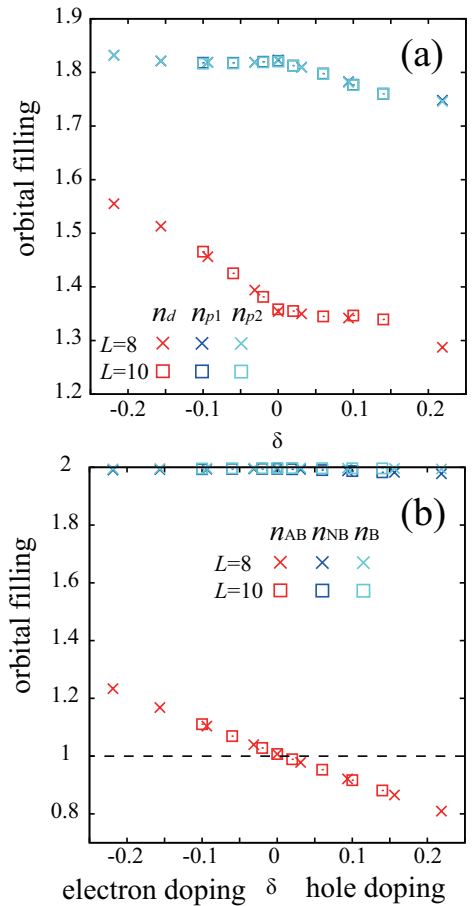


FIG. 19. (Color online) Doping dependence of the occupation number of the Cu $x^2 - y^2$ and O $2p$ orbitals in La calculated by the VMC. (a) Orbital occupation in the basis of $d_{x^2-y^2}$ and $2p_\sigma$ atomic-like Wannier orbitals (b) Orbital occupation in the basis of bonding, nonbonding and antibonding Wannier orbitals, which represents three diagonalized bands in Fig. 16, respectively.

4. Strong hybridization of p , $d_{3z^2-r^2}$ and $d_{x^2-y^2}$ orbitals in the La compound

If we try to derive a single-band Hamiltonian in a similar way to the Hg compound, one encounters a difficulty, where strongly hybridizing $d_{3z^2-r^2}$ and the antibonding band constructed from the $d_{x^2-y^2}$ and p_σ orbitals generate substantial off-diagonal self-energy between the $d_{3z^2-r^2}$ and the anti-bonding bands. However, when we derive the effective one-band Hamiltonian, the entanglement between the anti-bonding and the $d_{3z^2-r^2}$ orbitals has to be disentangled and the off-diagonal part of the self-energy has to be ignored. If only the diagonal self-energy for the anti-bonding band is retained, this truncation results in unphysical wiggly behavior of the bands, which is much more serious than the case of the cGW-SIC discussed in Ref.22. This suggests that the quantitatively precise estimate of the electronic properties must be estimated by including the $d_{3z^2-r^2}$ orbital

degrees of freedom in the effective Hamiltonian. Therefore we do not derive the effective single-band Hamiltonian for the La compound.

When we attempt to derive the effective two-band Hamiltonian, the disentanglement and elimination of the non-bonding and anti-bonding bands and resultant neglect of the off-diagonal self-energy involving the bonding/non-bonding electrons again induces weird wavy structure in the two bands, suggesting the necessity to include the bonding/nonbonding states. Therefore, from the obtained band structure, the reasonable effective Hamiltonian can be obtained only for three-band Hamiltonian or four-band Hamiltonian including all the e_g and p_σ orbitals on the present level of cGW-SIC+LRFB.

IV. CONCLUSION AND OUTLOOK

We have derived three-types (three-band, two-band and one-band) of effective Hamiltonians for the $\text{HgBa}_2\text{CuO}_4$ and three-band effective Hamiltonian for La_2CuO_4 beyond the cGW-SIC effective Hamiltonians derived in Ref.22 by improving the treatment of the inter-band Hartree energy. More complete effective Hamiltonian parameters including the transfers and interactions at farther distances are listed in Tables in Supplementary Materials.

The necessity of this improvement is clear in our estimates of the Mott gap and antiferromagnetic ordered moment, if one wishes realistic estimates with predictive power. In other words, quantitative accuracy of our derived Hamiltonians by the cGW-SIC+LRFB (or cGW-SIC+ $\Delta\mu$) is proven from our VMC solution of the three-band effective Hamiltonian for the La compound: The Mott gap estimated as 2eV and $0.6 \mu_B$ for the antiferromagnetic ordered moment are in good agreement with the experimental results of La_2CuO_4 . Although the cuprate compounds have rather complicated band structure with entanglement, the present MACE scheme offers a reasonably accurate effective Hamiltonian for the purpose of understanding physics of copper oxide superconductors.

The obtained Hamiltonians will further serve to clarify physical properties of these copper oxide superconductors, particularly for carrier doped cases, where the mechanism of high- T_c superconductivity remains to be a grand challenge in condensed matter physics. We will discuss physics and properties of carrier doped cases including superconducting properties in a separate publication.

Appendix A: Rigidity of orbital filling

To examine the rigidity of the orbital occupations, we estimate the energy cost to change the orbital occupation by employing the following simple charge diagonal part

of Coulomb energy,

$$V_C = \frac{v_d}{2} n_d^2 + 2v'_d n_d^2 + \frac{1}{2} v_p (n_{p1}^2 + n_{p2}^2) + v'_p n_{p1} n_{p2} + v_{d,p} n_d (n_{p1} + n_{p2}) - \mu_d n_d - \mu_p (n_{p1} + n_{p2}), \quad (\text{A1})$$

where the bare intra-orbital onsite Coulomb interaction between two electrons at the $d_{x^2-y^2}$ ($2p_\sigma$) orbital is denoted by v_d (v_p) and the bare onsite inter-orbital Coulomb interaction between electrons at the $d_{x^2-y^2}$ and $2p_\sigma$ is $v_{d,p}$ and v'_d and v'_p are nearest-neighbor intra-orbital interaction of the $d_{x^2-y^2}$ and $2p_\sigma$ orbitals, respectively. Here, we take into account only up to the nearest-neighbor interaction, because they are the dominant terms.

In this analysis, we only take into account the atomic Coulomb repulsions of the Cu $x^2 - y^2$ and O $2p$, because the interaction between a $d_{x^2-y^2}$ or $2p$ electron and an electron at other orbitals are considered in the chemical potential μ_d and μ_p provided that the levels of other orbitals are far from the Fermi level and their fillings are rigidly full or empty. Of course, in μ_d and μ_p , the potential from the nuclei is also included.

Under the constraint $n_d + 2n_p = 5$, and $n_p = n_{p1} = n_{p2}$, the Coulomb energy is rewritten as a function of n_d only, as

$$V_C = A n_d^2 + B n_d + C, \quad (\text{A2})$$

where A and B are

$$A = \frac{v_d}{2} + 2v'_d + \frac{v_p + 2v'_p}{4} - v_{d,p}, \quad (\text{A3})$$

$$B = \frac{5(v_p + 2v'_p)}{2} + 5v_{d,p} - \mu_d + \mu_p \quad (\text{A4})$$

and C is a constant. By taking $\delta n_d = n_d - N_d$, one obtains

$$V_C = A \delta n_d^2 + (2N_d + B) \delta n_d + C', \quad (\text{A5})$$

where $C' = A N_d^2 + B N_d + C$. Therefore, when V_C has the minimum at N_d , the coefficient of the linear term, $2N_d + B = 0$ is required. Then

$$V_C = A(n_d - N_d)^2 + C', \quad (\text{A6})$$

is obtained. When the relative filling between n_d and n_p changes, the energy cost is given by Eq.(A6).

Suppose this interaction energy gives the minimum at $N_d = 1.437$ as it is estimated by the full GW calculation (see Table I). The effect of strong correlation on the orbital occupation beyond the GW approximation can be roughly estimated from the solution of the mVMC within the effective three-band Hamiltonian of Hg compound with the parameters listed in Table I. The mVMC energy for several choices of lattice sizes is plotted in Fig. 20. Since the size dependence is small, we employ $L = 10$ result, as the thermodynamic limit. Strong correlation effects makes the d -orbital filling smaller from the GW value, $n_d = 1.437$ to 1.32.

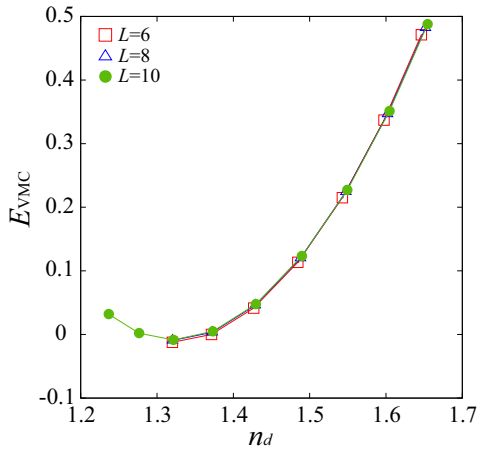


FIG. 20. (Color online) n_d dependence of total energy per site of the three-band effective Hamiltonian for the Hg compound estimated by the mVMC calculation. The obtained energy has the minimum at $n_d = 1.32$. Here, we added a constant in the energy so as to make the minimum energy zero.

Then although it is not a rigorous treatment, the rigidity of the orbital occupation is roughly estimated by adding the VMC energy E_{VMC} to the bare Coulomb energy given by Eq.(A6) with $A \simeq 20.9$ eV as can be estimated in the present paper for $\text{HgBa}_2\text{CuO}_4$ (see Table I). This means that electrons in the low-energy degrees of freedom follows the low-energy effective Hamiltonian under the parabolic potential given by Eq.(A6). Namely, the rigidity of the orbital occupation is roughly estimated by the shift of the minimum from N_d when we add the energy calculated from the solution of the low-energy effective Hamiltonian defined before the level renormalization.

The *ab initio* three-band effective Hamiltonian for the Hg compound with the parameters listed in Table VIII for cGW-SIC was solved by the mVMC. The resultant energy E_{VMC} is plotted in Fig. 21. When we plot $V_C + E_{\text{VMC}}$, n_d which gives the minimum value shifts from the minimum of V_C $n_d = 1.437$ to 1.415 with the amount 0.022 as one sees in Fig. 21. This little change proves the rigidity of the orbital filling n_d estimated by the GW approximation and justifies the present treatment to fix the orbital occupation determined from the DFT or GW approximation.

The self-consistent dynamical mean-field treatment was formulated by taking account of correlation-induced changes to the total charge density to impose the self-consistency for the charge density⁵⁵. It was applied to thin films of SrVO_3 and the self-consistent GW treatment shows that the orbital occupation of d_{xy} and d_{yz}/d_{zx} orbitals recovers to values similar to the DFT estimates.^{56,57} This again endorses the rigidity of the orbital occupation.

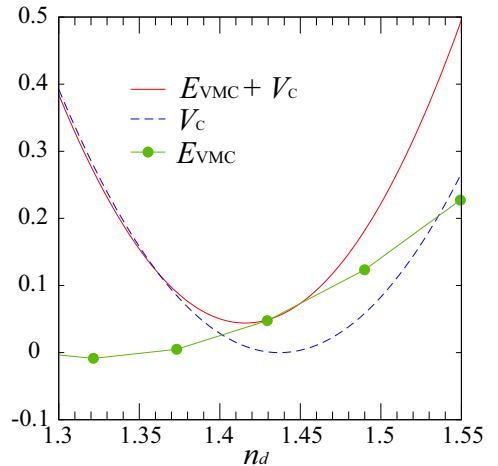


FIG. 21. (Color online) Comparison of n_d dependence of Coulomb energy V_C , E_{VMC} and $V_C + E_{\text{VMC}}$. Here, the minimum of V_C is taken to be zero by adding a constant to V_C .

ACKNOWLEDGMENTS

They are indebted to Takashi Miyake for his advice. The authors acknowledge Terumasa Tadano, Yusuke Nomura and Kota Ido for useful discussions. This work is financially supported by the MEXT HPCI Strategic Programs, and the Creation of New Functional Devices and High-Performance Materials to Support Next Generation Industries (CDMSI). This work was also supported by a Grant-in-Aid for Scientific Research (Nos. 16H06345 and 16K17746) from MEXT, Japan. TM was supported

by Building of Consortia for the Development of Human Resources in Science and Technology from the MEXT of Japan. TO was supported by a Grant-in-Aid for Scientific Research No.18K13477. The simulations were partially performed on the K computer provided by the RIKEN Advanced Institute for Computational Science under the HPCI System Research project (the project number hp170263 and hp180170). The calculations were also performed on computers at the Supercomputer Center, Institute for Solid State Physics, University of Tokyo.

-
- ¹ Bednortz and A Müller, Z. Phys. **87**, 195144 (1986).
² J. M. Tranquada, J. D. Axe, N. Ichikawa, A. R. Moodenbaugh, Y. Nakamura, and S. Uchida, Phys. Rev. Lett. **78**, 338 (1997).
³ K. Yamada, *et al.*, Phys. Rev. B **57**, 6165 (1998).
⁴ G. Ghiringhelli, *et al.*, Science **337**, 821 (2012).
⁵ W. Tabis, *et al.*, Nat. Commun. **5**, 5875 (2014).
⁶ R. Comin, *et al.*, Science **347**, 1335 (2015).
⁷ E. M. Forgan, *et al.*, Nat. Commun. **6**, 10064 (2015).
⁸ Y. Y. Peng, *et al.*, Phys. Rev. B **94**, 184511 (2016).
⁹ H. Eduardo, *et al.*, Science **343**, 393 (2014).
¹⁰ K. Fujita, *et al.*, Proc. Natl. Acad. Sci. USA **111**, E3026 (2014).
¹¹ A. Mesaros, *et al.*, Proc. Natl. Acad. Sci. USA **113**, 12661 (2016).
¹² B. Keimer, *et al.*, Nature **518**, 179 (2015).
¹³ R. Comin and A. Damascelli, Annu. Rev. Condens. Matter Phys. **7**, 369 (2016).
¹⁴ S. R. White and D. J. Scalapino, Phys. Rev. B **61**, 6320 (2000).
¹⁵ M. Capone and G. Kotliar, Phys. Rev. B **74**, 054513 (2006).
¹⁶ T. Misawa and M. Imada, Phys. Rev. B **90**, 115137 (2014).
¹⁷ P. Corboz, T. M. Rice, and M. Troyer, Phys. Rev. Lett. **113**, 046402 (2014).
¹⁸ J. Otsuki, H. Hafermann, and A. I. Lichtenstein, Phys. Rev. B **90**, 235132 (2014).
¹⁹ H.-H. Zhao, K. Ido, S. Morita, and M. Imada, Phys. Rev. B **96**, 085103 (2017).
²⁰ B.-X. Zheng, C.-M. Chung, P. Corboz, G. Ehlers, M.-P. Qin, R. M. Noack, H. Shi, S. R. White, S. Zhang, and G. K.-L. Chan, Science **358**, 1155 (2017).
²¹ K. Ido, T. Ohgoe and M. Imada, Phys. Rev. B **97**, 045138 (2018).
²² M. Hirayama, Y. Yamaji, T. Misawa, and M. Imada, Phys. Rev. B **98**, 134501 (2018).
²³ M. Imada and T. Miyake, J. Phys. Soc. Jpn. **79**, 112001 (2010).
²⁴ M. Hirayama, T. Miyake, and M. Imada, Phys. Rev. B **87**, 195144 (2013).
²⁵ M. Hirayama, T. Miyake, M. Imada and S. Biermann, Phys. Rev. B **96**, 075102 (2017).
²⁶ M. S. Hybertsen, E. B. Stechel, M. Schluter, and D. R. Jennison, Phys. Rev. B **41**, 11068 (1990).
²⁷ V.I. Anisimov, M.A. Korotin, I.A. Nekrasov, Z.V. Pchelkina, S. Sorella, Phys. Rev. B **66**, 100502(R) (2002).
²⁸ Hirofumi Sakakibara, Katsuhiko Suzuki, Hidetomo Usui, Satoaki Miyao, Isao Maruyama, Koichi Kusakabe, Ryotaro Arita, Hideo Aoki, and Kazuhiko Kuroki, Phys. Rev. B **89**, 224505 (2014).
²⁹ M. S. Hybertsen and S. G. Louie, Phys. Rev. B **34**, 5390 (1986).
³⁰ F. Aryasetiawan, J. M. Tomczak, T. Miyake, and R. Sakuma, Phys. Rev. Lett. **102**, 176402 (2009).
³¹ C. Gros, Ann. Phys. **53**, 189 (1989).
³² D. Tahara and M. Imada, J. Phys. Soc. Jpn. **77**, 114701 (2008).
³³ T. Misawa and M. Imada, Phys. Rev. B **90**, 115137 (2014).
³⁴ T. Misawa, S. Morita, K. Yoshimi, M. Kawamura, Y. Motoyama, K. Ido, T. Ohgoe, M. Imada, T. Kato, Comp. Phys. Commun. **235**, 447 (2019).
³⁵ <https://ma.issp.u-tokyo.ac.jp/en/app/518>.
³⁶ M. C. Gutzwiller, Phys. Rev. Lett. **10**, 159 (1963).
³⁷ R. Jastrow, Phys. Rev. **98**, 1479 (1955).
³⁸ P. Ring and P. Schuck, *The Nuclear Many-Body Problem* (Springer-Verlag Berlin Heidelberg New York, 2004).
³⁹ S. Sorella, Phys. Rev. B **64**, 024512 (2001).
⁴⁰ S. Putilin, E. Antipov, O. Chamaisssem, and M. Marezio, Nature **362**, 226 (1993).
⁴¹ J. D. Jorgensen, H. B. Schuttler, D. G. Hinks, D.W. Capone, K. Zhang, M. B. Brodsky, and D. J. Scalapino, Phys. Rev. Lett. **58**, 1024 (1987).
⁴² M. Methfessel, M. van Schilfhaarde, and R. A. Casali, in *Lecture Notes in Physics*, Vol. 535, edited by H. Dreyse (Springer-Verlag, Berlin., 2000).
⁴³ D. M. Ceperley and B. J. Alder, Phys. Rev. Lett. **45**, 566 (1980).
⁴⁴ M. van Schilfhaarde, T. Kotani, and S. V. Faleev, Phys. Rev. B **74**, 245125 (2006).
⁴⁵ T. Miyake, F. Aryasetiawan, and M. Imada, Phys. Rev. B **80**, 155134 (2009).
⁴⁶ T. Miyake, K. Nakamura, R. Arita and M. Imada, J. Phys. Soc. Jpn. **79**, 044705 (2010).
⁴⁷ T. Misawa, K. Nakamura, and M. Imada, J. Phys. Soc. Jpn. **80**, 023704 (2011).
⁴⁸ A. W. Sandvik, Phys. Rev. B, **56**, 11678 (1997).
⁴⁹ M. A. Kastner, R. J. Birgeneau, G. Shirane, and Y. Endoh, Rev. Mod. Phys., **70**, 897 (1998).
⁵⁰ J. Zaanen, G. A. Sawatzky, and J. W. Allen, Phys. Rev. Lett. **55**, 418 (1985).
⁵¹ P. W. Anderson *The Theory of Superconductivity in the High-T_c Cuprate Superconductors* (Princeton University Press, 1997).
⁵² K.Yamada, E.Kudo, Y.Endoh, Y.Hidaka, M.Oda,

- M.Suzuki and T.Murakami, Solid State Commun. **64** 753 (1987).
- ⁵³ S. Uchida, T. Ido, H. Takagi, T. Arima, Y. Tokura, and S. Tajima, Phys. Rev. B **43**, 7942 (1991).
- ⁵⁴ In the Supplemental Material, the complete tables of the transfer integrals and effective interactions are given in the cGW-SIC+ $\Delta\mu$ for the three-band Hamiltonian and cGW-SIC+LRFB for the three-, two-, and one-band Hamiltonian.
- ⁵⁵ L.V. Pourovskii, B. Amadon, S. Biermann, A. Georges, Phys. Rev. B **76**, 235101 (2007).
- ⁵⁶ S. Bhandary, E. Assmann, M. Aichhorn, and K. Held, Phys. Rev. B **94**, 155131 (2016).
- ⁵⁷ M. Schüler, O. E. Peil, G. J. Kraberger, R. Pordzik, M. Marsman, G. Kresse, T. O. Wehling and M. Aichhorn, J. Phys.: Condens. Matter **30**, 475901 (2018)

TABLE I. Transfer integrals and effective interactions for three-band Hamiltonian of $\text{HgBa}_2\text{CuO}_4$ (in eV). We show the transfer integral in the cGW-SIC+ $\Delta\mu$ as well as that in the GWA for comparison, while the effective interaction is the result of the cRPA. The data for the cGW-SIC+ $\Delta\mu$ except for the orbital level of p_1 and p_2 are taken from Table IV of Ref.22 obtained by the cGW-SIC. For the p_1 and p_2 levels, $\Delta_{dp} = 1$ eV is added to the level in Ref.22. v and J_v represent the bare Coulomb and exchange interactions, respectively. $U(0)$ and $J(0)$ represent the static values of the effective Coulomb and exchange interactions, respectively (at $\omega = 0$). The index 'n' and 'nn' represent the nearest, $[1,0,0]$ and the next-nearest sites $[1,1,0]$ respectively. The occupation number in the GWA is also given in the bottom column "occu.(GWA)" in this Table. The parameters for further neighbor transfer integrals and interactions by the cGW-SIC+ $\Delta\mu$ are given in the Supplemental Material⁵⁴.

$t(\text{GWA})$	(0, 0, 0)			(1, 0, 0)			(1, 1, 0)			(2, 0, 0)		
	$x^2 - y^2$	p_1	p_2	$x^2 - y^2$	p_1	p_2	$x^2 - y^2$	p_1	p_2	$x^2 - y^2$	p_1	p_2
$x^2 - y^2$	-1.597	-1.184	1.184	-0.014	-0.026	-0.016	0.020	0.004	-0.004	0.002	-0.005	-0.002
p_1	-1.184	-3.909	-0.659	1.184	0.111	0.659	-0.016	0.039	0.003	0.026	-0.008	0.003
p_2	1.184	-0.659	-3.909	-0.016	-0.003	-0.061	0.016	0.003	0.039	-0.002	0.006	-0.004
$t(\text{cGW-SIC})$	(0, 0, 0)			(1, 0, 0)			(1, 1, 0)			(2, 0, 0)		
	$x^2 - y^2$	p_1	p_2	$x^2 - y^2$	p_1	p_2	$x^2 - y^2$	p_1	p_2	$x^2 - y^2$	p_1	p_2
$x^2 - y^2$	-1.696	-1.257	1.257	-0.012	-0.033	-0.056	0.021	-0.012	0.012	-0.012	0.004	-0.003
p_1	-1.257	-4.112	-0.751	1.257	0.181	0.751	-0.056	0.054	0.004	0.033	-0.006	0.004
p_2	1.257	-0.751	-4.112	-0.056	-0.004	-0.060	0.056	0.004	0.054	-0.003	0.001	-0.004
$t(\text{cGW-SIC}+\Delta\mu)$	(0, 0, 0)			(1, 0, 0)			(1, 1, 0)			(2, 0, 0)		
	$x^2 - y^2$	p_1	p_2	$x^2 - y^2$	p_1	p_2	$x^2 - y^2$	p_1	p_2	$x^2 - y^2$	p_1	p_2
$x^2 - y^2$	-1.696	-1.257	1.257	-0.012	-0.033	-0.056	0.021	-0.012	0.012	-0.012	0.004	-0.003
p_1	-1.257	-3.112	-0.751	1.257	0.181	0.751	-0.056	0.054	0.004	0.033	-0.006	0.004
p_2	1.257	-0.751	-3.112	-0.056	-0.004	-0.060	0.056	0.004	0.054	-0.003	0.001	-0.004
	v			$U(0)$			J_v			$J(0)$		
	$x^2 - y^2$	p_1	p_2	$x^2 - y^2$	p_1	p_2	$x^2 - y^2$	p_1	p_2	$x^2 - y^2$	p_1	p_2
$x^2 - y^2$	28.821	8.010	8.010	8.837	1.985	1.985		0.063	0.063		0.048	0.048
p_1	8.010	17.114	5.319	1.985	5.311	1.210	0.063		0.041	0.048	-	0.020
p_2	8.010	5.319	17.114	1.985	1.210	5.311	0.063	0.041		0.048	0.020	
	v_n			$V_n(0)$			v_{nn}			$V_{nn}(0)$		
	$x^2 - y^2$	p_1	p_2	$x^2 - y^2$	p_1	p_2	$x^2 - y^2$	p_1	p_2	$x^2 - y^2$	p_1	p_2
$x^2 - y^2$	3.798	8.010	3.339	0.804	1.985	0.650	2.706	3.339	3.339	0.380	0.545	0.544
p_1	2.577	3.877	2.417	0.499	0.847	0.450	2.172	2.678	2.417	0.286	0.415	0.356
p_2	3.339	5.319	3.601	0.650	1.210	0.705	2.172	2.417	2.678	0.286	0.356	0.414
occu.(GWA)	$x^2 - y^2$	p_1	p_2									
	1.437	1.781	1.781									

TABLE II. Transfer integrals and effective interactions for three-band Hamiltonian of $\text{HgBa}_2\text{CuO}_4$ (in eV). Both the transfer integrals and the effective interactions are calculated based on the GW+LRFB band structure. Transfer integrals denoted by GW+LRFB are obtained from the Wannier orbital constructed to fit the GW+LRFB band structure. On the other hand, transfer integrals denoted as cGW-SIC+LRFB is obtained by the cGW-SIC procedure using the GW+LRFB bandstructure/Green's functions. The effective interactions are the result of the cRPA applied to the GW+LRFB Green's functions. v and J_v represent the bare Coulomb and exchange interactions, respectively. $U(0)$ and $J(0)$ represent the static values of the effective Coulomb and exchange interactions, respectively (at $\omega = 0$). The index 'n' and 'nn' represent the nearest, [1,0,0] and the next-nearest sites [1,1,0] respectively. The occupation number in the GWA is also given in the bottom column "occ.(GWA)" in this Table. The parameters for further neighbor transfer integrals and interactions by the cGW-SIC+LRFB are given in the Supplemental Material⁵⁴.

$t(\text{GW+LRFB})$	(0, 0, 0)			(1, 0, 0)			(1, 1, 0)			(2, 0, 0)		
	$x^2 - y^2$	p_1	p_2	$x^2 - y^2$	p_1	p_2	$x^2 - y^2$	p_1	p_2	$x^2 - y^2$	p_1	p_2
$x^2 - y^2$	-2.105	-1.189	1.189	-0.014	-0.027	-0.013	0.020	0.006	-0.006	0.002	-0.006	-0.003
p_1	-1.189	-3.587	-0.680	1.189	0.108	0.680	-0.013	0.034	0.006	0.027	-0.013	0.006
p_2	1.189	-0.680	-3.587	-0.013	-0.006	-0.063	0.013	0.006	0.0394	-0.003	0.006	-0.005
$t(\text{cGW-SIC+LRFB})$	(0, 0, 0)			(1, 0, 0)			(1, 1, 0)			(2, 0, 0)		
	$x^2 - y^2$	p_1	p_2	$x^2 - y^2$	p_1	p_2	$x^2 - y^2$	p_1	p_2	$x^2 - y^2$	p_1	p_2
$x^2 - y^2$	-1.801	-1.261	1.261	-0.014	-0.034	-0.056	0.023	-0.011	0.012	-0.012	0.004	-0.004
p_1	-1.261	-3.975	-0.753	1.261	0.183	0.753	-0.057	0.053	0.007	0.034	-0.009	0.007
p_2	1.261	-0.753	-3.975	-0.057	-0.007	-0.060	0.056	0.007	0.053	-0.004	0.001	-0.006
	v			$U(0)$			J_v			$J(0)$		
	$x^2 - y^2$	p_1	p_2	$x^2 - y^2$	p_1	p_2	$x^2 - y^2$	p_1	p_2	$x^2 - y^2$	p_1	p_2
$x^2 - y^2$	28.821	8.010	8.010	8.986	2.053	2.053		0.063	0.063		0.048	0.048
p_1	8.010	17.114	5.319	2.053	5.404	1.253	0.063		0.041	0.048		0.020
p_2	8.010	5.319	17.114	2.053	1.253	5.404	0.063	0.041		0.048	0.020	
	v_n			$V_n(0)$			v_{nn}			$V_{nn}(0)$		
	$x^2 - y^2$	p_1	p_2	$x^2 - y^2$	p_1	p_2	$x^2 - y^2$	p_1	p_2	$x^2 - y^2$	p_1	p_2
$x^2 - y^2$	3.798	8.010	3.339	0.844	2.053	0.681	2.706	3.339	3.339	0.513	0.681	0.681
p_1	2.577	3.877	2.417	0.525	0.887	0.473	2.172	2.678	2.417	0.404	0.535	0.473
p_2	3.339	5.319	3.601	0.681	1.253	0.736	2.172	2.417	2.678	0.405	0.473	0.535
occ.(GWA)	$x^2 - y^2$	p_1	p_2									
	1.437	1.781	1.781									

TABLE III. Transfer integral and effective interaction in two-band Hamiltonian for $\text{HgBa}_2\text{CuO}_4$ (in eV). We show the transfer integral in the cGW-SIC and also in the GWA for comparison. The transfer integrals denoted as GWA are calculated from the Wannier orbitals constructed to fit the GW band structure. The transfer integrals denoted as cGW-SIC are calculated from the cGW procedure applied to the GWA band structure/Green's functions. The effective interaction is the result of the cRPA applied to the GWA Green's functions. v and J_v represent the bare Coulomb interaction/exchange interactions respectively. $U(0)$ and $J(0)$ represent the static values of the effective Coulomb interaction/exchange interactions (at $\omega = 0$). The data are the same as and taken from Table II of Ref.22.

$t(\text{GWA})$	(0, 0, 0)		(1, 0, 0)		(1, 1, 0)		(2, 0, 0)	
	$3z^2 - r^2$		$x^2 - y^2$		$3z^2 - r^2$		$x^2 - y^2$	
$3z^2 - r^2$	-2.282	0.000	-0.018	0.084	-0.006	0.000	-0.003	0.010
$x^2 - y^2$	0.000	0.144	0.084	-0.453	0.000	0.074	0.010	-0.051
$t(\text{cGW-SIC})$	(0, 0, 0)		(1, 0, 0)		(1, 1, 0)		(2, 0, 0)	
	$3z^2 - r^2$		$x^2 - y^2$		$3z^2 - r^2$		$x^2 - y^2$	
$3z^2 - r^2$	-3.811	0.000	0.013	0.033	-0.003	0.000	0.000	0.002
$x^2 - y^2$	0.000	0.197	0.033	-0.426	0.000	0.102	0.002	-0.048
	v		$U(0)$		J_v		$J(0)$	
	$3z^2 - r^2$		$x^2 - y^2$		$3z^2 - r^2$		$x^2 - y^2$	
$3z^2 - r^2$	24.348	18.672	6.922	3.998	0.808		0.726	
$x^2 - y^2$	18.672	17.421	3.998	4.508	0.808		0.726	
	v_n		$V_n(0)$		v_{nn}		$V_{nn}(0)$	
	$3z^2 - r^2$		$x^2 - y^2$		$3z^2 - r^2$		$x^2 - y^2$	
$3z^2 - r^2$	3.669	3.922	0.764	0.833	2.657	2.696	0.486	0.502
$x^2 - y^2$	3.922	4.155	0.833	0.901	2.696	2.749	0.502	0.522
occ.(GWA)	$3z^2 - r^2$		$x^2 - y^2$					
	1.992	1.008						

TABLE IV. Transfer integrals and effective interactions for two-band Hamiltonian of $\text{HgBa}_2\text{CuO}_4$ (in eV). Both the transfer integrals and the effective interactions are calculated based on the GW+LRFB band structure and the GW+LRFB Green's functions. The transfer integral denoted as GW+LRFB is obtained from the Wannier orbitals constructed to fit this GW+LRFB band structure. On the other hand, the transfer integrals denoted as cGW-SIC+LRFB is obtained by the cGW-SIC+LRFB procedure, where the cGW-SIC is applied to the GW+LRFB band structure/Green's functions. The effective interaction is the result of the cRPA obtained by using the GW+LRFB Green's functions. v and J_v represent the bare Coulomb interaction/exchange interactions respectively. $U(0)$ and $J(0)$ represent the static values of the effective Coulomb interaction/exchange interactions (at $\omega = 0$). The index 'n' and 'nn' represent the nearest unit cell $[1,0,0]$ and the next-nearest unit cell $[1,1,0]$ respectively. The occupation number in the GWA is also given in this Table. The parameters for further neighbor transfer integrals and interactions by the cGW-SIC+LRFB are given in the Supplemental Material⁵⁴.

$t(\text{GW+LRFB})$	(0, 0, 0)		(1, 0, 0)		(1, 1, 0)		(2, 0, 0)	
	$3z^2 - r^2$		$x^2 - y^2$		$3z^2 - r^2$		$x^2 - y^2$	
$3z^2 - r^2$	-2.556	0.000	0.003	0.113	-0.011	0.000	-0.006	0.012
$x^2 - y^2$	0.000	-0.109	0.113	-0.512	0.000	0.079	0.012	-0.064
$t(\text{cGW-SIC+LRFB})$	(0, 0, 0)		(1, 0, 0)		(1, 1, 0)		(2, 0, 0)	
	$3z^2 - r^2$		$x^2 - y^2$		$3z^2 - r^2$		$x^2 - y^2$	
$3z^2 - r^2$	-3.518	0.000	0.002	0.029	-0.003	0.000	-0.003	0.004
$x^2 - y^2$	0.000	0.187	0.029	-0.455	0.000	0.096	0.004	-0.040
	v		$U(0)$		J_v		$J(0)$	
	$3z^2 - r^2$		$x^2 - y^2$		$3z^2 - r^2$		$x^2 - y^2$	
$3z^2 - r^2$	21.816	17.022	5.962	3.497	0.737		0.645	
$x^2 - y^2$	17.022	16.197	3.497	4.029	0.737		0.645	
	v_n		$V_n(0)$		v_{nn}		$V_{nn}(0)$	
	$3z^2 - r^2$		$x^2 - y^2$		$3z^2 - r^2$		$x^2 - y^2$	
$3z^2 - r^2$	3.584	3.889	0.733	0.820	2.608	2.670	0.470	0.492
$x^2 - y^2$	3.889	4.194	0.820	0.911	2.670	2.755	0.492	0.520
occ.(GWA)	$3z^2 - r^2$		$x^2 - y^2$					
	1.992	1.008						

TABLE V. Transfer integral and effective interaction in one-band Hamiltonian for $\text{HgBa}_2\text{CuO}_4$ (in eV). We show the transfer integral in the cGW and also in the GWA for comparison. The transfer integrals denoted as GWA are calculated from the Wannier orbitals constructed to fit the GW band structure. The transfer integrals denoted as cGW-SIC are calculated from the cGW procedure applied to the GWA band structure/Green's functions. The effective interaction is the result of the cRPA applied to the GWA Green's functions. v and J_v represent the bare Coulomb interaction/exchange interactions respectively. $U(0)$ and $J(0)$ represent the static values of the effective Coulomb interaction/exchange interactions (at $\omega = 0$). The data are the same as and taken from Table II of Ref.22.

$t(\text{GWA})$	(0, 0, 0)	(1, 0, 0)	(1, 1, 0)	(2, 0, 0)
$x^2 - y^2$	0.164	-0.453	0.074	-0.051
$t(\text{cGW})$	(0, 0, 0)	(1, 0, 0)	(1, 1, 0)	(2, 0, 0)
$x^2 - y^2$	0.190	-0.461	0.119	-0.072
	v	$U(0)$		
$x^2 - y^2$	17.421	4.374		

TABLE VI. Transfer integrals and effective interactions for one-band Hamiltonian of $\text{HgBa}_2\text{CuO}_4$ (in eV). We show the transfer integrals obtained from the Wannier function constructed from the fitting to the GW+LRFB band structure, which are denoted as GW+LRFB. Transfer integrals obtained by the cGW procedure by using the GW+LRFB bands and Green's functions are denoted by the cGW+LRFB. Effective interaction is obtained by using cRPA applied to the GW+LRFB Green's function. v represents the bare Coulomb interaction. $U(0)$ represent the static values of the effective Coulomb interaction (at $\omega = 0$). The index 'n' and 'nn' represent the nearest unit cell $[1,0,0]$ and the next-nearest unit cell $[1,1,0]$ respectively. The parameters for further neighbor transfer integrals and interactions by the cGW-SIC+LRFB are given in the Supplemental Material⁵⁴.

$t(\text{GW+LRFB})$	$(0, 0, 0)$	$(1, 0, 0)$	$(1, 1, 0)$	$(2, 0, 0)$		
$x^2 - y^2$	-0.111	-0.512	0.082	-0.066		
$t(\text{cGW+LRFB})$	$(0, 0, 0)$	$(1, 0, 0)$	$(1, 1, 0)$	$(2, 0, 0)$		
$x^2 - y^2$	0.229	-0.509	0.127	-0.077		
	v	$U(0)$	v_n	$V_n(0)$	v_{nn}	$V_{nn}(0)$
$x^2 - y^2$	16.197	3.846	4.194	0.834	2.755	0.460

TABLE VII. Summary of effective Hamiltonian parameters for $\text{HgBa}_2\text{CuO}_4$ in the cGW-SIC+LRFB (in eV). We show the transfer integral calculated from the GW as well as that calculated from the GW-SIC+LRFB procedure. t and t' for one- and two-band Hamiltonians are for nearest and next nearest-neighbor transfers between Cu $3d$ orbitals, respectively. Onsite and nearest-neighbor interactions U and V , respectively for Cu $3d$ orbitals are given as well. The orbital level is given by ϵ_X with $X = x^2 - y^2$ or $3z^2 - r^2$. Left panel: 1-band Hamiltonians. Middle two panels: two-band Hamiltonians. Right panel: three-band Hamiltonians t_{dp} (t_{pp}) is for largest nearest-neighbor transfer between Cu $3d_{x^2-y^2}$ and O $2p_\sigma$ (two O $2p_\sigma$) orbitals. Onsite (U) and nearest-neighbor (V) interactions for Cu $3d_{x^2-y^2}$ and O $2p_\sigma$ are given as well. The level difference between $3d_{x^2-y^2}$ and $2p_\sigma$ is given by $\Delta\mu_{dp}$.

					from GW			from GW+LRFB			from GW		3-band	
					1-band			2-band			1-band		3-band	
					t			t			t_{dp}		1.257	
					t'			t'			t_{pp}		0.751	
					$ t'/t $			$ t'/t $			Δ_{dp}		2.416	
					U			U			U_{dd}		8.84	
					V			V			V_{dd}		0.80	
					$ U/t $			$ U/t $			V_{dp}		1.99	
					$ U_{dd}/t_{dp} $			$ U_{dd}/t_{dp} $			U_{pp}		5.31	
					$\epsilon_{x^2-y^2} - \epsilon_{3z^2-r^2}$			$\epsilon_{x^2-y^2} - \epsilon_{3z^2-r^2}$			V_{pp}		1.21	
					$\epsilon_{x^2-y^2} - \epsilon_{3z^2-r^2}$			$\epsilon_{x^2-y^2} - \epsilon_{3z^2-r^2}$			$ U_{dd}/t_{dp} $		7.03	
					from GW+LRFB 1-band			from GW+LRFB 2-band			from GW+LRFB 1-band		from GW+LRFB 3-band	
					t			t			t_{dp}		1.261	
					t'			t'			t_{pp}		0.753	
					$ t'/t $			$ t'/t $			Δ_{dp}		2.174	
					U			U			U_{dd}		8.99	
					V			V			V_{dd}		0.84	
					$ U/t $			$ U/t $			V_{dp}		2.05	
					$ U_{dd}/t_{dp} $			$ U_{dd}/t_{dp} $			U_{pp}		5.40	
					$\epsilon_{x^2-y^2} - \epsilon_{3z^2-r^2}$			$\epsilon_{x^2-y^2} - \epsilon_{3z^2-r^2}$			V_{pp}		1.25	
					$\epsilon_{x^2-y^2} - \epsilon_{3z^2-r^2}$			$\epsilon_{x^2-y^2} - \epsilon_{3z^2-r^2}$			$ U_{dd}/t_{dp} $		7.13	
from GW	1-band	t	$3z^2 - r^2$	$x^2 - y^2$	from GW+LRFB	2-band	t	$3z^2 - r^2$	$x^2 - y^2$	from GW				
t	-0.461	$3z^2 - r^2$	0.013	0.033	$3z^2 - r^2$	0.002	$3z^2 - r^2$	0.002	0.029					
		$x^2 - y^2$	0.033	-0.426	$x^2 - y^2$	0.029	$x^2 - y^2$	0.029	-0.455					
t'	0.119	t'	$3z^2 - r^2$	$x^2 - y^2$	t'	$3z^2 - r^2$	$3z^2 - r^2$	$3z^2 - r^2$	$x^2 - y^2$					
$ t'/t $	0.26		-0.003	0.000		-0.003		-0.003	0.000					
U	4.37	$x^2 - y^2$	0.000	0.102	$x^2 - y^2$	0.000	$x^2 - y^2$	0.000	0.096					
V	1.09	$ t'_{x^2-y^2}/t_{x^2-y^2} $	0.24		$ t'_{x^2-y^2}/t_{x^2-y^2} $	0.21								
$ U/t $	9.48	$\epsilon_{x^2-y^2} - \epsilon_{3z^2-r^2}$	4.01		$\epsilon_{x^2-y^2} - \epsilon_{3z^2-r^2}$	3.71								
from GW+LRFB	1-band	U	$3z^2 - r^2$	$x^2 - y^2$	from GW+LRFB	2-band	U	$3z^2 - r^2$	$x^2 - y^2$	from GW+LRFB				
t	-0.509	$3z^2 - r^2$	6.92	4.00	$3z^2 - r^2$	5.96	$3z^2 - r^2$	5.96	3.50					
		$x^2 - y^2$	4.00	4.51	$x^2 - y^2$	3.50	$x^2 - y^2$	3.50	4.03					
t'	0.127	V	$3z^2 - r^2$	$x^2 - y^2$	V	$3z^2 - r^2$	$3z^2 - r^2$	$3z^2 - r^2$	$x^2 - y^2$					
$ t'/t $	0.25		0.76	0.83		0.73		0.73	0.82					
U	3.85	$x^2 - y^2$	0.83	0.90	$x^2 - y^2$	0.82	$x^2 - y^2$	0.82	0.91					
V	0.83	$ U/t_{x^2-y^2} $	$3z^2 - r^2$	$x^2 - y^2$	$ U/t_{x^2-y^2} $	$3z^2 - r^2$	$3z^2 - r^2$	$3z^2 - r^2$	$x^2 - y^2$					
$ U/t $	7.56		16.2	9.4		13.1		13.1	7.7					
		$x^2 - y^2$	9.4	10.6	$x^2 - y^2$	7.7	$x^2 - y^2$	7.7	8.9					

TABLE VIII. Transfer integrals and effective interactions for three-band Hamiltonian of La_2CuO_4 in the cGW-SIC (in eV) as well as in the GWA. The notations are the same as Table I. The GWA and cGW-SIC data are taken from Table VII in Ref.22. The parameters for further neighbor interactions by the cGW-SIC+ $\Delta\mu$ are given in the Supplemental Material⁵⁴.

$t(\text{GWA})$	(0, 0, 0)			(1, 0, 0)			(1, 1, 0)			(2, 0, 0)		
	$x^2 - y^2$	p_1	p_2	$x^2 - y^2$	p_1	p_2	$x^2 - y^2$	p_1	p_2	$x^2 - y^2$	p_1	p_2
$x^2 - y^2$	-1.743	-1.399	1.399	-0.010	-0.012	-0.042	0.013	-0.006	0.006	-0.004	-0.000	-0.001
p_1	-1.399	-4.657	-0.659	1.399	0.120	0.659	-0.042	0.041	-0.000	0.012	-0.002	-0.000
p_2	1.399	-0.659	-4.657	-0.042	0.000	-0.011	0.042	-0.000	0.041	-0.002	0.000	-0.002
$t(\text{cGW-SIC})$	(0, 0, 0)			(1, 0, 0)			(1, 1, 0)			(2, 0, 0)		
	$x^2 - y^2$	p_1	p_2	$x^2 - y^2$	p_1	p_2	$x^2 - y^2$	p_1	p_2	$x^2 - y^2$	p_1	p_2
$x^2 - y^2$	-1.538	-1.369	1.369	0.038	-0.036	-0.028	0.025	-0.020	0.020	-0.005	0.005	0.005
p_1	-1.369	-5.237	-0.753	1.369	0.189	0.754	-0.028	0.047	0.010	0.036	-0.005	0.009
p_2	1.369	-0.753	-5.237	-0.029	-0.010	0.021	0.028	0.009	0.047	0.005	-0.002	0.002
$t(\text{cGW-SIC}+\Delta\mu)$	(0, 0, 0)			(1, 0, 0)			(1, 1, 0)			(2, 0, 0)		
	$x^2 - y^2$	p_1	p_2	$x^2 - y^2$	p_1	p_2	$x^2 - y^2$	p_1	p_2	$x^2 - y^2$	p_1	p_2
$x^2 - y^2$	-1.538	-1.369	1.369	0.038	-0.036	-0.028	0.025	-0.020	0.020	-0.005	0.005	0.005
p_1	-1.369	-2.737	-0.753	1.369	0.189	0.754	-0.028	0.047	0.010	0.036	-0.005	0.009
p_2	1.369	-0.753	-2.737	-0.029	-0.010	0.021	0.028	0.009	0.047	0.005	-0.002	0.002
	v			$U(0)$			J_v			$J(0)$		
	$x^2 - y^2$	p_1	p_2	$x^2 - y^2$	p_1	p_2	$x^2 - y^2$	p_1	p_2	$x^2 - y^2$	p_1	p_2
$x^2 - y^2$	28.784	8.246	8.246	9.612	2.680	2.680		0.065	0.065		0.049	0.049
p_1	8.246	17.777	5.501	2.680	6.128	1.861	0.065		0.036	0.049	-	0.019
p_2	8.246	5.501	17.777	2.680	1.861	6.128	0.065	0.036		0.049	0.019	
	v_n			$V_n(0)$			v_{nn}			$V_{nn}(0)$		
	$x^2 - y^2$	p_1	p_2	$x^2 - y^2$	p_1	p_2	$x^2 - y^2$	p_1	p_2	$x^2 - y^2$	p_1	p_2
$x^2 - y^2$	3.897	8.246	3.441	1.511	2.680	1.353	2.779	3.441	3.441	1.208	1.354	1.354
p_1	2.656	4.002	2.502	1.199	1.503	1.156	2.241	2.770	2.502	1.104	1.217	1.157
p_2	3.441	5.501	3.727	1.354	1.862	1.394	2.241	2.502	2.770	1.104	1.157	1.217
occ.(GWA)	$x^2 - y^2$	p_1	p_2									
	1.350	1.825	1.825									

Supplementary material for Effective Hamiltonian for cuprate superconductors derived from multi-scale *ab initio* scheme with level renormalization

S.1 DETAILS OF HAMILTONIANS

In this supplementary material, we list up the whole parameters including relatively small one-body and two-body parameters. We show all the transfer integrals when they are above 10meV. Beyond the relative distance (3,3,0) all the one-body parameters are below 10 meV. We also show two-body parameters up to the distance (3,3,0). Within the distance (3,3,0), we list up interactions only when the value is above 50 meV. Interactions for further neighbor unit-cell pairs very well follows $1/r$ dependence inferred from the list. One-body parameters in the cGW-SIC+ $\Delta\mu$ for the three-band hamiltonian of HgBa₂CuO₄ are listed in Table A and the interaction parameters are given in Tables S.2, S.3, S.4, S.5, and S.6. One-body parameters in the cGW-SIC+LRFB for the three-band hamiltonian of HgBa₂CuO₄ are listed in Table S.7 and the interaction parameters are given in Tables S.8, S.9, S.10, S.11, and S.12. The two-band hamiltonian parameters in the cGW-SIC+LRF are listed in Tables S.13, S.14, S.15, and S.16. In the same way, the one-band hamiltonian parameters are listed in Tables S.17 and S.18. The hamiltonian parameters in the cGW-SIC+ $\Delta\mu$ for the three-band hamiltonian of La₂CuO₄ are given in the same order in Tables S.19-S.23. Note that the unit cell of La₂CuO₄ has two copper atoms in the z direction.

TABLE S.1. Transfer integrals in the cGW-SIC+ $\Delta\mu$ for three-band hamiltonian of HgBa₂CuO₄ (in eV). The inter-layer hopping is omitted because its energy scale is under 10 meV.

$t(\text{cGW-SIC}+\Delta\mu)$	(0, 0, 0)			(1, 0, 0)			(1, 1, 0)			(2, 0, 0)		
	$x^2 - y^2$	p_1	p_2	$x^2 - y^2$	p_1	p_2	$x^2 - y^2$	p_1	p_2	$x^2 - y^2$	p_1	p_2
$x^2 - y^2$	-1.696	-1.257	1.257	-0.012	-0.033	-0.056	0.021	-0.012	0.012	-0.012	0.004	-0.003
p_1	-1.257	-3.112	-0.751	1.257	0.181	0.751	-0.056	0.054	0.004	0.033	-0.006	0.004
p_2	1.257	-0.751	-3.112	-0.056	-0.004	-0.060	0.056	0.004	0.054	-0.003	0.001	-0.004
	(2, 1, 0)			(2, 2, 0)			(3, 0, 0)			(3, 1, 0)		
	$x^2 - y^2$	p_1	p_2	$x^2 - y^2$	p_1	p_2	$x^2 - y^2$	p_1	p_2	$x^2 - y^2$	p_1	p_2
$x^2 - y^2$	-0.007	0.003	-0.008	0.009	-0.001	0.001	0.004	-0.002	0.001	0.003	-0.001	0.001
p_1	0.012	0.000	0.013	-0.008	0.004	-0.002	-0.002	0.000	0.000	-0.001	0.000	-0.001
p_2	0.003	-0.001	-0.003	0.008	-0.002	0.004	0.001	0.000	0.001	-0.001	0.000	0.000
	(3, 2, 0)			(3, 3, 0)								
	$x^2 - y^2$	p_1	p_2	$x^2 - y^2$	p_1	p_2						
$x^2 - y^2$	0.002	0.000	0.003	-0.006	0.002	-0.002						
p_1	0.000	0.000	-0.001	0.002	-0.001	0.000						
p_2	-0.001	0.001	0.001	-0.002	0.000	-0.001						

TABLE S.2. Diagonal effective interactions in the cGW-SIC+ $\Delta\mu$ for three-band hamiltonian of HgBa₂CuO₄ (in eV). The interactions are indexed as $\langle\phi_{\ell_1\mathbf{R}_{i_1}}\phi_{\ell_2\mathbf{R}_{i_2}}|X|\phi_{\ell_3\mathbf{R}_{i_3}}\phi_{\ell_4\mathbf{R}_{i_4}}\rangle$ ($X = v, W^r$). The orbital indices 1, 2, and 3 stand for the $x^2 - y^2$, p_1 and p_2 orbitals, respectively.

\mathbf{R}_{i_1}	ℓ_1	\mathbf{R}_{i_2}	ℓ_2	\mathbf{R}_{i_3}	ℓ_3	\mathbf{R}_{i_4}	ℓ_4	v	W^r
(0,0,0)	1	(0,0,0)	1	(0,0,0)	1	(0,0,0)	1	28.821	8.837
(0,0,0)	1	(0,0,0)	1	(0,0,0)	2	(0,0,0)	2	8.010	1.985
(0,0,0)	1	(0,0,0)	1	(0,0,0)	2	(0,0,0)	3	0.327	0.105
(0,0,0)	1	(0,0,0)	1	(0,0,0)	3	(0,0,0)	2	0.327	0.105
(0,0,0)	1	(0,0,0)	1	(0,0,0)	3	(0,0,0)	3	8.010	1.985
(0,0,0)	1	(0,0,0)	2	(0,0,0)	2	(0,0,0)	2	0.170	0.104
(0,0,0)	2	(0,0,0)	1	(0,0,0)	2	(0,0,0)	2	0.170	0.104
(0,0,0)	2	(0,0,0)	2	(0,0,0)	1	(0,0,0)	1	8.010	1.985
(0,0,0)	2	(0,0,0)	2	(0,0,0)	1	(0,0,0)	2	0.170	0.104
(0,0,0)	2	(0,0,0)	2	(0,0,0)	2	(0,0,0)	1	0.170	0.104
(0,0,0)	2	(0,0,0)	2	(0,0,0)	2	(0,0,0)	2	17.114	5.311
(0,0,0)	2	(0,0,0)	2	(0,0,0)	3	(0,0,0)	3	5.319	1.210
(0,0,0)	2	(0,0,0)	3	(0,0,0)	1	(0,0,0)	1	0.327	0.105
(0,0,0)	3	(0,0,0)	2	(0,0,0)	1	(0,0,0)	1	0.327	0.105
(0,0,0)	3	(0,0,0)	3	(0,0,0)	1	(0,0,0)	1	8.010	1.985
(0,0,0)	3	(0,0,0)	3	(0,0,0)	2	(0,0,0)	2	5.319	1.210
(0,0,0)	3	(0,0,0)	3	(0,0,0)	3	(0,0,0)	3	17.114	5.311
(0,0,0)	1	(0,0,0)	1	(1,0,0)	1	(1,0,0)	1	3.798	0.804
(0,0,0)	1	(0,0,0)	1	(1,0,0)	2	(1,0,0)	2	8.010	1.985
(0,0,0)	1	(0,0,0)	1	(1,0,0)	3	(1,0,0)	3	3.339	0.650
(0,0,0)	2	(0,0,0)	2	(1,0,0)	1	(1,0,0)	1	2.577	0.499
(0,0,0)	2	(0,0,0)	2	(1,0,0)	2	(1,0,0)	2	3.877	0.847
(0,0,0)	2	(0,0,0)	2	(1,0,0)	3	(1,0,0)	3	2.417	0.450
(0,0,0)	3	(0,0,0)	3	(1,0,0)	1	(1,0,0)	1	3.339	0.650
(0,0,0)	3	(0,0,0)	3	(1,0,0)	2	(1,0,0)	2	5.319	1.210
(0,0,0)	3	(0,0,0)	3	(1,0,0)	3	(1,0,0)	3	3.601	0.705
(0,0,0)	1	(0,0,0)	1	(1,1,0)	1	(1,1,0)	1	2.706	0.487
(0,0,0)	1	(0,0,0)	1	(1,1,0)	2	(1,1,0)	2	3.339	0.650
(0,0,0)	1	(0,0,0)	1	(1,1,0)	3	(1,1,0)	3	3.339	0.650
(0,0,0)	2	(0,0,0)	2	(1,1,0)	1	(1,1,0)	1	2.172	0.384
(0,0,0)	2	(0,0,0)	2	(1,1,0)	2	(1,1,0)	2	2.678	0.511
(0,0,0)	2	(0,0,0)	2	(1,1,0)	3	(1,1,0)	3	2.417	0.450
(0,0,0)	3	(0,0,0)	3	(1,1,0)	1	(1,1,0)	1	2.172	0.384
(0,0,0)	3	(0,0,0)	3	(1,1,0)	2	(1,1,0)	2	2.417	0.450
(0,0,0)	3	(0,0,0)	3	(1,1,0)	3	(1,1,0)	3	2.678	0.511
(0,0,0)	1	(0,0,0)	1	(2,0,0)	1	(2,0,0)	1	2.033	0.357
(0,0,0)	1	(0,0,0)	1	(2,0,0)	2	(2,0,0)	2	2.577	0.499
(0,0,0)	1	(0,0,0)	1	(2,0,0)	3	(2,0,0)	3	1.959	0.339
(0,0,0)	2	(0,0,0)	2	(2,0,0)	1	(2,0,0)	1	1.770	0.297
(0,0,0)	2	(0,0,0)	2	(2,0,0)	2	(2,0,0)	2	2.024	0.362

TABLE S.3. (Continued from Table S2.) Diagonal effective interactions in the cGW-SIC+ $\Delta\mu$ for three-band hamiltonian of $\text{HgBa}_2\text{CuO}_4$ (in eV). Notations are the same as Table S2.

(0, 0, 0) 2 (0, 0, 0) 2 (2, 0, 0) 3 (2, 0, 0) 3	1.724	0.288
(0, 0, 0) 3 (0, 0, 0) 3 (2, 0, 0) 1 (2, 0, 0) 1	1.959	0.339
(0, 0, 0) 3 (0, 0, 0) 3 (2, 0, 0) 2 (2, 0, 0) 2	2.417	0.450
(0, 0, 0) 3 (0, 0, 0) 3 (2, 0, 0) 3 (2, 0, 0) 3	1.989	0.348
(0, 0, 0) 1 (0, 0, 0) 1 (2, 1, 0) 1 (2, 1, 0) 1	1.855	0.310
(0, 0, 0) 1 (0, 0, 0) 1 (2, 1, 0) 2 (2, 1, 0) 2	2.172	0.384
(0, 0, 0) 1 (0, 0, 0) 1 (2, 1, 0) 3 (2, 1, 0) 3	1.959	0.339
(0, 0, 0) 2 (0, 0, 0) 2 (2, 1, 0) 1 (2, 1, 0) 1	1.668	0.273
(0, 0, 0) 2 (0, 0, 0) 2 (2, 1, 0) 2 (2, 1, 0) 2	1.839	0.315
(0, 0, 0) 2 (0, 0, 0) 2 (2, 1, 0) 3 (2, 1, 0) 3	1.724	0.289
(0, 0, 0) 3 (0, 0, 0) 3 (2, 1, 0) 1 (2, 1, 0) 1	1.693	0.278
(0, 0, 0) 3 (0, 0, 0) 3 (2, 1, 0) 2 (2, 1, 0) 2	1.884	0.326
(0, 0, 0) 3 (0, 0, 0) 3 (2, 1, 0) 3 (2, 1, 0) 3	1.824	0.312
(0, 0, 0) 1 (0, 0, 0) 1 (2, 2, 0) 1 (2, 2, 0) 1	1.584	0.251
(0, 0, 0) 1 (0, 0, 0) 1 (2, 2, 0) 2 (2, 2, 0) 2	1.693	0.278
(0, 0, 0) 1 (0, 0, 0) 1 (2, 2, 0) 3 (2, 2, 0) 3	1.693	0.278
(0, 0, 0) 2 (0, 0, 0) 2 (2, 2, 0) 1 (2, 2, 0) 1	1.491	0.234
(0, 0, 0) 2 (0, 0, 0) 2 (2, 2, 0) 2 (2, 2, 0) 2	1.563	0.253
(0, 0, 0) 2 (0, 0, 0) 2 (2, 2, 0) 3 (2, 2, 0) 3	1.562	0.253
(0, 0, 0) 3 (0, 0, 0) 3 (2, 2, 0) 1 (2, 2, 0) 1	1.491	0.234
(0, 0, 0) 3 (0, 0, 0) 3 (2, 2, 0) 2 (2, 2, 0) 2	1.562	0.253
(0, 0, 0) 3 (0, 0, 0) 3 (2, 2, 0) 3 (2, 2, 0) 3	1.563	0.253
(0, 0, 0) 1 (0, 0, 0) 1 (3, 0, 0) 1 (3, 0, 0) 1	1.704	0.279
(0, 0, 0) 1 (0, 0, 0) 1 (3, 0, 0) 2 (3, 0, 0) 2	1.770	0.297
(0, 0, 0) 1 (0, 0, 0) 1 (3, 0, 0) 3 (3, 0, 0) 3	1.664	0.272
(0, 0, 0) 2 (0, 0, 0) 2 (3, 0, 0) 1 (3, 0, 0) 1	1.770	0.297
(0, 0, 0) 2 (0, 0, 0) 2 (3, 0, 0) 2 (3, 0, 0) 2	1.691	0.282
(0, 0, 0) 2 (0, 0, 0) 2 (3, 0, 0) 3 (3, 0, 0) 3	1.724	0.289
(0, 0, 0) 3 (0, 0, 0) 3 (3, 0, 0) 1 (3, 0, 0) 1	1.664	0.272
(0, 0, 0) 3 (0, 0, 0) 3 (3, 0, 0) 2 (3, 0, 0) 2	1.724	0.289
(0, 0, 0) 3 (0, 0, 0) 3 (3, 0, 0) 3 (3, 0, 0) 3	1.673	0.276
(0, 0, 0) 1 (0, 0, 0) 1 (3, 1, 0) 1 (3, 1, 0) 1	1.623	0.260
(0, 0, 0) 1 (0, 0, 0) 1 (3, 1, 0) 2 (3, 1, 0) 2	1.668	0.273
(0, 0, 0) 1 (0, 0, 0) 1 (3, 1, 0) 3 (3, 1, 0) 3	1.664	0.272
(0, 0, 0) 2 (0, 0, 0) 2 (3, 1, 0) 1 (3, 1, 0) 1	1.668	0.273
(0, 0, 0) 2 (0, 0, 0) 2 (3, 1, 0) 2 (3, 1, 0) 2	1.608	0.262
(0, 0, 0) 2 (0, 0, 0) 2 (3, 1, 0) 3 (3, 1, 0) 3	1.724	0.288
(0, 0, 0) 3 (0, 0, 0) 3 (3, 1, 0) 1 (3, 1, 0) 1	1.532	0.243
(0, 0, 0) 3 (0, 0, 0) 3 (3, 1, 0) 2 (3, 1, 0) 2	1.562	0.253
(0, 0, 0) 3 (0, 0, 0) 3 (3, 1, 0) 3 (3, 1, 0) 3	1.596	0.259

TABLE S.4. (Continued from Table S3.) Diagonal effective interactions in the cGW-SIC+ $\Delta\mu$ for three-band hamiltonian of $\text{HgBa}_2\text{CuO}_4$ (in eV). Notations are the same as Table S2.

(0, 0, 0) 1 (0, 0, 0) 1 (3, 2, 0) 1 (3, 2, 0) 1	1.476	0.229
(0, 0, 0) 1 (0, 0, 0) 1 (3, 2, 0) 2 (3, 2, 0) 2	1.491	0.234
(0, 0, 0) 1 (0, 0, 0) 1 (3, 2, 0) 3 (3, 2, 0) 3	1.532	0.243
(0, 0, 0) 2 (0, 0, 0) 2 (3, 2, 0) 1 (3, 2, 0) 1	1.491	0.234
(0, 0, 0) 2 (0, 0, 0) 2 (3, 2, 0) 2 (3, 2, 0) 2	1.458	0.230
(0, 0, 0) 2 (0, 0, 0) 2 (3, 2, 0) 3 (3, 2, 0) 3	1.562	0.253
(0, 0, 0) 3 (0, 0, 0) 3 (3, 2, 0) 1 (3, 2, 0) 1	1.414	0.218
(0, 0, 0) 3 (0, 0, 0) 3 (3, 2, 0) 2 (3, 2, 0) 2	1.423	0.223
(0, 0, 0) 3 (0, 0, 0) 3 (3, 2, 0) 3 (3, 2, 0) 3	1.455	0.229
(0, 0, 0) 1 (0, 0, 0) 1 (3, 3, 0) 1 (3, 3, 0) 1	1.408	0.215
(0, 0, 0) 1 (0, 0, 0) 1 (3, 3, 0) 2 (3, 3, 0) 2	1.414	0.218
(0, 0, 0) 1 (0, 0, 0) 1 (3, 3, 0) 3 (3, 3, 0) 3	1.414	0.218
(0, 0, 0) 2 (0, 0, 0) 2 (3, 3, 0) 1 (3, 3, 0) 1	1.414	0.218
(0, 0, 0) 2 (0, 0, 0) 2 (3, 3, 0) 2 (3, 3, 0) 2	1.390	0.215
(0, 0, 0) 2 (0, 0, 0) 2 (3, 3, 0) 3 (3, 3, 0) 3	1.423	0.222
(0, 0, 0) 3 (0, 0, 0) 3 (3, 3, 0) 1 (3, 3, 0) 1	1.414	0.218
(0, 0, 0) 3 (0, 0, 0) 3 (3, 3, 0) 2 (3, 3, 0) 2	1.423	0.222
(0, 0, 0) 3 (0, 0, 0) 3 (3, 3, 0) 3 (3, 3, 0) 3	1.390	0.215
(0, 0, 0) 1 (0, 0, 0) 1 (0, 0, 1) 1 (0, 0, 1) 1	1.612	0.350
(0, 0, 0) 1 (0, 0, 0) 1 (0, 0, 1) 2 (0, 0, 1) 2	1.574	0.324
(0, 0, 0) 1 (0, 0, 0) 1 (0, 0, 1) 3 (0, 0, 1) 3	1.574	0.324
(0, 0, 0) 2 (0, 0, 0) 2 (0, 0, 1) 1 (0, 0, 1) 1	1.574	0.324
(0, 0, 0) 2 (0, 0, 0) 2 (0, 0, 1) 2 (0, 0, 1) 2	1.590	0.325
(0, 0, 0) 2 (0, 0, 0) 2 (0, 0, 1) 3 (0, 0, 1) 3	1.539	0.306
(0, 0, 0) 3 (0, 0, 0) 3 (0, 0, 1) 1 (0, 0, 1) 1	1.574	0.324
(0, 0, 0) 3 (0, 0, 0) 3 (0, 0, 1) 2 (0, 0, 1) 2	1.539	0.306
(0, 0, 0) 3 (0, 0, 0) 3 (0, 0, 1) 3 (0, 0, 1) 3	1.590	0.325
(0, 0, 0) 1 (0, 0, 0) 1 (1, 0, 1) 1 (1, 0, 1) 1	1.524	0.300
(0, 0, 0) 1 (0, 0, 0) 1 (1, 0, 1) 2 (1, 0, 1) 2	1.574	0.324
(0, 0, 0) 1 (0, 0, 0) 1 (1, 0, 1) 3 (1, 0, 1) 3	1.492	0.287
(0, 0, 0) 2 (0, 0, 0) 2 (1, 0, 1) 1 (1, 0, 1) 1	1.434	0.266
(0, 0, 0) 2 (0, 0, 0) 2 (1, 0, 1) 2 (1, 0, 1) 2	1.505	0.293
(0, 0, 0) 2 (0, 0, 0) 2 (1, 0, 1) 3 (1, 0, 1) 3	1.407	0.258
(0, 0, 0) 3 (0, 0, 0) 3 (1, 0, 1) 1 (1, 0, 1) 1	1.492	0.287
(0, 0, 0) 3 (0, 0, 0) 3 (1, 0, 1) 2 (1, 0, 1) 2	1.539	0.306
(0, 0, 0) 3 (0, 0, 0) 3 (1, 0, 1) 3 (1, 0, 1) 3	1.503	0.290
(0, 0, 0) 1 (0, 0, 0) 1 (1, 1, 1) 1 (1, 1, 1) 1	1.455	0.272
(0, 0, 0) 1 (0, 0, 0) 1 (1, 1, 1) 2 (1, 1, 1) 2	1.492	0.287
(0, 0, 0) 1 (0, 0, 0) 1 (1, 1, 1) 3 (1, 1, 1) 3	1.492	0.287
(0, 0, 0) 2 (0, 0, 0) 2 (1, 1, 1) 1 (1, 1, 1) 1	1.380	0.247

TABLE S.5. (Continued from Table S4.) Diagonal effective interactions in the cGW-SIC+ $\Delta\mu$ for three-band hamiltonian of HgBa₂CuO₄ (in eV). Notations are the same as Table S2.

(0, 0, 0) 2	(0, 0, 0) 2	(1, 1, 1) 2	(1, 1, 1) 2	1.436	0.267
(0, 0, 0) 2	(0, 0, 0) 2	(1, 1, 1) 3	(1, 1, 1) 3	1.407	0.258
(0, 0, 0) 3	(0, 0, 0) 3	(1, 1, 1) 1	(1, 1, 1) 1	1.380	0.247
(0, 0, 0) 3	(0, 0, 0) 3	(1, 1, 1) 2	(1, 1, 1) 2	1.407	0.258
(0, 0, 0) 3	(0, 0, 0) 3	(1, 1, 1) 3	(1, 1, 1) 3	1.436	0.267
(0, 0, 0) 1	(0, 0, 0) 1	(2, 0, 1) 1	(2, 0, 1) 1	1.374	0.242
(0, 0, 0) 1	(0, 0, 0) 1	(2, 0, 1) 2	(2, 0, 1) 2	1.434	0.266
(0, 0, 0) 1	(0, 0, 0) 1	(2, 0, 1) 3	(2, 0, 1) 3	1.350	0.237
(0, 0, 0) 2	(0, 0, 0) 2	(2, 0, 1) 1	(2, 0, 1) 1	1.315	0.225
(0, 0, 0) 2	(0, 0, 0) 2	(2, 0, 1) 2	(2, 0, 1) 2	1.358	0.241
(0, 0, 0) 2	(0, 0, 0) 2	(2, 0, 1) 3	(2, 0, 1) 3	1.295	0.221
(0, 0, 0) 3	(0, 0, 0) 3	(2, 0, 1) 1	(2, 0, 1) 1	1.350	0.237
(0, 0, 0) 3	(0, 0, 0) 3	(2, 0, 1) 2	(2, 0, 1) 2	1.407	0.258
(0, 0, 0) 3	(0, 0, 0) 3	(2, 0, 1) 3	(2, 0, 1) 3	1.354	0.239
(0, 0, 0) 1	(0, 0, 0) 1	(2, 1, 1) 1	(2, 1, 1) 1	1.334	0.229
(0, 0, 0) 1	(0, 0, 0) 1	(2, 1, 1) 2	(2, 1, 1) 2	1.380	0.247
(0, 0, 0) 1	(0, 0, 0) 1	(2, 1, 1) 3	(2, 1, 1) 3	1.350	0.237
(0, 0, 0) 2	(0, 0, 0) 2	(2, 1, 1) 1	(2, 1, 1) 1	1.283	0.216
(0, 0, 0) 2	(0, 0, 0) 2	(2, 1, 1) 2	(2, 1, 1) 2	1.317	0.228
(0, 0, 0) 2	(0, 0, 0) 2	(2, 1, 1) 3	(2, 1, 1) 3	1.295	0.221
(0, 0, 0) 3	(0, 0, 0) 3	(2, 1, 1) 1	(2, 1, 1) 1	1.283	0.216
(0, 0, 0) 3	(0, 0, 0) 3	(2, 1, 1) 2	(2, 1, 1) 2	1.319	0.230
(0, 0, 0) 3	(0, 0, 0) 3	(2, 1, 1) 3	(2, 1, 1) 3	1.314	0.227
(0, 0, 0) 1	(0, 0, 0) 1	(2, 2, 1) 1	(2, 2, 1) 1	1.257	0.206
(0, 0, 0) 1	(0, 0, 0) 1	(2, 2, 1) 2	(2, 2, 1) 2	1.283	0.216
(0, 0, 0) 1	(0, 0, 0) 1	(2, 2, 1) 3	(2, 2, 1) 3	1.283	0.216
(0, 0, 0) 2	(0, 0, 0) 2	(2, 2, 1) 1	(2, 2, 1) 1	1.220	0.198
(0, 0, 0) 2	(0, 0, 0) 2	(2, 2, 1) 2	(2, 2, 1) 2	1.240	0.205
(0, 0, 0) 2	(0, 0, 0) 2	(2, 2, 1) 3	(2, 2, 1) 3	1.240	0.205
(0, 0, 0) 3	(0, 0, 0) 3	(2, 2, 1) 1	(2, 2, 1) 1	1.220	0.198
(0, 0, 0) 3	(0, 0, 0) 3	(2, 2, 1) 2	(2, 2, 1) 2	1.240	0.205
(0, 0, 0) 3	(0, 0, 0) 3	(2, 2, 1) 3	(2, 2, 1) 3	1.240	0.205
(0, 0, 0) 1	(0, 0, 0) 1	(3, 0, 1) 1	(3, 0, 1) 1	1.309	0.221
(0, 0, 0) 1	(0, 0, 0) 1	(3, 0, 1) 2	(3, 0, 1) 2	1.315	0.225
(0, 0, 0) 1	(0, 0, 0) 1	(3, 0, 1) 3	(3, 0, 1) 3	1.288	0.217
(0, 0, 0) 2	(0, 0, 0) 2	(3, 0, 1) 1	(3, 0, 1) 1	1.315	0.225
(0, 0, 0) 2	(0, 0, 0) 2	(3, 0, 1) 2	(3, 0, 1) 2	1.294	0.220
(0, 0, 0) 2	(0, 0, 0) 2	(3, 0, 1) 3	(3, 0, 1) 3	1.295	0.221
(0, 0, 0) 3	(0, 0, 0) 3	(3, 0, 1) 1	(3, 0, 1) 1	1.288	0.217
(0, 0, 0) 3	(0, 0, 0) 3	(3, 0, 1) 2	(3, 0, 1) 2	1.295	0.221

TABLE S.6. (Continued from Table S5.) Diagonal and off-diagonal effective interactions in the cGW-SIC+ $\Delta\mu$ for three-band hamiltonian of $\text{HgBa}_2\text{CuO}_4$ (in eV). Notations are the same as Table S2.

(0, 0, 0) 3 (0, 0, 0) 3 (3, 0, 1) 3 (3, 0, 1) 3	1.289 0.218
(0, 0, 0) 1 (0, 0, 0) 1 (3, 1, 1) 1 (3, 1, 1) 1	1.279 0.212
(0, 0, 0) 1 (0, 0, 0) 1 (3, 1, 1) 2 (3, 1, 1) 2	1.283 0.216
(0, 0, 0) 1 (0, 0, 0) 1 (3, 1, 1) 3 (3, 1, 1) 3	1.288 0.217
(0, 0, 0) 2 (0, 0, 0) 2 (3, 1, 1) 1 (3, 1, 1) 1	1.283 0.216
(0, 0, 0) 2 (0, 0, 0) 2 (3, 1, 1) 2 (3, 1, 1) 2	1.264 0.211
(0, 0, 0) 2 (0, 0, 0) 2 (3, 1, 1) 3 (3, 1, 1) 3	1.295 0.221
(0, 0, 0) 3 (0, 0, 0) 3 (3, 1, 1) 1 (3, 1, 1) 1	1.238 0.203
(0, 0, 0) 3 (0, 0, 0) 3 (3, 1, 1) 2 (3, 1, 1) 2	1.240 0.205
(0, 0, 0) 3 (0, 0, 0) 3 (3, 1, 1) 3 (3, 1, 1) 3	1.260 0.210
(0, 0, 0) 1 (0, 0, 0) 1 (3, 2, 1) 1 (3, 2, 1) 1	1.222 0.196
(0, 0, 0) 1 (0, 0, 0) 1 (3, 2, 1) 2 (3, 2, 1) 2	1.220 0.198
(0, 0, 0) 1 (0, 0, 0) 1 (3, 2, 1) 3 (3, 2, 1) 3	1.238 0.203
(0, 0, 0) 2 (0, 0, 0) 2 (3, 2, 1) 1 (3, 2, 1) 1	1.220 0.198
(0, 0, 0) 2 (0, 0, 0) 2 (3, 2, 1) 2 (3, 2, 1) 2	1.206 0.195
(0, 0, 0) 2 (0, 0, 0) 2 (3, 2, 1) 3 (3, 2, 1) 3	1.240 0.205
(0, 0, 0) 3 (0, 0, 0) 3 (3, 2, 1) 1 (3, 2, 1) 1	1.190 0.189
(0, 0, 0) 3 (0, 0, 0) 3 (3, 2, 1) 2 (3, 2, 1) 2	1.188 0.191
(0, 0, 0) 3 (0, 0, 0) 3 (3, 2, 1) 3 (3, 2, 1) 3	1.204 0.195
(0, 0, 0) 1 (0, 0, 0) 1 (3, 3, 1) 1 (3, 3, 1) 1	1.194 0.188
(0, 0, 0) 1 (0, 0, 0) 1 (3, 3, 1) 2 (3, 3, 1) 2	1.190 0.189
(0, 0, 0) 1 (0, 0, 0) 1 (3, 3, 1) 3 (3, 3, 1) 3	1.190 0.189
(0, 0, 0) 2 (0, 0, 0) 2 (3, 3, 1) 1 (3, 3, 1) 1	1.190 0.189
(0, 0, 0) 2 (0, 0, 0) 2 (3, 3, 1) 2 (3, 3, 1) 2	1.178 0.188
(0, 0, 0) 2 (0, 0, 0) 2 (3, 3, 1) 3 (3, 3, 1) 3	1.188 0.191
(0, 0, 0) 3 (0, 0, 0) 3 (3, 3, 1) 1 (3, 3, 1) 1	1.190 0.189
(0, 0, 0) 3 (0, 0, 0) 3 (3, 3, 1) 2 (3, 3, 1) 2	1.188 0.191
(0, 0, 0) 3 (0, 0, 0) 3 (3, 3, 1) 3 (3, 3, 1) 3	1.178 0.187
(0, 1, 0) 3 (0, 0, 0) 1 (0, 1, 0) 3 (0, 1, 0) 3	0.170 0.104
(0, -1, 0) 1 (0, 0, 0) 3 (0, 0, 0) 3 (0, 0, 0) 3	0.170 0.104
(1 - 10) 2 (0, 0, 0) 3 (0, -1, 0) 1 (0, -1, 0) 1	0.327 0.105
(-110) 3 (0, 0, 0) 2 (-1, 0, 0) 1 (-1, 0, 0) 1	0.327 0.105
(0, 0, 0) 3 (0, 0, 0) 3 (0, -1, 0) 1 (0, 0, 0) 3	0.170 0.104
(0, 0, 0) 3 (0, 0, 0) 3 (0, 0, 0) 3 (0, -1, 0) 1	0.170 0.104
(0, 0, 0) 1 (0, 0, 0) 1 (0, 1, 0) 3 (1, 0, 0) 2	0.327 0.105
(0, 0, 0) 1 (0, 0, 0) 1 (1, 0, 0) 2 (0, 1, 0) 3	0.327 0.105

TABLE S.7. Transfer integrals in the cGW-SIC+LRFB for three-band hamiltonian of $\text{HgBa}_2\text{CuO}_4$ (in eV). The inter-layer hopping is omitted because its energy scale is under 10 meV.

$t(\text{cGW-SIC+LRFB})$	(0, 0, 0)			(1, 0, 0)			(1, 1, 0)			(2, 0, 0)		
	$x^2 - y^2$	p_1	p_2	$x^2 - y^2$	p_1	p_2	$x^2 - y^2$	p_1	p_2	$x^2 - y^2$	p_1	p_2
$x^2 - y^2$	-1.801	-1.261	1.261	-0.014	-0.034	-0.056	0.023	-0.011	0.012	-0.012	0.004	-0.004
p_1	-1.261	-3.975	-0.753	1.261	0.183	0.753	-0.057	0.053	0.007	0.034	-0.009	0.007
p_2	1.261	-0.753	-3.975	-0.057	-0.007	-0.060	0.056	0.007	0.053	-0.004	0.001	-0.006
	(2, 1, 0)			(2, 2, 0)			(3, 0, 0)			(3, 1, 0)		
	$x^2 - y^2$	p_1	p_2	$x^2 - y^2$	p_1	p_2	$x^2 - y^2$	p_1	p_2	$x^2 - y^2$	p_1	p_2
$x^2 - y^2$	-0.006	0.003	-0.008	0.009	-0.001	0.001	0.004	-0.002	0.001	0.002	-0.002	0.002
p_1	0.011	0.000	0.014	-0.008	0.005	-0.002	-0.002	0.000	0.000	-0.002	0.001	-0.001
p_2	0.004	-0.001	-0.003	0.008	-0.002	0.005	0.001	0.000	0.001	-0.001	0.000	0.000
	(3, 2, 0)			(3, 3, 0)								
	$x^2 - y^2$	p_1	p_2	$x^2 - y^2$	p_1	p_2						
$x^2 - y^2$	0.001	0.001	0.003	-0.006	0.002	-0.002						
p_1	0.001	0.000	-0.001	0.002	-0.002	0.001						
p_2	-0.002	0.001	0.001	-0.002	0.001	-0.002						

TABLE S.8. Diagonal effective interactions in the cGW-SIC+LRFB for three-band hamiltonian of $\text{HgBa}_2\text{CuO}_4$ (in eV). The interactions are indexed as $\langle \phi_{\ell_1 \mathbf{R}_{i_1}} \phi_{\ell_2 \mathbf{R}_{i_2}} | X | \phi_{\ell_3 \mathbf{R}_{i_3}} \phi_{\ell_4 \mathbf{R}_{i_4}} \rangle$ ($X = v, W^r$). The orbital indices 1, 2, and 3 stand for the $x^2 - y^2$, p_1 and p_2 orbitals, respectively.

\mathbf{R}_{i_1}	ℓ_1	\mathbf{R}_{i_2}	ℓ_2	\mathbf{R}_{i_3}	ℓ_3	\mathbf{R}_{i_4}	ℓ_4	v	W^r
(0,0,0)	1	(0,0,0)	1	(0,0,0)	1	(0,0,0)	1	28.821	8.986
(0,0,0)	1	(0,0,0)	1	(0,0,0)	2	(0,0,0)	2	8.010	2.053
(0,0,0)	1	(0,0,0)	1	(0,0,0)	2	(0,0,0)	3	0.327	0.107
(0,0,0)	1	(0,0,0)	1	(0,0,0)	3	(0,0,0)	2	0.327	0.107
(0,0,0)	1	(0,0,0)	1	(0,0,0)	3	(0,0,0)	3	8.010	2.053
(0,0,0)	1	(0,0,0)	2	(0,0,0)	2	(0,0,0)	2	0.170	0.105
(0,0,0)	2	(0,0,0)	1	(0,0,0)	2	(0,0,0)	2	0.170	0.105
(0,0,0)	2	(0,0,0)	2	(0,0,0)	1	(0,0,0)	1	8.010	2.053
(0,0,0)	2	(0,0,0)	2	(0,0,0)	1	(0,0,0)	2	0.170	0.105
(0,0,0)	2	(0,0,0)	2	(0,0,0)	2	(0,0,0)	1	0.170	0.105
(0,0,0)	2	(0,0,0)	2	(0,0,0)	2	(0,0,0)	2	17.114	5.404
(0,0,0)	2	(0,0,0)	2	(0,0,0)	3	(0,0,0)	3	5.319	1.253
(0,0,0)	2	(0,0,0)	3	(0,0,0)	1	(0,0,0)	1	0.327	0.107
(0,0,0)	3	(0,0,0)	2	(0,0,0)	1	(0,0,0)	1	0.327	0.107
(0,0,0)	3	(0,0,0)	3	(0,0,0)	1	(0,0,0)	1	8.010	2.053
(0,0,0)	3	(0,0,0)	3	(0,0,0)	2	(0,0,0)	2	5.319	1.253
(0,0,0)	3	(0,0,0)	3	(0,0,0)	3	(0,0,0)	3	17.114	5.404
(0,0,0)	1	(0,0,0)	1	(1,0,0)	1	(1,0,0)	1	3.798	0.844
(0,0,0)	1	(0,0,0)	1	(1,0,0)	2	(1,0,0)	2	8.010	2.053
(0,0,0)	1	(0,0,0)	1	(1,0,0)	3	(1,0,0)	3	3.339	0.681
(0,0,0)	2	(0,0,0)	2	(1,0,0)	1	(1,0,0)	1	2.577	0.525
(0,0,0)	2	(0,0,0)	2	(1,0,0)	2	(1,0,0)	2	3.877	0.887
(0,0,0)	2	(0,0,0)	2	(1,0,0)	3	(1,0,0)	3	2.417	0.473
(0,0,0)	3	(0,0,0)	3	(1,0,0)	1	(1,0,0)	1	3.339	0.681
(0,0,0)	3	(0,0,0)	3	(1,0,0)	2	(1,0,0)	2	5.319	1.253
(0,0,0)	3	(0,0,0)	3	(1,0,0)	3	(1,0,0)	3	3.601	0.736
(0,0,0)	1	(0,0,0)	1	(1,1,0)	1	(1,1,0)	1	2.706	0.513
(0,0,0)	1	(0,0,0)	1	(1,1,0)	2	(1,1,0)	2	3.339	0.681
(0,0,0)	1	(0,0,0)	1	(1,1,0)	3	(1,1,0)	3	3.339	0.681
(0,0,0)	2	(0,0,0)	2	(1,1,0)	1	(1,1,0)	1	2.172	0.404
(0,0,0)	2	(0,0,0)	2	(1,1,0)	2	(1,1,0)	2	2.678	0.535
(0,0,0)	2	(0,0,0)	2	(1,1,0)	3	(1,1,0)	3	2.417	0.473
(0,0,0)	3	(0,0,0)	3	(1,1,0)	1	(1,1,0)	1	2.172	0.405
(0,0,0)	3	(0,0,0)	3	(1,1,0)	2	(1,1,0)	2	2.417	0.473
(0,0,0)	3	(0,0,0)	3	(1,1,0)	3	(1,1,0)	3	2.678	0.535
(0,0,0)	1	(0,0,0)	1	(2,0,0)	1	(2,0,0)	1	2.033	0.377
(0,0,0)	1	(0,0,0)	1	(2,0,0)	2	(2,0,0)	2	2.577	0.525
(0,0,0)	1	(0,0,0)	1	(2,0,0)	3	(2,0,0)	3	1.959	0.358
(0,0,0)	2	(0,0,0)	2	(2,0,0)	1	(2,0,0)	1	1.770	0.315
(0,0,0)	2	(0,0,0)	2	(2,0,0)	2	(2,0,0)	2	2.024	0.382

TABLE S.9. (Continued from Table S8.) Diagonal effective interactions in the cGW-SIC+LRFB for three-band hamiltonian of $\text{HgBa}_2\text{CuO}_4$ (in eV). Notations are the same as Table S8.

(0, 0, 0) 2	(0, 0, 0) 2	(2, 0, 0) 3	(2, 0, 0) 3	1.724	0.305
(0, 0, 0) 3	(0, 0, 0) 3	(2, 0, 0) 1	(2, 0, 0) 1	1.959	0.358
(0, 0, 0) 3	(0, 0, 0) 3	(2, 0, 0) 2	(2, 0, 0) 2	2.417	0.473
(0, 0, 0) 3	(0, 0, 0) 3	(2, 0, 0) 3	(2, 0, 0) 3	1.989	0.366
(0, 0, 0) 1	(0, 0, 0) 1	(2, 1, 0) 1	(2, 1, 0) 1	1.855	0.328
(0, 0, 0) 1	(0, 0, 0) 1	(2, 1, 0) 2	(2, 1, 0) 2	2.172	0.404
(0, 0, 0) 1	(0, 0, 0) 1	(2, 1, 0) 3	(2, 1, 0) 3	1.959	0.358
(0, 0, 0) 2	(0, 0, 0) 2	(2, 1, 0) 1	(2, 1, 0) 1	1.668	0.289
(0, 0, 0) 2	(0, 0, 0) 2	(2, 1, 0) 2	(2, 1, 0) 2	1.839	0.333
(0, 0, 0) 2	(0, 0, 0) 2	(2, 1, 0) 3	(2, 1, 0) 3	1.724	0.305
(0, 0, 0) 3	(0, 0, 0) 3	(2, 1, 0) 1	(2, 1, 0) 1	1.693	0.295
(0, 0, 0) 3	(0, 0, 0) 3	(2, 1, 0) 2	(2, 1, 0) 2	1.884	0.344
(0, 0, 0) 3	(0, 0, 0) 3	(2, 1, 0) 3	(2, 1, 0) 3	1.824	0.329
(0, 0, 0) 1	(0, 0, 0) 1	(2, 2, 0) 1	(2, 2, 0) 1	1.584	0.266
(0, 0, 0) 1	(0, 0, 0) 1	(2, 2, 0) 2	(2, 2, 0) 2	1.693	0.295
(0, 0, 0) 1	(0, 0, 0) 1	(2, 2, 0) 3	(2, 2, 0) 3	1.693	0.295
(0, 0, 0) 2	(0, 0, 0) 2	(2, 2, 0) 1	(2, 2, 0) 1	1.491	0.249
(0, 0, 0) 2	(0, 0, 0) 2	(2, 2, 0) 2	(2, 2, 0) 2	1.563	0.268
(0, 0, 0) 2	(0, 0, 0) 2	(2, 2, 0) 3	(2, 2, 0) 3	1.562	0.268
(0, 0, 0) 3	(0, 0, 0) 3	(2, 2, 0) 1	(2, 2, 0) 1	1.491	0.249
(0, 0, 0) 3	(0, 0, 0) 3	(2, 2, 0) 2	(2, 2, 0) 2	1.562	0.268
(0, 0, 0) 3	(0, 0, 0) 3	(2, 2, 0) 3	(2, 2, 0) 3	1.563	0.268
(0, 0, 0) 1	(0, 0, 0) 1	(3, 0, 0) 1	(3, 0, 0) 1	1.704	0.295
(0, 0, 0) 1	(0, 0, 0) 1	(3, 0, 0) 2	(3, 0, 0) 2	1.770	0.315
(0, 0, 0) 1	(0, 0, 0) 1	(3, 0, 0) 3	(3, 0, 0) 3	1.664	0.288
(0, 0, 0) 2	(0, 0, 0) 2	(3, 0, 0) 1	(3, 0, 0) 1	1.770	0.315
(0, 0, 0) 2	(0, 0, 0) 2	(3, 0, 0) 2	(3, 0, 0) 2	1.691	0.298
(0, 0, 0) 2	(0, 0, 0) 2	(3, 0, 0) 3	(3, 0, 0) 3	1.724	0.305
(0, 0, 0) 3	(0, 0, 0) 3	(3, 0, 0) 1	(3, 0, 0) 1	1.664	0.288
(0, 0, 0) 3	(0, 0, 0) 3	(3, 0, 0) 2	(3, 0, 0) 2	1.724	0.305
(0, 0, 0) 3	(0, 0, 0) 3	(3, 0, 0) 3	(3, 0, 0) 3	1.673	0.292
(0, 0, 0) 1	(0, 0, 0) 1	(3, 1, 0) 1	(3, 1, 0) 1	1.623	0.276
(0, 0, 0) 1	(0, 0, 0) 1	(3, 1, 0) 2	(3, 1, 0) 2	1.668	0.289
(0, 0, 0) 1	(0, 0, 0) 1	(3, 1, 0) 3	(3, 1, 0) 3	1.664	0.288
(0, 0, 0) 2	(0, 0, 0) 2	(3, 1, 0) 1	(3, 1, 0) 1	1.668	0.289
(0, 0, 0) 2	(0, 0, 0) 2	(3, 1, 0) 2	(3, 1, 0) 2	1.608	0.278
(0, 0, 0) 2	(0, 0, 0) 2	(3, 1, 0) 3	(3, 1, 0) 3	1.724	0.305
(0, 0, 0) 3	(0, 0, 0) 3	(3, 1, 0) 1	(3, 1, 0) 1	1.532	0.258
(0, 0, 0) 3	(0, 0, 0) 3	(3, 1, 0) 2	(3, 1, 0) 2	1.562	0.268
(0, 0, 0) 3	(0, 0, 0) 3	(3, 1, 0) 3	(3, 1, 0) 3	1.596	0.275

TABLE S.10. (Continued from Table S9.) Diagonal effective interactions in the cGW-SIC+LRFB for three-band hamiltonian of $\text{HgBa}_2\text{CuO}_4$ (in eV). Notations are the same as Table S8.

(0, 0, 0) 1	(0, 0, 0) 1	(3, 2, 0) 1	(3, 2, 0) 1	1.476	0.243
(0, 0, 0) 1	(0, 0, 0) 1	(3, 2, 0) 2	(3, 2, 0) 2	1.491	0.249
(0, 0, 0) 1	(0, 0, 0) 1	(3, 2, 0) 3	(3, 2, 0) 3	1.532	0.258
(0, 0, 0) 2	(0, 0, 0) 2	(3, 2, 0) 1	(3, 2, 0) 1	1.491	0.249
(0, 0, 0) 2	(0, 0, 0) 2	(3, 2, 0) 2	(3, 2, 0) 2	1.458	0.244
(0, 0, 0) 2	(0, 0, 0) 2	(3, 2, 0) 3	(3, 2, 0) 3	1.562	0.268
(0, 0, 0) 3	(0, 0, 0) 3	(3, 2, 0) 1	(3, 2, 0) 1	1.414	0.232
(0, 0, 0) 3	(0, 0, 0) 3	(3, 2, 0) 2	(3, 2, 0) 2	1.423	0.236
(0, 0, 0) 3	(0, 0, 0) 3	(3, 2, 0) 3	(3, 2, 0) 3	1.455	0.243
(0, 0, 0) 1	(0, 0, 0) 1	(3, 3, 0) 1	(3, 3, 0) 1	1.408	0.228
(0, 0, 0) 1	(0, 0, 0) 1	(3, 3, 0) 2	(3, 3, 0) 2	1.414	0.232
(0, 0, 0) 1	(0, 0, 0) 1	(3, 3, 0) 3	(3, 3, 0) 3	1.414	0.232
(0, 0, 0) 2	(0, 0, 0) 2	(3, 3, 0) 1	(3, 3, 0) 1	1.414	0.232
(0, 0, 0) 2	(0, 0, 0) 2	(3, 3, 0) 2	(3, 3, 0) 2	1.390	0.229
(0, 0, 0) 2	(0, 0, 0) 2	(3, 3, 0) 3	(3, 3, 0) 3	1.423	0.236
(0, 0, 0) 3	(0, 0, 0) 3	(3, 3, 0) 1	(3, 3, 0) 1	1.414	0.232
(0, 0, 0) 3	(0, 0, 0) 3	(3, 3, 0) 2	(3, 3, 0) 2	1.423	0.236
(0, 0, 0) 3	(0, 0, 0) 3	(3, 3, 0) 3	(3, 3, 0) 3	1.390	0.228
(0, 0, 0) 1	(0, 0, 0) 1	(0, 0, 1) 1	(0, 0, 1) 1	1.612	0.360
(0, 0, 0) 1	(0, 0, 0) 1	(0, 0, 1) 2	(0, 0, 1) 2	1.574	0.337
(0, 0, 0) 1	(0, 0, 0) 1	(0, 0, 1) 3	(0, 0, 1) 3	1.574	0.336
(0, 0, 0) 2	(0, 0, 0) 2	(0, 0, 1) 1	(0, 0, 1) 1	1.574	0.337
(0, 0, 0) 2	(0, 0, 0) 2	(0, 0, 1) 2	(0, 0, 1) 2	1.590	0.339
(0, 0, 0) 2	(0, 0, 0) 2	(0, 0, 1) 3	(0, 0, 1) 3	1.539	0.320
(0, 0, 0) 3	(0, 0, 0) 3	(0, 0, 1) 1	(0, 0, 1) 1	1.574	0.336
(0, 0, 0) 3	(0, 0, 0) 3	(0, 0, 1) 2	(0, 0, 1) 2	1.539	0.320
(0, 0, 0) 3	(0, 0, 0) 3	(0, 0, 1) 3	(0, 0, 1) 3	1.590	0.338
(0, 0, 0) 1	(0, 0, 0) 1	(1, 0, 1) 1	(1, 0, 1) 1	1.524	0.313
(0, 0, 0) 1	(0, 0, 0) 1	(1, 0, 1) 2	(1, 0, 1) 2	1.574	0.337
(0, 0, 0) 1	(0, 0, 0) 1	(1, 0, 1) 3	(1, 0, 1) 3	1.492	0.300
(0, 0, 0) 2	(0, 0, 0) 2	(1, 0, 1) 1	(1, 0, 1) 1	1.434	0.279
(0, 0, 0) 2	(0, 0, 0) 2	(1, 0, 1) 2	(1, 0, 1) 2	1.505	0.307
(0, 0, 0) 2	(0, 0, 0) 2	(1, 0, 1) 3	(1, 0, 1) 3	1.407	0.271
(0, 0, 0) 3	(0, 0, 0) 3	(1, 0, 1) 1	(1, 0, 1) 1	1.492	0.300
(0, 0, 0) 3	(0, 0, 0) 3	(1, 0, 1) 2	(1, 0, 1) 2	1.539	0.320
(0, 0, 0) 3	(0, 0, 0) 3	(1, 0, 1) 3	(1, 0, 1) 3	1.503	0.304
(0, 0, 0) 1	(0, 0, 0) 1	(1, 1, 1) 1	(1, 1, 1) 1	1.455	0.285
(0, 0, 0) 1	(0, 0, 0) 1	(1, 1, 1) 2	(1, 1, 1) 2	1.492	0.300
(0, 0, 0) 1	(0, 0, 0) 1	(1, 1, 1) 3	(1, 1, 1) 3	1.492	0.300
(0, 0, 0) 2	(0, 0, 0) 2	(1, 1, 1) 1	(1, 1, 1) 1	1.380	0.260

TABLE S.11. (Continued from Table S10.) Diagonal effective interactions in the cGW-SIC+LRFB for three-band hamiltonian of $\text{HgBa}_2\text{CuO}_4$ (in eV). Notations are the same as Table S8.

(0, 0, 0) 2 (0, 0, 0) 2 (1, 1, 1) 2 (1, 1, 1) 2	1.436	0.281
(0, 0, 0) 2 (0, 0, 0) 2 (1, 1, 1) 3 (1, 1, 1) 3	1.407	0.271
(0, 0, 0) 3 (0, 0, 0) 3 (1, 1, 1) 1 (1, 1, 1) 1	1.380	0.260
(0, 0, 0) 3 (0, 0, 0) 3 (1, 1, 1) 2 (1, 1, 1) 2	1.407	0.271
(0, 0, 0) 3 (0, 0, 0) 3 (1, 1, 1) 3 (1, 1, 1) 3	1.436	0.281
(0, 0, 0) 1 (0, 0, 0) 1 (2, 0, 1) 1 (2, 0, 1) 1	1.374	0.255
(0, 0, 0) 1 (0, 0, 0) 1 (2, 0, 1) 2 (2, 0, 1) 2	1.434	0.279
(0, 0, 0) 1 (0, 0, 0) 1 (2, 0, 1) 3 (2, 0, 1) 3	1.350	0.249
(0, 0, 0) 2 (0, 0, 0) 2 (2, 0, 1) 1 (2, 0, 1) 1	1.315	0.238
(0, 0, 0) 2 (0, 0, 0) 2 (2, 0, 1) 2 (2, 0, 1) 2	1.358	0.254
(0, 0, 0) 2 (0, 0, 0) 2 (2, 0, 1) 3 (2, 0, 1) 3	1.295	0.234
(0, 0, 0) 3 (0, 0, 0) 3 (2, 0, 1) 1 (2, 0, 1) 1	1.350	0.249
(0, 0, 0) 3 (0, 0, 0) 3 (2, 0, 1) 2 (2, 0, 1) 2	1.407	0.271
(0, 0, 0) 3 (0, 0, 0) 3 (2, 0, 1) 3 (2, 0, 1) 3	1.354	0.252
(0, 0, 0) 1 (0, 0, 0) 1 (2, 1, 1) 1 (2, 1, 1) 1	1.334	0.242
(0, 0, 0) 1 (0, 0, 0) 1 (2, 1, 1) 2 (2, 1, 1) 2	1.380	0.260
(0, 0, 0) 1 (0, 0, 0) 1 (2, 1, 1) 3 (2, 1, 1) 3	1.350	0.249
(0, 0, 0) 2 (0, 0, 0) 2 (2, 1, 1) 1 (2, 1, 1) 1	1.283	0.228
(0, 0, 0) 2 (0, 0, 0) 2 (2, 1, 1) 2 (2, 1, 1) 2	1.317	0.241
(0, 0, 0) 2 (0, 0, 0) 2 (2, 1, 1) 3 (2, 1, 1) 3	1.295	0.234
(0, 0, 0) 3 (0, 0, 0) 3 (2, 1, 1) 1 (2, 1, 1) 1	1.283	0.229
(0, 0, 0) 3 (0, 0, 0) 3 (2, 1, 1) 2 (2, 1, 1) 2	1.319	0.242
(0, 0, 0) 3 (0, 0, 0) 3 (2, 1, 1) 3 (2, 1, 1) 3	1.314	0.240
(0, 0, 0) 1 (0, 0, 0) 1 (2, 2, 1) 1 (2, 2, 1) 1	1.257	0.219
(0, 0, 0) 1 (0, 0, 0) 1 (2, 2, 1) 2 (2, 2, 1) 2	1.283	0.229
(0, 0, 0) 1 (0, 0, 0) 1 (2, 2, 1) 3 (2, 2, 1) 3	1.283	0.229
(0, 0, 0) 2 (0, 0, 0) 2 (2, 2, 1) 1 (2, 2, 1) 1	1.220	0.210
(0, 0, 0) 2 (0, 0, 0) 2 (2, 2, 1) 2 (2, 2, 1) 2	1.240	0.217
(0, 0, 0) 2 (0, 0, 0) 2 (2, 2, 1) 3 (2, 2, 1) 3	1.240	0.218
(0, 0, 0) 3 (0, 0, 0) 3 (2, 2, 1) 1 (2, 2, 1) 1	1.220	0.210
(0, 0, 0) 3 (0, 0, 0) 3 (2, 2, 1) 2 (2, 2, 1) 2	1.240	0.218
(0, 0, 0) 3 (0, 0, 0) 3 (2, 2, 1) 3 (2, 2, 1) 3	1.240	0.217
(0, 0, 0) 1 (0, 0, 0) 1 (3, 0, 1) 1 (3, 0, 1) 1	1.309	0.233
(0, 0, 0) 1 (0, 0, 0) 1 (3, 0, 1) 2 (3, 0, 1) 2	1.315	0.238
(0, 0, 0) 1 (0, 0, 0) 1 (3, 0, 1) 3 (3, 0, 1) 3	1.288	0.229
(0, 0, 0) 2 (0, 0, 0) 2 (3, 0, 1) 1 (3, 0, 1) 1	1.315	0.238
(0, 0, 0) 2 (0, 0, 0) 2 (3, 0, 1) 2 (3, 0, 1) 2	1.294	0.233
(0, 0, 0) 2 (0, 0, 0) 2 (3, 0, 1) 3 (3, 0, 1) 3	1.295	0.234
(0, 0, 0) 3 (0, 0, 0) 3 (3, 0, 1) 1 (3, 0, 1) 1	1.288	0.229
(0, 0, 0) 3 (0, 0, 0) 3 (3, 0, 1) 2 (3, 0, 1) 2	1.295	0.234

TABLE S.12. (Continued from Table S11.) Diagonal and off-diagonal effective interactions in the cGW-SIC+LRFB for three-band hamiltonian of $\text{HgBa}_2\text{CuO}_4$ (in eV). Notations are the same as Table S8.

(0, 0, 0) 3 (0, 0, 0) 3 (3, 0, 1) 3 (3, 0, 1) 3	1.289 0.231
(0, 0, 0) 1 (0, 0, 0) 1 (3, 1, 1) 1 (3, 1, 1) 1	1.279 0.225
(0, 0, 0) 1 (0, 0, 0) 1 (3, 1, 1) 2 (3, 1, 1) 2	1.283 0.228
(0, 0, 0) 1 (0, 0, 0) 1 (3, 1, 1) 3 (3, 1, 1) 3	1.288 0.229
(0, 0, 0) 2 (0, 0, 0) 2 (3, 1, 1) 1 (3, 1, 1) 1	1.283 0.228
(0, 0, 0) 2 (0, 0, 0) 2 (3, 1, 1) 2 (3, 1, 1) 2	1.264 0.224
(0, 0, 0) 2 (0, 0, 0) 2 (3, 1, 1) 3 (3, 1, 1) 3	1.295 0.234
(0, 0, 0) 3 (0, 0, 0) 3 (3, 1, 1) 1 (3, 1, 1) 1	1.238 0.215
(0, 0, 0) 3 (0, 0, 0) 3 (3, 1, 1) 2 (3, 1, 1) 2	1.240 0.218
(0, 0, 0) 3 (0, 0, 0) 3 (3, 1, 1) 3 (3, 1, 1) 3	1.260 0.223
(0, 0, 0) 1 (0, 0, 0) 1 (3, 2, 1) 1 (3, 2, 1) 1	1.222 0.208
(0, 0, 0) 1 (0, 0, 0) 1 (3, 2, 1) 2 (3, 2, 1) 2	1.220 0.210
(0, 0, 0) 1 (0, 0, 0) 1 (3, 2, 1) 3 (3, 2, 1) 3	1.238 0.215
(0, 0, 0) 2 (0, 0, 0) 2 (3, 2, 1) 1 (3, 2, 1) 1	1.220 0.210
(0, 0, 0) 2 (0, 0, 0) 2 (3, 2, 1) 2 (3, 2, 1) 2	1.206 0.207
(0, 0, 0) 2 (0, 0, 0) 2 (3, 2, 1) 3 (3, 2, 1) 3	1.240 0.218
(0, 0, 0) 3 (0, 0, 0) 3 (3, 2, 1) 1 (3, 2, 1) 1	1.190 0.201
(0, 0, 0) 3 (0, 0, 0) 3 (3, 2, 1) 2 (3, 2, 1) 2	1.188 0.203
(0, 0, 0) 3 (0, 0, 0) 3 (3, 2, 1) 3 (3, 2, 1) 3	1.204 0.207
(0, 0, 0) 1 (0, 0, 0) 1 (3, 3, 1) 1 (3, 3, 1) 1	1.194 0.200
(0, 0, 0) 1 (0, 0, 0) 1 (3, 3, 1) 2 (3, 3, 1) 2	1.190 0.201
(0, 0, 0) 1 (0, 0, 0) 1 (3, 3, 1) 3 (3, 3, 1) 3	1.190 0.201
(0, 0, 0) 2 (0, 0, 0) 2 (3, 3, 1) 1 (3, 3, 1) 1	1.190 0.201
(0, 0, 0) 2 (0, 0, 0) 2 (3, 3, 1) 2 (3, 3, 1) 2	1.178 0.199
(0, 0, 0) 2 (0, 0, 0) 2 (3, 3, 1) 3 (3, 3, 1) 3	1.188 0.203
(0, 0, 0) 3 (0, 0, 0) 3 (3, 3, 1) 1 (3, 3, 1) 1	1.190 0.201
(0, 0, 0) 3 (0, 0, 0) 3 (3, 3, 1) 2 (3, 3, 1) 2	1.188 0.203
(0, 0, 0) 3 (0, 0, 0) 3 (3, 3, 1) 3 (3, 3, 1) 3	1.178 0.199
(0, 1, 0) 3 (0, 0, 0) 1 (0, 1, 0) 3 (0, 1, 0) 3	0.170 0.105
(0, -1, 0) 1 (0, 0, 0) 3 (0, 0, 0) 3 (0, 0, 0) 3	0.170 0.105
(1, -1, 0) 2 (0, 0, 0) 3 (0, -1, 0) 1 (0, -1, 0) 1	0.327 0.107
(-1, 1, 0) 3 (0, 0, 0) 2 (-1, 0, 0) 1 (-1, 0, 0) 1	0.327 0.107
(0, 0, 0) 3 (0, 0, 0) 3 (0, -1, 0) 1 (0, 0, 0) 3	0.170 0.105
(0, 0, 0) 3 (0, 0, 0) 3 (0, 0, 0) 3 (0, -1, 0) 1	0.170 0.105
(0, 0, 0) 1 (0, 0, 0) 1 (0, 1, 0) 3 (1, 0, 0) 2	0.327 0.107
(0, 0, 0) 1 (0, 0, 0) 1 (1, 0, 0) 2 (0, 1, 0) 3	0.327 0.107

TABLE S.13. Transfer integrals and onsite potentials in the cGW-SIC+LRFB for the two-band hamiltonian of $\text{HgBa}_2\text{CuO}_4$ (in eV). The inter-layer hopping except for that in $(0, 0, 1)$ is omitted because its energy scale is under 10 meV.

$t(\text{cGW-SIC+LRFB})$	$(0, 0, 0)$		$(1, 0, 0)$		$(1, 1, 0)$		$(2, 0, 0)$	
	$3z^2 - r^2$	$x^2 - y^2$	$3z^2 - r^2$	$x^2 - y^2$	$3z^2 - r^2$	$x^2 - y^2$	$3z^2 - r^2$	$x^2 - y^2$
$3z^2 - r^2$	-3.518	0.000	0.002	0.029	-0.003	0.000	-0.003	0.004
$x^2 - y^2$	0.000	0.187	0.029	-0.455	0.000	0.096	0.004	-0.040
	$(2, 1, 0)$		$(2, 2, 0)$		$(3, 0, 0)$		$(3, 1, 0)$	
	$3z^2 - r^2$	$x^2 - y^2$	$3z^2 - r^2$	$x^2 - y^2$	$3z^2 - r^2$	$x^2 - y^2$	$3z^2 - r^2$	$x^2 - y^2$
$3z^2 - r^2$	0.002	-0.002	-0.014	0.000	0.005	0.001	-0.006	-0.003
$x^2 - y^2$	-0.002	0.003	0.000	0.005	0.001	-0.002	-0.003	0.010
	$(3, 2, 0)$		$(3, 3, 0)$		$(0, 0, 1)$			
	$3z^2 - r^2$	$x^2 - y^2$	$3z^2 - r^2$	$x^2 - y^2$	$3z^2 - r^2$	$x^2 - y^2$		
$3z^2 - r^2$	0.001	0.001	-0.005	0.000	-0.046	0.000		
$x^2 - y^2$	0.001	-0.001	0.000	-0.008	0.000	0.000		

TABLE S.14. Diagonal effective interactions within the same CuO₂ plane in the cGW-SIC+LRFB for two-band hamiltonian of HgBa₂CuO₄ (in eV). The interactions are indexed as $\langle \phi_{\ell_1 \mathbf{R}_{i_1}} | \phi_{\ell_2 \mathbf{R}_{i_2}} | X | \phi_{\ell_3 \mathbf{R}_{i_3}} \phi_{\ell_4 \mathbf{R}_{i_4}} \rangle (X = v, W^r)$. For the orbital index ℓ , 1 and 2 stand for the $3z^2 - r^2$ and $x^2 - y^2$ orbitals, respectively.

\mathbf{R}_{i_1}	ℓ_1	\mathbf{R}_{i_2}	ℓ_2	\mathbf{R}_{i_3}	ℓ_3	\mathbf{R}_{i_4}	ℓ_4	v	W^r
(0,0,0)	1	(0,0,0)	1	(0,0,0)	1	(0,0,0)	1	21.816	5.962
(0,0,0)	1	(0,0,0)	1	(0,0,0)	2	(0,0,0)	2	17.022	3.497
(0,0,0)	1	(0,0,0)	2	(0,0,0)	1	(0,0,0)	2	0.737	0.645
(0,0,0)	1	(0,0,0)	2	(0,0,0)	2	(0,0,0)	1	0.737	0.645
(0,0,0)	2	(0,0,0)	1	(0,0,0)	1	(0,0,0)	2	0.737	0.645
(0,0,0)	2	(0,0,0)	1	(0,0,0)	2	(0,0,0)	1	0.737	0.645
(0,0,0)	2	(0,0,0)	2	(0,0,0)	1	(0,0,0)	1	17.022	3.497
(0,0,0)	2	(0,0,0)	2	(0,0,0)	2	(0,0,0)	2	16.197	4.029
(0,0,0)	1	(0,0,0)	1	(1,0,0)	1	(1,0,0)	1	3.584	0.733
(0,0,0)	1	(0,0,0)	1	(1,0,0)	2	(1,0,0)	2	3.889	0.820
(0,0,0)	2	(0,0,0)	2	(1,0,0)	1	(1,0,0)	1	3.889	0.820
(0,0,0)	2	(0,0,0)	2	(1,0,0)	2	(1,0,0)	2	4.194	0.911
(0,0,0)	1	(0,0,0)	1	(1,1,0)	1	(1,1,0)	1	2.608	0.470
(0,0,0)	1	(0,0,0)	1	(1,1,0)	2	(1,1,0)	2	2.670	0.492
(0,0,0)	2	(0,0,0)	2	(1,1,0)	1	(1,1,0)	1	2.670	0.492
(0,0,0)	2	(0,0,0)	2	(1,1,0)	2	(1,1,0)	2	2.755	0.520
(0,0,0)	1	(0,0,0)	1	(2,0,0)	1	(2,0,0)	1	1.989	0.341
(0,0,0)	1	(0,0,0)	1	(2,0,0)	2	(2,0,0)	2	2.033	0.356
(0,0,0)	2	(0,0,0)	2	(2,0,0)	1	(2,0,0)	1	2.033	0.356
(0,0,0)	2	(0,0,0)	2	(2,0,0)	2	(2,0,0)	2	2.084	0.375
(0,0,0)	1	(0,0,0)	1	(2,1,0)	1	(2,1,0)	1	1.822	0.305
(0,0,0)	1	(0,0,0)	1	(2,1,0)	2	(2,1,0)	2	1.849	0.315
(0,0,0)	2	(0,0,0)	2	(2,1,0)	1	(2,1,0)	1	1.849	0.315
(0,0,0)	2	(0,0,0)	2	(2,1,0)	2	(2,1,0)	2	1.878	0.326
(0,0,0)	1	(0,0,0)	1	(2,2,0)	1	(2,2,0)	1	1.564	0.252
(0,0,0)	1	(0,0,0)	1	(2,2,0)	2	(2,2,0)	2	1.579	0.257
(0,0,0)	2	(0,0,0)	2	(2,2,0)	1	(2,2,0)	1	1.579	0.257
(0,0,0)	2	(0,0,0)	2	(2,2,0)	2	(2,2,0)	2	1.595	0.263
(0,0,0)	1	(0,0,0)	1	(3,0,0)	1	(3,0,0)	1	1.679	0.271
(0,0,0)	1	(0,0,0)	1	(3,0,0)	2	(3,0,0)	2	1.700	0.278
(0,0,0)	2	(0,0,0)	2	(3,0,0)	1	(3,0,0)	1	1.700	0.278
(0,0,0)	2	(0,0,0)	2	(3,0,0)	2	(3,0,0)	2	1.723	0.287
(0,0,0)	1	(0,0,0)	1	(3,1,0)	1	(3,1,0)	1	1.602	0.259
(0,0,0)	1	(0,0,0)	1	(3,1,0)	2	(3,1,0)	2	1.619	0.266
(0,0,0)	2	(0,0,0)	2	(3,1,0)	1	(3,1,0)	1	1.619	0.266
(0,0,0)	2	(0,0,0)	2	(3,1,0)	2	(3,1,0)	2	1.638	0.273
(0,0,0)	1	(0,0,0)	1	(3,2,0)	1	(3,2,0)	1	1.460	0.231
(0,0,0)	1	(0,0,0)	1	(3,2,0)	2	(3,2,0)	2	1.472	0.236
(0,0,0)	2	(0,0,0)	2	(3,2,0)	1	(3,2,0)	1	1.472	0.236
(0,0,0)	2	(0,0,0)	2	(3,2,0)	2	(3,2,0)	2	1.485	0.241
(0,0,0)	1	(0,0,0)	1	(3,3,0)	1	(3,3,0)	1	1.396	0.219
(0,0,0)	1	(0,0,0)	1	(3,3,0)	2	(3,3,0)	2	1.406	0.223
(0,0,0)	2	(0,0,0)	2	(3,3,0)	1	(3,3,0)	1	1.406	0.223
(0,0,0)	2	(0,0,0)	2	(3,3,0)	2	(3,3,0)	2	1.416	0.227

TABLE S.15. Diagonal effective interactions for interlayer pair in the cGW-SIC+LRFB for two-band hamiltonian of HgBa₂CuO₄ (in eV). Same notation as Table S14.

(0,0,0)	1	(0,0,0)	1	(0,0,1)	1	(0,0,1)	1	1.677	0.326
(0,0,0)	1	(0,0,0)	1	(0,0,1)	2	(0,0,1)	2	1.620	0.300
(0,0,0)	2	(0,0,0)	2	(0,0,1)	1	(0,0,1)	1	1.620	0.300
(0,0,0)	2	(0,0,0)	2	(0,0,1)	2	(0,0,1)	2	1.574	0.282
(0,0,0)	1	(0,0,0)	1	(1,0,1)	1	(1,0,1)	1	1.556	0.277
(0,0,0)	1	(0,0,0)	1	(1,0,1)	2	(1,0,1)	2	1.526	0.268
(0,0,0)	2	(0,0,0)	2	(1,0,1)	1	(1,0,1)	1	1.526	0.268
(0,0,0)	2	(0,0,0)	2	(1,0,1)	2	(1,0,1)	2	1.498	0.260
(0,0,0)	1	(0,0,0)	1	(1,1,1)	1	(1,1,1)	1	1.473	0.252
(0,0,0)	1	(0,0,0)	1	(1,1,1)	2	(1,1,1)	2	1.455	0.248
(0,0,0)	2	(0,0,0)	2	(1,1,1)	1	(1,1,1)	1	1.455	0.248
(0,0,0)	2	(0,0,0)	2	(1,1,1)	2	(1,1,1)	2	1.436	0.243
(0,0,0)	1	(0,0,0)	1	(2,0,1)	1	(2,0,1)	1	1.382	0.227
(0,0,0)	1	(0,0,0)	1	(2,0,1)	2	(2,0,1)	2	1.373	0.226
(0,0,0)	2	(0,0,0)	2	(2,0,1)	1	(2,0,1)	1	1.373	0.226
(0,0,0)	2	(0,0,0)	2	(2,0,1)	2	(2,0,1)	2	1.363	0.224
(0,0,0)	1	(0,0,0)	1	(2,1,1)	1	(2,1,1)	1	1.339	0.216
(0,0,0)	1	(0,0,0)	1	(2,1,1)	2	(2,1,1)	2	1.332	0.216
(0,0,0)	2	(0,0,0)	2	(2,1,1)	1	(2,1,1)	1	1.332	0.216
(0,0,0)	2	(0,0,0)	2	(2,1,1)	2	(2,1,1)	2	1.325	0.215
(0,0,0)	1	(0,0,0)	1	(2,2,1)	1	(2,2,1)	1	1.260	0.198
(0,0,0)	1	(0,0,0)	1	(2,2,1)	2	(2,2,1)	2	1.256	0.199
(0,0,0)	2	(0,0,0)	2	(2,2,1)	1	(2,2,1)	1	1.256	0.199
(0,0,0)	2	(0,0,0)	2	(2,2,1)	2	(2,2,1)	2	1.252	0.199
(0,0,0)	1	(0,0,0)	1	(3,0,1)	1	(3,0,1)	1	1.312	0.209
(0,0,0)	1	(0,0,0)	1	(3,0,1)	2	(3,0,1)	2	1.307	0.209
(0,0,0)	2	(0,0,0)	2	(3,0,1)	1	(3,0,1)	1	1.307	0.209
(0,0,0)	2	(0,0,0)	2	(3,0,1)	2	(3,0,1)	2	1.303	0.209
(0,0,0)	1	(0,0,0)	1	(3,1,1)	1	(3,1,1)	1	1.282	0.202
(0,0,0)	1	(0,0,0)	1	(3,1,1)	2	(3,1,1)	2	1.278	0.203
(0,0,0)	2	(0,0,0)	2	(3,1,1)	1	(3,1,1)	1	1.278	0.203
(0,0,0)	2	(0,0,0)	2	(3,1,1)	2	(3,1,1)	2	1.274	0.203
(0,0,0)	1	(0,0,0)	1	(3,2,1)	1	(3,2,1)	1	1.223	0.190
(0,0,0)	1	(0,0,0)	1	(3,2,1)	2	(3,2,1)	2	1.220	0.191
(0,0,0)	2	(0,0,0)	2	(3,2,1)	1	(3,2,1)	1	1.220	0.191
(0,0,0)	2	(0,0,0)	2	(3,2,1)	2	(3,2,1)	2	1.218	0.191
(0,0,0)	1	(0,0,0)	1	(3,3,1)	1	(3,3,1)	1	1.195	0.184
(0,0,0)	1	(0,0,0)	1	(3,3,1)	2	(3,3,1)	2	1.193	0.185
(0,0,0)	2	(0,0,0)	2	(3,3,1)	1	(3,3,1)	1	1.193	0.185
(0,0,0)	2	(0,0,0)	2	(3,3,1)	2	(3,3,1)	2	1.191	0.186

TABLE S.16. Off-diagonal effective interactions in the cGW-SIC+LRFB for two-band hamiltonian of $\text{HgBa}_2\text{CuO}_4$ (in eV). Same notation as Table S14.

(0, 1, 0) 2 (0, 0, 0) 1 (0, 0, 0) 1 (0, 0, 0) 1	0.339 0.088
(0, 1, 0) 2 (0, 0, 0) 2 (0, 0, 0) 1 (0, 0, 0) 1	0.347 0.062
(0, 1, 0) 2 (0, 0, 0) 2 (0, 0, 0) 2 (0, 0, 0) 2	0.247 0.061
(0, 1, 0) 1 (0, 0, 0) 2 (0, 1, 0) 1 (0, 1, 0) 1	0.339 0.088
(0, 1, 0) 2 (0, 0, 0) 2 (0, 1, 0) 1 (0, 1, 0) 1	0.347 0.062
(0, 1, 0) 2 (0, 0, 0) 2 (0, 1, 0) 2 (0, 1, 0) 2	0.247 0.061
(0, -1, 0) 2 (0, 0, 0) 1 (0, 0, 0) 1 (0, 0, 0) 1	0.339 0.088
(0, -1, 0) 2 (0, 0, 0) 2 (0, 0, 0) 1 (0, 0, 0) 1	0.347 0.062
(0, -1, 0) 2 (0, 0, 0) 2 (0, 0, 0) 2 (0, 0, 0) 2	0.247 0.061
(0, -1, 0) 1 (0, 0, 0) 2 (0, -1, 0) 1 (0, -1, 0) 1	0.339 0.088
(0, -1, 0) 2 (0, 0, 0) 2 (0, -1, 0) 1 (0, -1, 0) 1	0.347 0.062
(0, -1, 0) 2 (0, 0, 0) 2 (0, -1, 0) 2 (0, -1, 0) 2	0.247 0.061
(1, 0, 0) 2 (0, 0, 0) 2 (0, 0, 0) 1 (0, 0, 0) 1	0.347 0.062
(1, 0, 0) 2 (0, 0, 0) 2 (0, 0, 0) 2 (0, 0, 0) 2	0.247 0.061
(1, 0, 0) 2 (0, 0, 0) 2 (1, 0, 0) 1 (1, 0, 0) 1	0.347 0.062
(1, 0, 0) 2 (0, 0, 0) 2 (1, 0, 0) 2 (1, 0, 0) 2	0.247 0.061
(-1, 0, 0) 2 (0, 0, 0) 2 (0, 0, 0) 1 (0, 0, 0) 1	0.347 0.062
(-1, 0, 0) 2 (0, 0, 0) 2 (0, 0, 0) 2 (0, 0, 0) 2	0.247 0.061
(-1, 0, 0) 2 (0, 0, 0) 2 (-1, 0, 0) 1 (-1, 0, 0) 1	0.347 0.062
(-1, 0, 0) 2 (0, 0, 0) 2 (-1, 0, 0) 2 (-1, 0, 0) 2	0.247 0.061
(0, 0, 0) 1 (0, 0, 0) 1 (0, 0, 0) 1 (0, 1, 0) 2	0.339 0.088
(0, 0, 0) 1 (0, 0, 0) 1 (0, 0, 0) 2 (0, 1, 0) 2	0.347 0.062
(0, 0, 0) 2 (0, 0, 0) 2 (0, 0, 0) 2 (0, 1, 0) 2	0.247 0.061
(0, 0, 0) 1 (0, 0, 0) 1 (0, -1, 0) 2 (0, 0, 0) 1	0.339 0.088
(0, 0, 0) 1 (0, 0, 0) 1 (0, -1, 0) 2 (0, 0, 0) 2	0.347 0.062
(0, 0, 0) 2 (0, 0, 0) 2 (0, -1, 0) 2 (0, 0, 0) 2	0.247 0.061
(0, 0, 0) 1 (0, 0, 0) 1 (0, 0, 0) 1 (0, -1, 0) 2	0.339 0.088
(0, 0, 0) 1 (0, 0, 0) 1 (0, 0, 0) 2 (0, -1, 0) 2	0.347 0.062
(0, 0, 0) 2 (0, 0, 0) 2 (0, 0, 0) 2 (0, -1, 0) 2	0.247 0.061
(0, 0, 0) 1 (0, 0, 0) 1 (0, 1, 0) 2 (0, 0, 0) 1	0.339 0.088
(0, 0, 0) 1 (0, 0, 0) 1 (0, 1, 0) 2 (0, 0, 0) 2	0.347 0.062
(0, 0, 0) 2 (0, 0, 0) 2 (0, 1, 0) 2 (0, 0, 0) 2	0.247 0.061
(0, 0, 0) 1 (0, 0, 0) 1 (0, 0, 0) 2 (1, 0, 0) 2	0.347 0.062
(0, 0, 0) 2 (0, 0, 0) 2 (0, 0, 0) 2 (1, 0, 0) 2	0.247 0.061
(0, 0, 0) 1 (0, 0, 0) 1 (-1, 0, 0) 2 (0, 0, 0) 2	0.347 0.062
(0, 0, 0) 2 (0, 0, 0) 2 (-1, 0, 0) 2 (0, 0, 0) 2	0.247 0.061
(0, 0, 0) 1 (0, 0, 0) 1 (0, 0, 0) 2 (-1, 0, 0) 2	0.347 0.062
(0, 0, 0) 2 (0, 0, 0) 2 (0, 0, 0) 2 (-1, 0, 0) 2	0.247 0.061
(0, 0, 0) 1 (0, 0, 0) 1 (1, 0, 0) 2 (0, 0, 0) 2	0.347 0.062
(0, 0, 0) 2 (0, 0, 0) 2 (1, 0, 0) 2 (0, 0, 0) 2	0.247 0.061

TABLE S.17. Transfer integrals in the cGW+LRFB for one-band hamiltonian of $\text{HgBa}_2\text{CuO}_4$ (in eV). The inter-layer hopping is omitted because its energy scale is under 10 meV.

$t(\text{cGW+LRFB})$	(0, 0, 0)	(1, 0, 0)	(1, 1, 0)	(2, 0, 0)
$x^2 - y^2$	0.229	-0.509	0.127	-0.077
	(2, 1, 0)	(2, 2, 0)	(3, 0, 0)	(3, 1, 0)
$x^2 - y^2$	0.018	0.004	-0.004	0.007
	(3, 2, 0)	(3, 3, 0)		
$x^2 - y^2$	0.004	-0.009		

TABLE S.18. Effective interactions in the cGW+LRFB for one-band hamiltonian of $\text{HgBa}_2\text{CuO}_4$ (in eV). $\langle \phi_{\ell_1 \mathbf{R}_{i_1}} \phi_{\ell_2 \mathbf{R}_{i_2}} | X | \phi_{\ell_3 \mathbf{R}_{i_3}} \phi_{\ell_4 \mathbf{R}_{i_4}} \rangle (X = v, W^r)$ are shown.

\mathbf{R}_{i_1}	ℓ_1	\mathbf{R}_{i_2}	ℓ_2	\mathbf{R}_{i_3}	ℓ_3	\mathbf{R}_{i_4}	ℓ_4	v	W^r
(0, 0, 0)	1	(0, 0, 0)	1	(0, 0, 0)	1	(0, 0, 0)	1	16.197	3.846
(0, 0, 0)	1	(0, 0, 0)	1	(1, 0, 0)	1	(1, 0, 0)	1	4.194	0.834
(0, 0, 0)	1	(0, 0, 0)	1	(1, 1, 0)	1	(1, 1, 0)	1	2.755	0.460
(0, 0, 0)	1	(0, 0, 0)	1	(2, 0, 0)	1	(2, 0, 0)	1	2.084	0.318
(0, 0, 0)	1	(0, 0, 0)	1	(2, 1, 0)	1	(2, 1, 0)	1	1.878	0.271
(0, 0, 0)	1	(0, 0, 0)	1	(2, 2, 0)	1	(2, 2, 0)	1	1.595	0.209
(0, 0, 0)	1	(0, 0, 0)	1	(3, 0, 0)	1	(3, 0, 0)	1	1.723	0.233
(0, 0, 0)	1	(0, 0, 0)	1	(3, 1, 0)	1	(3, 1, 0)	1	1.638	0.219
(0, 0, 0)	1	(0, 0, 0)	1	(3, 2, 0)	1	(3, 2, 0)	1	1.485	0.187
(0, 0, 0)	1	(0, 0, 0)	1	(3, 3, 0)	1	(3, 3, 0)	1	1.416	0.173
(0, 0, 0)	1	(0, 0, 0)	1	(0, 0, 1)	1	(0, 0, 1)	1	1.574	0.252
(0, 0, 0)	1	(0, 0, 0)	1	(1, 0, 1)	1	(1, 0, 1)	1	1.498	0.224
(0, 0, 0)	1	(0, 0, 0)	1	(1, 1, 1)	1	(1, 1, 1)	1	1.436	0.204
(0, 0, 0)	1	(0, 0, 0)	1	(2, 0, 1)	1	(2, 0, 1)	1	1.363	0.183
(0, 0, 0)	1	(0, 0, 0)	1	(2, 1, 1)	1	(2, 1, 1)	1	1.325	0.172
(0, 0, 0)	1	(0, 0, 0)	1	(2, 2, 1)	1	(2, 2, 1)	1	1.252	0.154
(0, 0, 0)	1	(0, 0, 0)	1	(3, 0, 1)	1	(3, 0, 1)	1	1.303	0.166
(0, 0, 0)	1	(0, 0, 0)	1	(3, 1, 1)	1	(3, 1, 1)	1	1.274	0.159
(0, 0, 0)	1	(0, 0, 0)	1	(3, 2, 1)	1	(3, 2, 1)	1	1.218	0.145
(0, 0, 0)	1	(0, 0, 0)	1	(3, 3, 1)	1	(3, 3, 1)	1	1.191	0.139
(0, 1, 0)	1	(0, 0, 0)	1	(0, 0, 0)	1	(0, 0, 0)	1	0.247	0.057
(0, 1, 0)	1	(0, 0, 0)	1	(0, 1, 0)	1	(0, 1, 0)	1	0.247	0.057
(0, -1, 0)	1	(0, 0, 0)	1	(0, 0, 0)	1	(0, 0, 0)	1	0.247	0.057
(0, -1, 0)	1	(0, 0, 0)	1	(0, -1, 0)	1	(0, -1, 0)	1	0.247	0.057
(1, 0, 0)	1	(0, 0, 0)	1	(0, 0, 0)	1	(0, 0, 0)	1	0.247	0.057
(1, 0, 0)	1	(0, 0, 0)	1	(1, 0, 0)	1	(1, 0, 0)	1	0.247	0.057
(-1, 0, 0)	1	(0, 0, 0)	1	(0, 0, 0)	1	(0, 0, 0)	1	0.247	0.057
(-1, 0, 0)	1	(0, 0, 0)	1	(-1, 0, 0)	1	(-1, 0, 0)	1	0.247	0.057
(0, 0, 0)	1	(0, 0, 0)	1	(0, 0, 0)	1	(0, 1, 0)	1	0.247	0.057
(0, 0, 0)	1	(0, 0, 0)	1	(0, -1, 0)	1	(0, 0, 0)	1	0.247	0.057
(0, 0, 0)	1	(0, 0, 0)	1	(0, 0, 0)	1	(0, -1, 0)	1	0.247	0.057
(0, 0, 0)	1	(0, 0, 0)	1	(0, 1, 0)	1	(0, 0, 0)	1	0.247	0.057
(0, 0, 0)	1	(0, 0, 0)	1	(0, 0, 0)	1	(1, 0, 0)	1	0.247	0.057
(0, 0, 0)	1	(0, 0, 0)	1	(-1, 0, 0)	1	(0, 0, 0)	1	0.247	0.057
(0, 0, 0)	1	(0, 0, 0)	1	(0, 0, 0)	1	(-1, 0, 0)	1	0.247	0.057
(0, 0, 0)	1	(0, 0, 0)	1	(1, 0, 0)	1	(0, 0, 0)	1	0.247	0.057

TABLE S.19. Transfer integrals in the cGW-SIC for three-band hamiltonian of La_2CuO_4 (in eV). The inter-layer hopping is omitted because its energy scale is under 10 meV.

$t(\text{cGW-SIC})$	(0, 0, 0)			(1, 0, 0)			(1, 1, 0)			(2, 0, 0)		
	$x^2 - y^2$	p_1	p_2	$x^2 - y^2$	p_1	p_2	$x^2 - y^2$	p_1	p_2	$x^2 - y^2$	p_1	p_2
$x^2 - y^2$	-1.538	-1.369	1.369	0.038	-0.036	-0.028	0.025	-0.020	0.020	-0.005	0.005	0.005
p_1	-1.369	-5.237	-0.753	1.369	0.189	0.754	-0.028	0.047	0.010	0.036	-0.005	0.009
p_2	1.369	-0.753	-5.237	-0.029	-0.010	0.021	0.028	0.009	0.047	0.005	-0.002	0.002
	(2, 1, 0)			(2, 2, 0)			(3, 0, 0)			(3, 1, 0)		
	$x^2 - y^2$	p_1	p_2	$x^2 - y^2$	p_1	p_2	$x^2 - y^2$	p_1	p_2	$x^2 - y^2$	p_1	p_2
$x^2 - y^2$	-0.025	0.007	-0.020	0.017	-0.002	0.002	0.009	-0.002	0.002	0.001	-0.003	-0.001
p_1	0.020	-0.006	0.021	-0.020	0.011	-0.005	-0.002	0.002	0.001	-0.003	0.003	-0.003
p_2	-0.005	0.002	-0.012	0.020	-0.005	0.011	0.002	0.001	0.001	-0.002	-0.001	0.000
	(3, 2, 0)			(3, 3, 0)								
	$x^2 - y^2$	p_1	p_2	$x^2 - y^2$	p_1	p_2						
$x^2 - y^2$	0.005	0.001	0.010	-0.009	0.005	-0.005						
p_1	0.001	-0.001	-0.003	0.005	-0.004	0.002						
p_2	0.001	0.003	0.004	-0.005	0.002	-0.004						

TABLE S.20. Diagonal effective interactions in the cGW-SIC for three-band hamiltonian of La_2CuO_4 (in eV). The interactions are indexed as $\langle \phi_{\ell_1 \mathbf{R}_{i_1}} \phi_{\ell_2 \mathbf{R}_{i_2}} | X | \phi_{\ell_3 \mathbf{R}_{i_3}} \phi_{\ell_4 \mathbf{R}_{i_4}} \rangle$ ($X = v, W^r$). The orbital indices 1, 2, and 3 stand for the $x^2 - y^2$, p_1 and p_2 orbitals, respectively.

$\mathbf{R}_{i_1} \ell_1 \mathbf{R}_{i_2} \ell_2 \mathbf{R}_{i_3} \ell_3 \mathbf{R}_{i_4} \ell_4$	v	W^r
(0, 0, 0) 1 (0, 0, 0) 1 (0, 0, 0) 1 (0, 0, 0) 1	28.784	9.612
(0, 0, 0) 1 (0, 0, 0) 1 (0, 0, 0) 2 (0, 0, 0) 2	8.246	2.680
(0, 0, 0) 1 (0, 0, 0) 1 (0, 0, 0) 2 (0, 0, 0) 3	0.286	0.099
(0, 0, 0) 1 (0, 0, 0) 1 (0, 0, 0) 3 (0, 0, 0) 2	0.286	0.099
(0, 0, 0) 1 (0, 0, 0) 1 (0, 0, 0) 3 (0, 0, 0) 3	8.246	2.680
(0, 0, 0) 1 (0, 0, 0) 2 (0, 0, 0) 2 (0, 0, 0) 2	0.175	0.103
(0, 0, 0) 2 (0, 0, 0) 1 (0, 0, 0) 2 (0, 0, 0) 2	0.175	0.103
(0, 0, 0) 2 (0, 0, 0) 2 (0, 0, 0) 1 (0, 0, 0) 1	8.246	2.680
(0, 0, 0) 2 (0, 0, 0) 2 (0, 0, 0) 1 (0, 0, 0) 2	0.175	0.103
(0, 0, 0) 2 (0, 0, 0) 2 (0, 0, 0) 2 (0, 0, 0) 1	0.175	0.103
(0, 0, 0) 2 (0, 0, 0) 2 (0, 0, 0) 2 (0, 0, 0) 2	17.777	6.128
(0, 0, 0) 2 (0, 0, 0) 2 (0, 0, 0) 3 (0, 0, 0) 3	5.501	1.861
(0, 0, 0) 2 (0, 0, 0) 3 (0, 0, 0) 1 (0, 0, 0) 1	0.286	0.099
(0, 0, 0) 3 (0, 0, 0) 2 (0, 0, 0) 1 (0, 0, 0) 1	0.286	0.099
(0, 0, 0) 3 (0, 0, 0) 3 (0, 0, 0) 1 (0, 0, 0) 1	8.246	2.680
(0, 0, 0) 3 (0, 0, 0) 3 (0, 0, 0) 2 (0, 0, 0) 2	5.501	1.861
(0, 0, 0) 3 (0, 0, 0) 3 (0, 0, 0) 3 (0, 0, 0) 3	17.777	6.128
(0, 0, 0) 1 (0, 0, 0) 1 (1, 0, 0) 1 (1, 0, 0) 1	3.897	1.511
(0, 0, 0) 1 (0, 0, 0) 1 (1, 0, 0) 2 (1, 0, 0) 2	8.246	2.680
(0, 0, 0) 1 (0, 0, 0) 1 (1, 0, 0) 3 (1, 0, 0) 3	3.441	1.353
(0, 0, 0) 2 (0, 0, 0) 2 (1, 0, 0) 1 (1, 0, 0) 1	2.656	1.199
(0, 0, 0) 2 (0, 0, 0) 2 (1, 0, 0) 2 (1, 0, 0) 2	4.002	1.503
(0, 0, 0) 2 (0, 0, 0) 2 (1, 0, 0) 3 (1, 0, 0) 3	2.502	1.156
(0, 0, 0) 3 (0, 0, 0) 3 (1, 0, 0) 1 (1, 0, 0) 1	3.441	1.354
(0, 0, 0) 3 (0, 0, 0) 3 (1, 0, 0) 2 (1, 0, 0) 2	5.501	1.862
(0, 0, 0) 3 (0, 0, 0) 3 (1, 0, 0) 3 (1, 0, 0) 3	3.727	1.394
(0, 0, 0) 1 (0, 0, 0) 1 (1, 1, 0) 1 (1, 1, 0) 1	2.779	1.208
(0, 0, 0) 1 (0, 0, 0) 1 (1, 1, 0) 2 (1, 1, 0) 2	3.441	1.354
(0, 0, 0) 1 (0, 0, 0) 1 (1, 1, 0) 3 (1, 1, 0) 3	3.441	1.354
(0, 0, 0) 2 (0, 0, 0) 2 (1, 1, 0) 1 (1, 1, 0) 1	2.241	1.104
(0, 0, 0) 2 (0, 0, 0) 2 (1, 1, 0) 2 (1, 1, 0) 2	2.770	1.217
(0, 0, 0) 2 (0, 0, 0) 2 (1, 1, 0) 3 (1, 1, 0) 3	2.502	1.157
(0, 0, 0) 3 (0, 0, 0) 3 (1, 1, 0) 1 (1, 1, 0) 1	2.241	1.104
(0, 0, 0) 3 (0, 0, 0) 3 (1, 1, 0) 2 (1, 1, 0) 2	2.502	1.157
(0, 0, 0) 3 (0, 0, 0) 3 (1, 1, 0) 3 (1, 1, 0) 3	2.770	1.217
(0, 0, 0) 1 (0, 0, 0) 1 (2, 0, 0) 1 (2, 0, 0) 1	2.089	1.076
(0, 0, 0) 1 (0, 0, 0) 1 (2, 0, 0) 2 (2, 0, 0) 2	2.656	1.199
(0, 0, 0) 1 (0, 0, 0) 1 (2, 0, 0) 3 (2, 0, 0) 3	2.022	1.060
(0, 0, 0) 2 (0, 0, 0) 2 (2, 0, 0) 1 (2, 0, 0) 1	1.828	1.021
(0, 0, 0) 2 (0, 0, 0) 2 (2, 0, 0) 2 (2, 0, 0) 2	2.095	1.077

TABLE S.21. (Continued from Table S20.) Diagonal effective interactions in the cGW-SIC for three-band hamiltonian of La_2CuO_4 (in eV). Notations are the same as Table S20.

(0, 0, 0) 2 (0, 0, 0) 2 (2, 0, 0) 3 (2, 0, 0) 3	1.787	1.012
(0, 0, 0) 3 (0, 0, 0) 3 (2, 0, 0) 1 (2, 0, 0) 1	2.022	1.060
(0, 0, 0) 3 (0, 0, 0) 3 (2, 0, 0) 2 (2, 0, 0) 2	2.502	1.157
(0, 0, 0) 3 (0, 0, 0) 3 (2, 0, 0) 3 (2, 0, 0) 3	2.060	1.068
(0, 0, 0) 1 (0, 0, 0) 1 (2, 1, 0) 1 (2, 1, 0) 1	1.908	1.038
(0, 0, 0) 1 (0, 0, 0) 1 (2, 1, 0) 2 (2, 1, 0) 2	2.241	1.104
(0, 0, 0) 1 (0, 0, 0) 1 (2, 1, 0) 3 (2, 1, 0) 3	2.022	1.060
(0, 0, 0) 2 (0, 0, 0) 2 (2, 1, 0) 1 (2, 1, 0) 1	1.724	1.001
(0, 0, 0) 2 (0, 0, 0) 2 (2, 1, 0) 2 (2, 1, 0) 2	1.906	1.039
(0, 0, 0) 2 (0, 0, 0) 2 (2, 1, 0) 3 (2, 1, 0) 3	1.787	1.013
(0, 0, 0) 3 (0, 0, 0) 3 (2, 1, 0) 1 (2, 1, 0) 1	1.750	1.008
(0, 0, 0) 3 (0, 0, 0) 3 (2, 1, 0) 2 (2, 1, 0) 2	1.953	1.048
(0, 0, 0) 3 (0, 0, 0) 3 (2, 1, 0) 3 (2, 1, 0) 3	1.890	1.037
(0, 0, 0) 1 (0, 0, 0) 1 (2, 2, 0) 1 (2, 2, 0) 1	1.631	0.985
(0, 0, 0) 1 (0, 0, 0) 1 (2, 2, 0) 2 (2, 2, 0) 2	1.750	1.008
(0, 0, 0) 1 (0, 0, 0) 1 (2, 2, 0) 3 (2, 2, 0) 3	1.750	1.008
(0, 0, 0) 2 (0, 0, 0) 2 (2, 2, 0) 1 (2, 2, 0) 1	1.544	0.967
(0, 0, 0) 2 (0, 0, 0) 2 (2, 2, 0) 2 (2, 2, 0) 2	1.622	0.984
(0, 0, 0) 2 (0, 0, 0) 2 (2, 2, 0) 3 (2, 2, 0) 3	1.621	0.981
(0, 0, 0) 3 (0, 0, 0) 3 (2, 2, 0) 1 (2, 2, 0) 1	1.544	0.967
(0, 0, 0) 3 (0, 0, 0) 3 (2, 2, 0) 2 (2, 2, 0) 2	1.621	0.981
(0, 0, 0) 3 (0, 0, 0) 3 (2, 2, 0) 3 (2, 2, 0) 3	1.622	0.984
(0, 0, 0) 1 (0, 0, 0) 1 (3, 0, 0) 1 (3, 0, 0) 1	1.753	1.007
(0, 0, 0) 1 (0, 0, 0) 1 (3, 0, 0) 2 (3, 0, 0) 2	1.828	1.021
(0, 0, 0) 1 (0, 0, 0) 1 (3, 0, 0) 3 (3, 0, 0) 3	1.719	0.999
(0, 0, 0) 2 (0, 0, 0) 2 (3, 0, 0) 1 (3, 0, 0) 1	1.828	1.021
(0, 0, 0) 2 (0, 0, 0) 2 (3, 0, 0) 2 (3, 0, 0) 2	1.752	1.007
(0, 0, 0) 2 (0, 0, 0) 2 (3, 0, 0) 3 (3, 0, 0) 3	1.787	1.013
(0, 0, 0) 3 (0, 0, 0) 3 (3, 0, 0) 1 (3, 0, 0) 1	1.719	0.999
(0, 0, 0) 3 (0, 0, 0) 3 (3, 0, 0) 2 (3, 0, 0) 2	1.787	1.013
(0, 0, 0) 3 (0, 0, 0) 3 (3, 0, 0) 3 (3, 0, 0) 3	1.735	1.003
(0, 0, 0) 1 (0, 0, 0) 1 (3, 1, 0) 1 (3, 1, 0) 1	1.671	0.991
(0, 0, 0) 1 (0, 0, 0) 1 (3, 1, 0) 2 (3, 1, 0) 2	1.724	1.001
(0, 0, 0) 1 (0, 0, 0) 1 (3, 1, 0) 3 (3, 1, 0) 3	1.719	0.999
(0, 0, 0) 2 (0, 0, 0) 2 (3, 1, 0) 1 (3, 1, 0) 1	1.724	1.001
(0, 0, 0) 2 (0, 0, 0) 2 (3, 1, 0) 2 (3, 1, 0) 2	1.667	0.991
(0, 0, 0) 2 (0, 0, 0) 2 (3, 1, 0) 3 (3, 1, 0) 3	1.787	1.012
(0, 0, 0) 3 (0, 0, 0) 3 (3, 1, 0) 1 (3, 1, 0) 1	1.585	0.975
(0, 0, 0) 3 (0, 0, 0) 3 (3, 1, 0) 2 (3, 1, 0) 2	1.621	0.981
(0, 0, 0) 3 (0, 0, 0) 3 (3, 1, 0) 3 (3, 1, 0) 3	1.655	0.989

TABLE S.22. (Continued from Table S21.) Diagonal effective interactions in the cGW-SIC for three-band hamiltonian of La_2CuO_4 (in eV). Notations are the same as Table S20.

(0, 0, 0) 1 (0, 0, 0) 1 (3, 2, 0) 1 (3, 2, 0) 1	1.521 0.963
(0, 0, 0) 1 (0, 0, 0) 1 (3, 2, 0) 2 (3, 2, 0) 2	1.544 0.967
(0, 0, 0) 1 (0, 0, 0) 1 (3, 2, 0) 3 (3, 2, 0) 3	1.585 0.975
(0, 0, 0) 2 (0, 0, 0) 2 (3, 2, 0) 1 (3, 2, 0) 1	1.543 0.967
(0, 0, 0) 2 (0, 0, 0) 2 (3, 2, 0) 2 (3, 2, 0) 2	1.514 0.962
(0, 0, 0) 2 (0, 0, 0) 2 (3, 2, 0) 3 (3, 2, 0) 3	1.621 0.981
(0, 0, 0) 3 (0, 0, 0) 3 (3, 2, 0) 1 (3, 2, 0) 1	1.465 0.952
(0, 0, 0) 3 (0, 0, 0) 3 (3, 2, 0) 2 (3, 2, 0) 2	1.479 0.954
(0, 0, 0) 3 (0, 0, 0) 3 (3, 2, 0) 3 (3, 2, 0) 3	1.511 0.962
(0, 0, 0) 1 (0, 0, 0) 1 (3, 3, 0) 1 (3, 3, 0) 1	1.453 0.950
(0, 0, 0) 1 (0, 0, 0) 1 (3, 3, 0) 2 (3, 3, 0) 2	1.465 0.952
(0, 0, 0) 1 (0, 0, 0) 1 (3, 3, 0) 3 (3, 3, 0) 3	1.465 0.952
(0, 0, 0) 2 (0, 0, 0) 2 (3, 3, 0) 1 (3, 3, 0) 1	1.465 0.952
(0, 0, 0) 2 (0, 0, 0) 2 (3, 3, 0) 2 (3, 3, 0) 2	1.445 0.949
(0, 0, 0) 2 (0, 0, 0) 2 (3, 3, 0) 3 (3, 3, 0) 3	1.479 0.954
(0, 0, 0) 3 (0, 0, 0) 3 (3, 3, 0) 1 (3, 3, 0) 1	1.465 0.952
(0, 0, 0) 3 (0, 0, 0) 3 (3, 3, 0) 2 (3, 3, 0) 2	1.479 0.954
(0, 0, 0) 3 (0, 0, 0) 3 (3, 3, 0) 3 (3, 3, 0) 3	1.445 0.949
(0, 0, 0) 1 (0, 0, 0) 1 (0.5, 0.5, 1) 1 (0.5, 0.5, 1) 1	2.076 1.112
(0, 0, 0) 1 (0, 0, 0) 1 (0.5, 0.5, 1) 2 (0.5, 0.5, 1) 2	2.128 1.130
(0, 0, 0) 1 (0, 0, 0) 1 (0.5, 0.5, 1) 3 (0.5, 0.5, 1) 3	2.128 1.130
(0, 0, 0) 2 (0, 0, 0) 2 (0.5, 0.5, 1) 1 (0.5, 0.5, 1) 1	1.917 1.068
(0, 0, 0) 2 (0, 0, 0) 2 (0.5, 0.5, 1) 2 (0.5, 0.5, 1) 2	2.063 1.111
(0, 0, 0) 2 (0, 0, 0) 2 (0.5, 0.5, 1) 3 (0.5, 0.5, 1) 3	1.952 1.078
(0, 0, 0) 3 (0, 0, 0) 3 (0.5, 0.5, 1) 1 (0.5, 0.5, 1) 1	1.917 1.068
(0, 0, 0) 3 (0, 0, 0) 3 (0.5, 0.5, 1) 2 (0.5, 0.5, 1) 2	1.952 1.078
(0, 0, 0) 3 (0, 0, 0) 3 (0.5, 0.5, 1) 3 (0.5, 0.5, 1) 3	2.063 1.111
(0, 0, 0) 1 (0, 0, 0) 1 (1.5, 0.5, 1) 1 (1.5, 0.5, 1) 1	1.753 1.026
(0, 0, 0) 1 (0, 0, 0) 1 (1.5, 0.5, 1) 2 (1.5, 0.5, 1) 2	1.917 1.068
(0, 0, 0) 1 (0, 0, 0) 1 (1.5, 0.5, 1) 3 (1.5, 0.5, 1) 3	1.771 1.031
(0, 0, 0) 2 (0, 0, 0) 2 (1.5, 0.5, 1) 1 (1.5, 0.5, 1) 1	1.607 0.992
(0, 0, 0) 2 (0, 0, 0) 2 (1.5, 0.5, 1) 2 (1.5, 0.5, 1) 2	1.746 1.026
(0, 0, 0) 2 (0, 0, 0) 2 (1.5, 0.5, 1) 3 (1.5, 0.5, 1) 3	1.615 0.993
(0, 0, 0) 3 (0, 0, 0) 3 (1.5, 0.5, 1) 1 (1.5, 0.5, 1) 1	1.669 1.008
(0, 0, 0) 3 (0, 0, 0) 3 (1.5, 0.5, 1) 2 (1.5, 0.5, 1) 2	1.796 1.038
(0, 0, 0) 3 (0, 0, 0) 3 (1.5, 0.5, 1) 3 (1.5, 0.5, 1) 3	1.739 1.026
(0, 0, 0) 1 (0, 0, 0) 1 (1.5, 1.5, 1) 1 (1.5, 1.5, 1) 1	1.583 0.988
(0, 0, 0) 1 (0, 0, 0) 1 (1.5, 1.5, 1) 2 (1.5, 1.5, 1) 2	1.669 1.008
(0, 0, 0) 1 (0, 0, 0) 1 (1.5, 1.5, 1) 3 (1.5, 1.5, 1) 3	1.669 1.008
(0, 0, 0) 2 (0, 0, 0) 2 (1.5, 1.5, 1) 1 (1.5, 1.5, 1) 1	1.493 0.968

TABLE S.23. (Continued from Table S22.) Diagonal and off-diagonal effective interactions in the cGW-SIC for three-band hamiltonian of La_2CuO_4 (in eV). Notations are the same as Table S20.

(0, 0, 0) 2 (0, 0, 0) 2 (1.5, 1.5, 1) 2 (1.5, 1.5, 1) 2	1.574 0.988
(0, 0, 0) 2 (0, 0, 0) 2 (1.5, 1.5, 1) 3 (1.5, 1.5, 1) 3	1.550 0.980
(0, 0, 0) 3 (0, 0, 0) 3 (1.5, 1.5, 1) 1 (1.5, 1.5, 1) 1	1.493 0.968
(0, 0, 0) 3 (0, 0, 0) 3 (1.5, 1.5, 1) 2 (1.5, 1.5, 1) 2	1.550 0.980
(0, 0, 0) 3 (0, 0, 0) 3 (1.5, 1.5, 1) 3 (1.5, 1.5, 1) 3	1.574 0.988
(0, 0, 0) 1 (0, 0, 0) 1 (2.5, 0.5, 1) 1 (2.5, 0.5, 1) 1	1.523 0.973
(0, 0, 0) 1 (0, 0, 0) 1 (2.5, 0.5, 1) 2 (2.5, 0.5, 1) 2	1.607 0.992
(0, 0, 0) 1 (0, 0, 0) 1 (2.5, 0.5, 1) 3 (2.5, 0.5, 1) 3	1.526 0.973
(0, 0, 0) 2 (0, 0, 0) 2 (2.5, 0.5, 1) 1 (2.5, 0.5, 1) 1	1.487 0.964
(0, 0, 0) 2 (0, 0, 0) 2 (2.5, 0.5, 1) 2 (2.5, 0.5, 1) 2	1.518 0.972
(0, 0, 0) 2 (0, 0, 0) 2 (2.5, 0.5, 1) 3 (2.5, 0.5, 1) 3	1.488 0.964
(0, 0, 0) 3 (0, 0, 0) 3 (2.5, 0.5, 1) 1 (2.5, 0.5, 1) 1	1.481 0.964
(0, 0, 0) 3 (0, 0, 0) 3 (2.5, 0.5, 1) 2 (2.5, 0.5, 1) 2	1.550 0.980
(0, 0, 0) 3 (0, 0, 0) 3 (2.5, 0.5, 1) 3 (2.5, 0.5, 1) 3	1.510 0.971
(0, 0, 0) 1 (0, 0, 0) 1 (2.5, 1.5, 1) 1 (2.5, 1.5, 1) 1	1.442 0.957
(0, 0, 0) 1 (0, 0, 0) 1 (2.5, 1.5, 1) 2 (2.5, 1.5, 1) 2	1.493 0.968
(0, 0, 0) 1 (0, 0, 0) 1 (2.5, 1.5, 1) 3 (2.5, 1.5, 1) 3	1.481 0.964
(0, 0, 0) 2 (0, 0, 0) 2 (2.5, 1.5, 1) 1 (2.5, 1.5, 1) 1	1.415 0.950
(0, 0, 0) 2 (0, 0, 0) 2 (2.5, 1.5, 1) 2 (2.5, 1.5, 1) 2	1.435 0.956
(0, 0, 0) 2 (0, 0, 0) 2 (2.5, 1.5, 1) 3 (2.5, 1.5, 1) 3	1.449 0.956
(0, 0, 0) 3 (0, 0, 0) 3 (2.5, 1.5, 1) 1 (2.5, 1.5, 1) 1	1.390 0.945
(0, 0, 0) 3 (0, 0, 0) 3 (2.5, 1.5, 1) 2 (2.5, 1.5, 1) 2	1.426 0.953
(0, 0, 0) 3 (0, 0, 0) 3 (2.5, 1.5, 1) 3 (2.5, 1.5, 1) 3	1.432 0.956
(0, 0, 0) 1 (0, 0, 0) 1 (2.5, 2.5, 1) 1 (2.5, 2.5, 1) 1	1.363 0.940
(0, 0, 0) 1 (0, 0, 0) 1 (2.5, 2.5, 1) 2 (2.5, 2.5, 1) 2	1.390 0.945
(0, 0, 0) 1 (0, 0, 0) 1 (2.5, 2.5, 1) 3 (2.5, 2.5, 1) 3	1.390 0.945
(0, 0, 0) 2 (0, 0, 0) 2 (2.5, 2.5, 1) 1 (2.5, 2.5, 1) 1	1.343 0.935
(0, 0, 0) 2 (0, 0, 0) 2 (2.5, 2.5, 1) 2 (2.5, 2.5, 1) 2	1.354 0.939
(0, 0, 0) 2 (0, 0, 0) 2 (2.5, 2.5, 1) 3 (2.5, 2.5, 1) 3	1.367 0.940
(0, 0, 0) 3 (0, 0, 0) 3 (2.5, 2.5, 1) 1 (2.5, 2.5, 1) 1	1.343 0.935
(0, 0, 0) 3 (0, 0, 0) 3 (2.5, 2.5, 1) 2 (2.5, 2.5, 1) 2	1.367 0.940
(0, 0, 0) 3 (0, 0, 0) 3 (2.5, 2.5, 1) 3 (2.5, 2.5, 1) 3	1.354 0.939
(0, 1, 0) 3 (0, 0, 0) 1 (0, 1, 0) 3 (0, 1, 0) 3	0.175 0.103
(0, -1, 0) 1 (0, 0, 0) 3 (0, 0, 0) 3 (0, 0, 0) 3	0.175 0.103
(1, -1, 0) 2 (0, 0, 0) 3 (0, -1, 0) 1 (0, -1, 0) 1	0.286 0.099
(-1, 1, 0) 3 (0, 0, 0) 2 (-1, 0, 0) 1 (-1, 0, 0) 1	0.286 0.099
(0, 0, 0) 3 (0, 0, 0) 3 (0, -1, 0) 1 (0, 0, 0) 3	0.175 0.103
(0, 0, 0) 3 (0, 0, 0) 3 (0, 0, 0) 3 (0, -1, 0) 1	0.175 0.103
(0, 0, 0) 1 (0, 0, 0) 1 (0, 1, 0) 3 (1, 0, 0) 2	0.286 0.099
(0, 0, 0) 1 (0, 0, 0) 1 (1, 0, 0) 2 (0, 1, 0) 3	0.286 0.099